DRY POWDER FOR INHALATION - INFLUENCE OF MIXING PROCESS AND ADDITION OF MAGNESIUM STEARATE

LUND UNIVERSITY

EMMACE CONSULTING AB

GALENICA

Love Ivarsson

EMMACE CONSULTING AB | FACULTY OF ENGINEERING, LTH | GALENICA AB

Abstract

For efficient treatment of many diseases of the lung, it is beneficial to deliver the medicine to the respiratory tract directly. This ensures a rapid response since it can enter the bloodstream directly through the alveolar epithelium. Consequently, also decreases systemic effects due to the local treatment.

Dry powder inhaler (DPI) is today one of the most used inhalers for pulmonary delivery. The DPI formulations often consist of a micronized active pharmaceutical ingredient (API) which is mixed with larger carrier particles, creating an adhesive mixture. For a successful API delivery, there are four main factors that need to be considered; the formulation, the device used for the delivery, the physicochemical properties of the drug and the patient. In this thesis, the focus is to determine how the mixing energy, mixing speed, mixing time and use of coatings, affects the formulation and drug delivery.

These effects were studied using a Turbula T2C low shear and a Diosna P1-6 high shear mixer, set to different mixing speeds and mixing times to manufacture prototype formulations. To some of the batches, a coating of Magnesium Stearate was added. The formulations were studied using different analytical techniques.

Evidently, all the above-mentioned parameters play a part in the performance of the formulations. However, it is indicated that it is rather the mixing energy that controls the quality, than the individual parameters. Neither too low nor too high mixing energy is beneficial when manufacturing formulations.

Comparing the results of the Diosna and Turbula mixed formulations, it may be assumed that both are suitable for mixing of the API, however when mixing the coating agent, the Diosna high-shear mixer is favored. Adding a coating agent continually improved the performance of all formulations manufactured.

Acknowledgements

This master´s thesis has been performed at the department of food technology in collaboration with Emmace consulting AB and Galenica AB.

I would like to express my gratitude towards both my supervisors Kyrre Thalberg and Ann-Marie Lyberg, both of whom have offered great support, time and guidance in the making of this diploma work.

Furthermore, I would like to extend my appreciation to both Emmace consulting AB and Galenica AB for the opportunity they offered me by accepting this project and showing an interest in its progress.

An extra thank you is dedicated to Peter Elfman and Jackie Stuckel for their guidance and help with many of the practical aspects. And to Jackie and the many pleasant lunch breaks during this summer's work together.

To Marie Wahlgren, for accepting to be my examinator during this thesis and helping when needed. My thank you to Crispin Hetherington for operating the SEM.

And to Rasia Ahmadi and Rebecka Cattani, for their continued support. I also greatly appreciated the expertise offered by Rasia when problems occurred with the ACI setup.

There are many more people who have contributed and supported me during this thesis, but the list would be too long to go on. However, I am extremely thankful to all. And I am thankful for all the years at LTH, the knowledge gained, and that it has soon come to an end.

Table of content

1 Introduction

1.1 Background

The treatment of many diseases of the lung is delivered to the respiratory tract directly. The reason for this is to ensure a rapid response as well as being able to administrate smaller doses, due to local treatment, thus also avoiding systemic side effects. Another beneficial aspect of pulmonary delivery is the great surface area of the lungs and additionally, due to it being the site for gas exchange, a very large number of capillaries and thin air-blood barrier. By delivering drugs via the pulmonary tract, it is possible to avoid the liver metabolizing the drug which is occurrent with oral delivery (though the lung has some metabolic effects on its own). This also makes pulmonary delivery a potential route for other treatments. (Aulton & Taylor, 2017, p. 654) However due to the low buffering capacity of the lung, compared to the GI tract e.g., the excipients that could be used to improve delivery is limited (Telko & Hickey, 2005).

The concept of drug delivery through inhalation is a much older concept than might be thought. The oldest records date back to ancient Egypt, though it was not until the year 1778 that the word "inhaler" was first used. Moving forward to the year 1864, the first patent was filed for a device intended for the delivery of dry powders. (Sanders, 2007) Since then several advances have been made and today one of the most likely areas for innovation to occur is within formulation technology. One of the challenges that are remaining to be improved in this regard is the targeted delivery of medicine to the lungs. (Biddiscombe and Usmani, 2018)

1.2 Aim of the study

The purpose of the study is to determine the effects of mixing energy, mixing speed and mixing time on dry powder formulations (for inhalation), comparing the results for formulations with and without a magnesium stearate coating. Using both the Turbula T2C low shear- and the Diosna P1-6 high shear mixer, formulations will be prepared with and without adding a coating to the formulation. Three different mixing times will be compared for each batch, taking out samples that are to be used to measure bulk density. The formulations will be studied using different analytical techniques. For testing the formulation, the inhaler Novolizer was chosen, both due to enabling an easy switch of formulation and showing promising results in previous thesis studies.

1.2.1 Approach

Magnesium stearate-coated and uncoated batches will be manufactured using both the Turbula low-shear mixer and Diosna high-shear mixer. For the high-shear mixer, two different speeds will be used for mixing. The bulk density of each batch will be measured immediately after manufacturing and after being stored.

Investigation of the manufactured formulations will be conducted using cascade impactors to gain information regarding the amount, aerodynamic particle distribution, fine particle fraction

and fine particle dose. In addition, Malvern Mastersizer (dry) will be used to examine the particle distribution. The homogeneity of the formulations will be determined using UV-Vis spectroscopy and the morphology studied using secondary electron microscopy (SEM).

1.2.2 Goal

Contribute with knowledge regarding how the magnesium stearate coating affects the formulation when using the Turbula compared to a high-shear mixer, Diosna. How time and speed influence the mixing, further investigate the difference between the usage of a magnesium stearate coating compared to not using coating and how the coating affects the structure of the adhesive mixture.

2 Theory

2.1 Pulmonary drug delivery

For delivery to the lung, it is important that the drug is in the form of an aerosol. An aerosol is a suspension, of either solid particles or liquid droplets, in a gas. The particles or droplets must be of a sufficiently small size to be able to remain stable as a suspension. For the size of the particles, the measurement used is the aerodynamic diameter (d_a). This is the diameter of a sphere (of a unit density), traveling through air with the same velocity as that of the particle. For particles that can be viewed as spheres, the following equation can be used to determine d_a. (Aulton & Taylor, 2017, pp. 654-655, 667,669)

$$d_a = d_p(\rho/\rho_0)^{1/2}$$

Where d_p is the diameter of the particle (physically), ρ is the density of the particle and ρ_0 is the unit density. If the mass median diameter is used for d_p, the measurement d_a will be that of the mass median aerodynamic diameter (MMAD). The reason behind the importance of this measurement is that it can be used to assess how deep particles are carried down the respiratory tract. Meaning that a large but porous particle may have the same MMAD as a smaller but denser particle, which may offer advantages when formulating a drug. This measurement can be determined using a cascade impactor, where both information regarding the median aerodynamic diameter as well as polydispersity can be derived. The impactor fractionates the aerosols according to size on progressively finer jets as the aerosol is pulled in at a predetermined flow rate. (Aulton & Taylor, 2017, pp. 654-655, 667,669)

There are four main factors that contribute to the deposition of the drug. These are the formulation, the device used for the delivery, the physicochemical properties of the drug and the patient. The three main mechanisms for deposition within the lung are the following: impaction, sedimentation and diffusion. (Aulton & Taylor, 2017, p. 655)

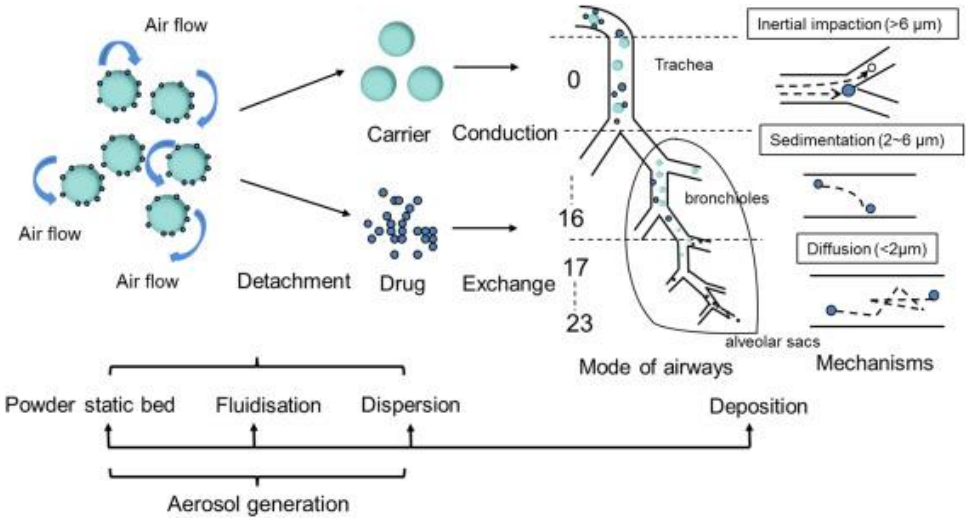

Figure 1. Illustration of the detachment- and deposition mechanisms of ordered mixtures. (Figure credit: Peng et al, 2016)

2.1.1 Inertial impaction

Inertial impaction is one of the deposition mechanisms in pulmonary drug delivery. Due to the high velocity of the air stream inspirated, there is an impaction in the back of the throat as the airflow changes direction down the respiratory tract. This type of deposition is especially important regarding large particles with a diameter of 5 µm or larger (>10 µm especially). Further down the tract, the velocity decreases and thus this mechanism loses significance. (Aulton & Taylor, 2017, p. 655)

2.1.2 Gravitational sedimentation

For particles ranging between 0.5 and 3 µm in diameter, the most important deposition method is that of gravitational sedimentation, which is determined by Stokes law. This type of deposition mainly occurs in the small airways and alveoli. (Aulton & Taylor, 2017, p. 655) According to several studies, the optimal size for lung deposition has proven to be within the range of 1-5 µm (Telko & Hickey, 2012).

2.1.3 Brownian diffusion

Particles finer than 0.5 µm in diameter are deposited by Brownian motion. Brownian motion occurs when very small particles collide with other particles and molecules, and thus resulting in a netto movement from high to low concentrations. The effect this has on the particles inhaled, is that they move from the aerosol cloud toward the lower concentrations at the walls of the airway. (Aulton & Taylor, 2017, p. 655) However, particles of this size (<0.5 µm) risk not being deposited at all since diffusion is a slow movement. (Telko & Hickey, 2005)

2.2 Dry powder formulations

The formulation used for dry powder inhalers (DPI) consists of a micronized active pharmaceutical ingredient (API) together with a larger carrier particle, often lactose is used. Micronizing decreases the particle size which is important since the API has to be small enough to be inhaled, while the carrier particles´ main purpose is to make the formula administrable. The reason being that the micronized drug on its own most often has poor flowability. (Aulton & Taylor, 2017, p. 137) By introducing a carrier particle, the number of aggregates is also lowered. After micronization, the size of the particles range between 5-10 µm in size. (Thalberg, Berg & Fransson, 2012)

The DPI formulation, after actuation, is inhaled as a fine powder cloud (Aulton & Taylor, 2017, p. 660). It is under the influence of the airflow inspirated, that the API separates from the carrier particle and continues down while the carrier impacts the oropharyngeal surfaces. (Telko & Hickey, 2005)

An advantage of using DPIs instead of other systems, such as pressurized metered-dose inhalers (pMDIs), is that there is often no need of additional excipients, not counting the carrier particles. Additionally, the devices are breath actuated, meaning that the coordination of actuation and inhalation need not be considered. One disadvantage with DPIs however is that they are limited by the inhalation capacity of the patient, since the disaggregation of the formulation is dependent on the airflow (inhalation). This of course can prove to be a problem since many

patients requiring treatment with inhalers have some form of respiratory impairment. (Aulton & Taylor, 2017, p. 660)

2.2.1 Flowability

Flowability of a DPI formulation is affected by its physical characteristics; such as density, roughness of the particle surfaces, moisture content, bulk density, hardness, shape and size of the particles. To aid the flowability of the drug, a carrier is often, but not always used. The carrier is a larger particle, often between 30 and 150 µm in diameter, and of inert nature. Together with the API, the carrier is mixed to create an ordered mixture. In the ordered mixture the smaller particles of the API are attached to the surface of the larger carrier. The benefits of the ordered mix approach are that it both facilitates the release of API from the inhaler by improving the flow of the powder, as well as improving the uniformity of the actuated doses. When the particles have left the device, the turbulent airflow from within the device is what detaches the drug from the carrier. This results in the carrier impacting the throat, while the much smaller micronized drug particles are able to continue further down the respiratory tract. (Aulton & Taylor, 2017, pp. 660-661)

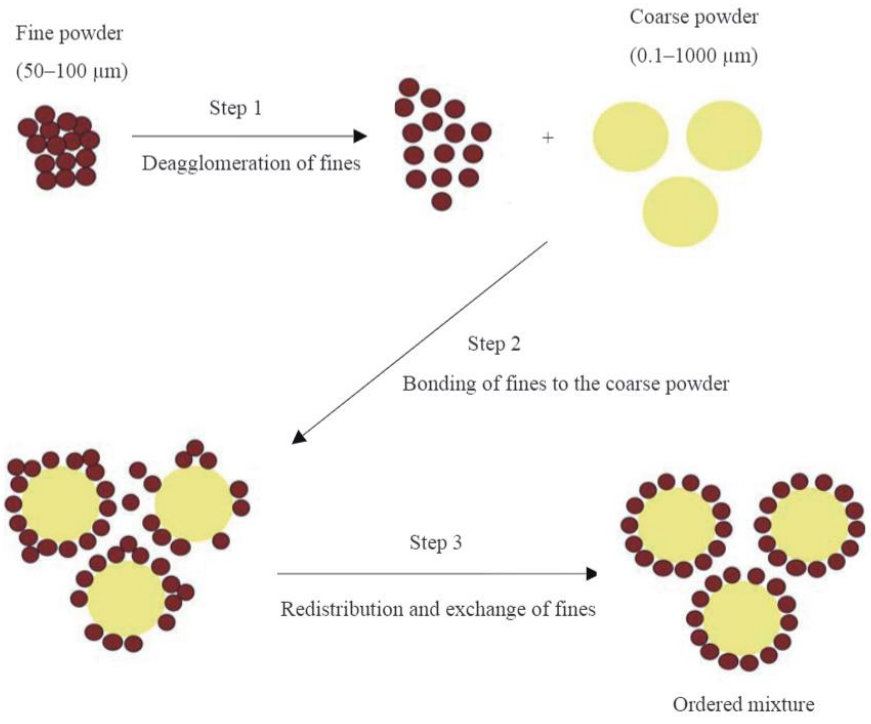

Figure 2. Illustration of an ordered mixture and its processing steps. (Figure credit: Saharan et.al. 2008)

Important aspects of the success of a DPI is the adhesiveness between carrier and API and the ability to detach when a dose is actuated. These aspects are dependent on the morphology and surface of the particles as well as the surface energy. Factors contributing to this are the processing of the formulation and the chemical qualities of the material. Another way of changing the adhesive qualities of the particles is by adding a coating (flow activator) to the

carrier, such as magnesium stearate, that can aid the drug release. (Aulton & Taylor, 2017, p. 661)

2.2.1.1 Shape and surface properties

With formulations for DPIs, it is necessary to take into consideration the shape and properties of the surface of the particles to ensure successful delivery. The roughness of the surface of the carrier particles affects how strongly the API adheres to it. For example, a very rough surface may cause the drug to not separate and thus leading to a low delivered dose of API. On the other hand, if the surface of the carrier is too smooth the opposite effect may occur, that the drug does not adhere well enough when filling the inhaler or actuating a dose. One approach to this problem is the addition of micronized excipient particles, before adding the API. This may lead to the micronized excipients (fines) occupying the deeper cavities of a rough carrier particle, thus making the API adhere to more easily dispatched sites. However, this has not been proved beyond doubt and other possible reasons for an enhanced delivery are possible. This further proves the importance of studying the surface of the carrier when designing a new DPI. (Aulton & Taylor, 2017, pp. 137-138)

In addition, a more spherical particle often exhibits better flow qualities than one with an irregular shape. If the texture of the particles is irregular there is also an increased risk of them interlocking and thus contributing to poor flowability. (Aulton & Taylor, 2017, p. 199)

2.2.1.2 Moisture content

Other factors that contribute to the result are whether there is a presence of water, which is known to affect the adhesion, and why the need for humidity control when manufacturing is crucial. (Aulton & Taylor, 2017, pp. 137-138) Moisture, when adsorbed to the surface of a particle, may also cause an increase in bulk density and reduce the porosity, thus leading to lower flowability. (Aulton & Taylor, 2017, p. 199) Even very small amounts of moisture can cause capillary forces to act on the particles (Telko & Hickey, 2005). This can be counteracted by drying the formulation in a low-humidity storage (Aulton & Taylor, 2017, p. 199). But consideration must be given to the risk of surface charges (Telko & Hickey, 2005).

Another aspect of moisture uptake and loss is the risk of permanent aggregation by the formation of solid bridges. This is due to the moisture causing local dissolution and recrystallization. The creation of aggregates may cause an inability to create an aerosol cloud with particles of suitable size. (Telko & Hickey, 2005)

2.2.1.3 Size

The size of the particles has also proven to be important for flowability. Larger particles are often less cohesive than smaller particles and thus exhibit better flow qualities. To improve flowability it may thus be advantageous to decrease the portion of fines or increase the portion of large particles. (Aulton & Taylor, 2017, p. 199) Both adhesion and cohesion (the sum of the interparticular interactions) are properties related to the surface of the particles, thus a high surface-to-mass ratio (such as for small particles) tend to result in adhesive and cohesive effects (Aulton & Taylor, 2017, p. 191). For the particles to disperse into an aerosol, the cohesive forces need to be overcome. And the higher the cohesive energy, the lower the dispersibility of

the formulation. (Thalberg, Berg & Fransson, 2012) The risk is that the shear of the airflow will not be sufficient to detach the drug from the carrier (Telko & Hickey, 2005). This is more prominent for particles smaller than 100 µm and becomes extreme for particle sizes below 10 µm. It does however not apply to ordered mixtures, where the small particles are attached to the surface of larger since the flow properties then will be dictated by the large particles. (Aulton & Taylor, 2017, p. 191)

2.2.1.4 Electrostatic charges

Electrostatic charges in the powder also affect the flowability. By reducing these the flowability of the powder can be increased. The charges may originate from the manufacturing process or container. (Aulton & Taylor, 2017, p. 199)

2.2.1.5 Coating agents

Coating agents, also called glidants or flow activators, can be added to improve the flowability of a powder. What it does is reduce the cohesion and adhesion of the particles. (Aulton & Taylor, 2017, p. 199) A glidant, or coating agent, is smeared onto the carrier particle during mixing. These agents are often derived from surfactants, an example of this is magnesium stearate (MgSt). Magnesium stearate has previously been used as a "lubricant" for other drug formulations and has been gaining large interest in dry powders as well. The hope is for it to improve the fine particle dose and stability. (Shur, Jagdeep, et al. 2016, pp. 374-383) These glidants improve the dispersity of the mixture by making the surface of the carrier smoother and thus lower the surface energy and friction. (Thalberg et al, 2021)

2.2.1.6 Bulk density

The bulk density of a powder is dependent both on the packing of the particles and on the changes occurring as it consolidates. If the powder is consolidated there is a risk of it having poor powder flow. (Aulton & Taylor, 2017, p. 197)

Both the initial bulk density (poured bulk density) and the final bulk density (consolidated/tapped bulk density) can be measured. These measurements have gained interest since they correspond to flowability. One measurement that has proven to be useful is the Hausner ratio, which is the ratio between tapped and poured bulk density. The result can be used as a measurement of the flowability of the powder. (Aulton & Taylor, 2017, pp. 197-198)

For tightly packed powders to flow, a higher driving force/airflow is often required. (Aulton & Taylor, 2017, p. 192)

The bulk density, ρ_B can be calculated by using the following equation:

$$\rho_B = \frac{M}{V} kgm^{-3}$$

Due to voids and pores within a packed powder, the bulk density can never exceed the "true density" of the material. An increase in bulk density may indicate that there has been a decrease in porosity. Further, this leads to more contact surfaces between the particles which contribute to a higher degree of adhesion and cohesion. If the particles are sufficiently large, however this

may not be enough to overrule and affect the flow quality. If the bulk density instead is decreasing, this may not be beneficial for the flowability either, since a decrease may indicate finer particles with a looser packing. However finer particles also indicate a raise in adhesive and cohesive forces, meaning that although more porous, the flowability may be reduced. (Aulton & Taylor, 2017, p. 192)

Another possible packing phenomenon is the formation of bridges and arches. If there are bridge formations in the packed powder, two different states of packing may give the same bulk density/porosity. (Aulton & Taylor, 2017, pp. 192-193)

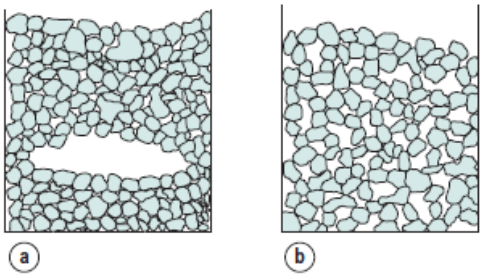

Figure 3. Both a and b display the same bulk density/porosity, but exhibit different packing geometries which is not represented using the bulk density measurement. (Figure credit: Aulton & Taylor, 2017, p. 193)

2.2.2 Dry powder inhalers

2.2.2.1 Novolizer

The Novolizer is a DPI device that is breath activated, a minimum inspirated airflow of between 35-50 l/min is required. When the dose has been delivered the dose indication window (seen in figure 4) will switch colour and a clicking sound is heard. (Kohler, 2004)

Inside the mouthpiece, a cyclone is situated. The cyclone aids in enabling the deagglomeration of the particles, making them able to flow down to deposit on the target site rather than in the upper respiratory tract. The Novolizer has been proven to give one of the highest depositions in the lung compared to other devices. In addition, it does not show the same flow rate dependence as many other devices. (Kohler, 2004)

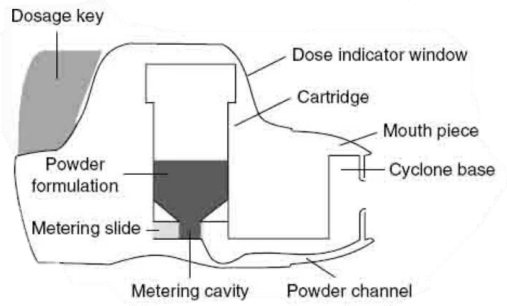

Figure 4. Figure illustrating the design and different parts of the Novolizer. (Figure credit: (Fenton, Keating, & Plosker, 2003))

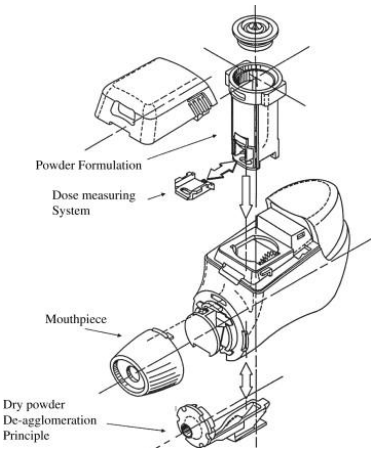

Figure 5. The different parts of the Novopulmon Novolizer. (Figure credit: Kulkarni, 2009).

2.3 Aerodynamic particle size distribution

2.3.1 Cascade impactors

A way of analyzing DPIs is with the use of cascade impactors. These impactors consist of jets which become increasingly finer the further down the devices, with collection plates at each stage. This enables a separation dependent on the aerodynamic diameter. This means that big and dense particles will deposit on the earlier collection plates while finer and more porous particles will move further down the impactor. Depending on the airflow through the device, the cut-off diameter of the different stages will change. Usually, the first stage of the impactor is a throat, traditionally made from metal, made to mimick that of a human. (Aulton & Taylor, 2017, p. 667) After each run, the impactor is dismantled and with the chosen analytical method, the amount deposited on each stage can be determined (Telko & Hickey, 2012)

When using cascade impactors to measure on DPIs, the pharmacopoeia dictates to use a pressure drop of 4.0 kPa. From this, a suitable flow rate can be calculated. (Aulton & Taylor, 2017, p. 669)

A disadvantage of using cascade impactors is the risk of bounce. Bounce is when particles "bounce" off the collection plate and continue further down the impactor. This may result in a wrongful decrease in the aerodynamic particle size. One way of combating this issue is by using a coating agent on the collection plates. Another limiting factor is that a single airflow rate does not adequately represent respiration, causing the dispersion and deposition profile of the drug to not reflect reality. The reason for this is that by having different flow rates during inspiration, which is the case for a person inhaling, the deposition profile changes as the breath is drawn. By using a "breath simulator", with a predetermined inhalation profile, this can be countered. (Aulton & Taylor, 2017, p. 669)

To ensure that the product tested is effective for treatment, an important measurement to take into consideration is the amount in percentages, finer than a set size (usually 5 µm), the so-

called fine particle fraction. The dose this corresponds to is called the fine particle dose. (Aulton & Taylor, 2017, p. 669)

There are two types of impactors which are commonly used. The Andersen cascade impactor (ACI) and the Next generation impactor (NGI). (Aulton & Taylor, 2017, p. 667)

2.3.1.1 Andersen Cascade Impactor

The Andersen Cascade Impactor, ACI, consists of eight stages, each with a collection plate, stacked on top of each other and lastly followed by a terminating filter. The ACI can be used for aerodynamic assessment of pMDIs and DPIs. (Aulton & Taylor, 2017, pp. 667-668)

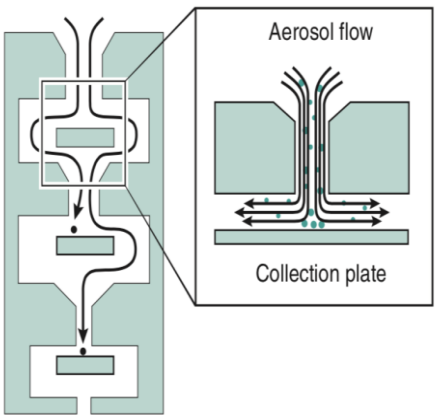

Figure 6. Schematic figure showing the airflow inside the Andersen Cascade Impactor. (Figure credit: Taylor & Aulton, 2017, p. 667)

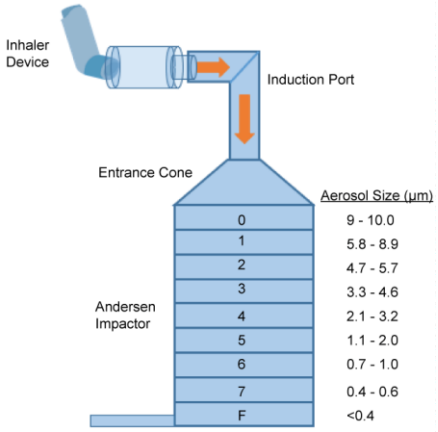

Figure 7. Illustration of the ACI device and the aerosol size each stage correlates to. (Figure credit: Gumani et al., 2016)

2.3.1.2 Next generation impactor

The NGI has seven different stages for impaction. After the impaction stages, a micro-orifice collector is situated. The NGI can be used for flowrates ranging between 15 L min^{-1} to 100 L min^{-1}. It is suitable for the aerodynamic assessment of DPIs, pMDIs and nebulizers. (Aulton & Taylor, 2017, p. 668)

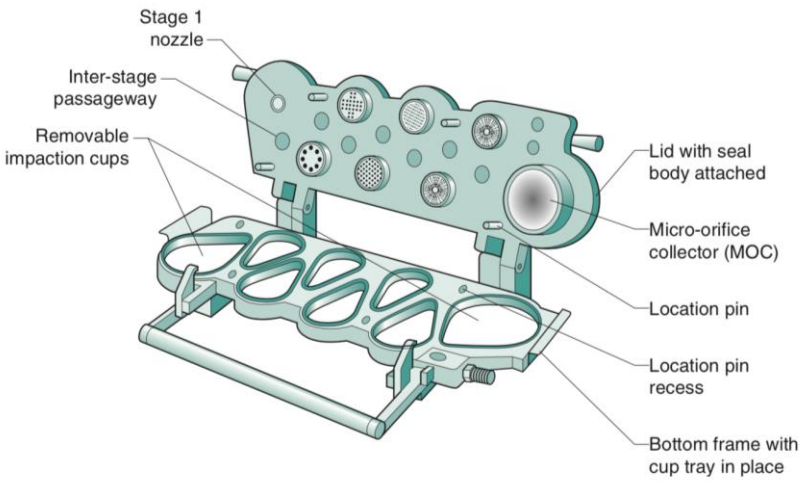

Figure 8. Schematic image of the Next Generation Impactor. (Figure credit: Taylor & Aulton, 2017, p. 668)

2.3.2 Fine particle fraction - FPF

Fine particle fraction (FPF), as previously mentioned, is the percentage of particles below a certain size (often <5 µm is used). Studies have shown that low FPF values often can be linked to poor performance with a high variety in the dose delivered to the lung. This is occurrent for formulations containing a low percentage of API. A more suitable range would be within 2-15 %, since this range enables a high fine particle fraction. If the drug load is higher, there is a risk of collapse of the fine particle fraction (regarding ordered mixtures). (Thalberg, Berg & Fransson, 2012)

Within the fine particle fraction, it is good to take the polydispersity into consideration since two formulations with vastly different size distributions can result in the same FPF. The degree of dispersity can affect both the quality and efficacy of the formulation. (Telko & Hickey, 2005)

The FPF is also to a high degree dependent on the processing of the formulation. The mixing process heavily influences the performance of a formulation, this can be seen in the impact of the FPF. With a higher degree of fine particles in a formulation, the number of aggregates on the surface of the carriers is also increased. (Thalberg, Berg & Fransson, 2012)

2.4 Effects of mixing

Ordered, or adhesive, mixtures can be categorized according to their mixing state. The first step is when the API occupies cavities on the surface of the carrier particle. The second is when the API instead adheres to the external surface of the carrier. Lastly, the third state occurs at high doses of API, when the API starts to form agglomerations which coexist along with the carrier particles. Since these different states exist, it is difficult to compare mixtures which are at different mixing stages to each other. (Thalberg et al., 2021)

The fine particle fraction may also be directly related to the mixing process of the formulation. Mixing is also correlated to other performance measurements and the degree of mixing is related to both which mixer and method are being employed. Additionally, the duration of mixing has been observed to impact the fine particle fraction. (Thalberg,et al., 2012)

2.4.1 Turbula low-shear mixer

Low-shear mixers such as the Turbula mixer, use a tumbling motion to blend powders. There are a limited number of studies examining the effects of blending (such as mixing time and mixing speed) in low-shear mixing and the results are unanimous. Some studies indicate that a prolonged mixing time does not correlate with blend uniformity. Others have shown that a prolonged mixing time is linked to an increased drug load, more electrostatic interactions and adhesive forces. Some have seen a decrease in drug detachment and FPF with longer mixing times. (Spahn, Zhang, & Smyth, 2022)

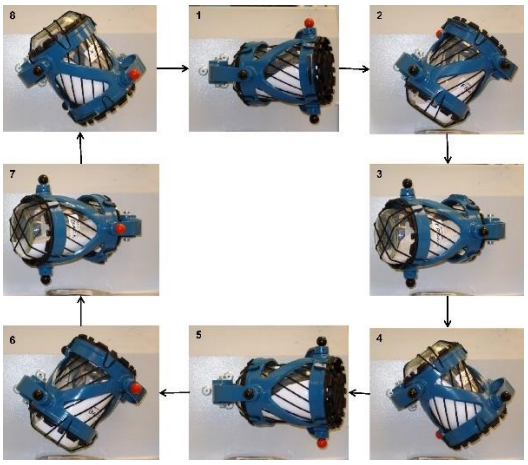

Figure 9. Images showing the blending cycle of the Turbula mixer. The mixer provides an rotation of 90° around the central axis as well as 360° around the radial axis during one mixing cycle.
(Figure credit: Kushner, 2012)

2.4.2 Diosna high shear mixer

The high-shear mixer consists of an impeller blade which blends the powder, contrary to the tumbling motion of the Turbula. Previous studies have indicated higher aerosol performance, but lower drug content linked to an increase in mixing intensity. Studies performed with magnesium stearate as a flow activator/lubricant showed an initial increase of FBF and then a decrease with prolonged mixing time. (Spahn, Zhang, & Smyth, 2022)

When mixing with a high-shear mixer, the dominating movement is the rotation of the impeller which moves the powder, and thus the centrifugal force is important. To model the force exerted on the particles, the following formulas can thus be used. (Thalberg et al., 2021)

Since the particles are confined by the walls of the mixing bowl, the force, F, and thus the acceleration, a, can be calculated according to:

$$a = \frac{v^2}{r}$$

Where v is the peripheral velocity and r is the radius of the mixing bowl. This can also be expressed as:

$$F = m * a = m\frac{v^2}{r}$$

Here, m is the mass of the carrier particle. To calculate the mixing energy, ME, the expression is multiplied by the distance travelled by the particles, d.

$$ME = F * d = F * v * t = m\frac{v^3 t}{r}$$

To express this with the rotational speed, which is used when mixing powders, the impeller frequency, f, can be expressed using the velocity v.

$$f = \frac{v}{2\pi r}$$

Thus the following formula can be used to calculate the mixing energy.

$$ME = 8\pi^3 m f^3 r^2 t$$

From this equation, it is evident that both the mixing time and speed are important parameters. It can also be seen that the mixing speed is of greater importance than the time (power of three compared to one), however this can be compensated with longer mixing times. (Thalberg et al., 2021)

There have also been studies conducted that report a prolonged mixing time/overmixing can lead to a lower FPF. Possible explanations offered are that a prolonged mixing results in the API being incorporated into the coating, or a loss of API (and thus fine particles) during the mixing process. (Thalberg et al., 2021)

3 Materials and methodology

3.1 Manufacturing of formulations

The formulations were manufactured using the Diosna P1-6 high-shear mixer and the Turbula T2C low-shear mixer. Different speeds and mixing times were studied for coated and naked formulations. Each batch has lactose as a carrier and contains 2% Budesonide (API). The coated batches contained ~1% magnesium stearate (used as coating agent). Further information regarding the raw material can be found in table 1, as well as composition in table 2 and amounts used in table 3 (Diosna batches) and 4 (Turbula batches).

Table 1. Raw materials.

Component	Supplier	Batch No.	Function
Magnesium Stearate	Peter Greven	4211059	Reduce friction/lubricant
Budesonide micronized	AstraZeneca	C723845	API
Lactose monohydrate Lactohale LH206	DFE Pharma	600365	Carrier

Table 2. Composition

Component	Composition in percent (%), Budesonide blends with MgSt	Composition in percent (%), Budesonide naked blends	Composition in percent (%), Coated carrier
Magnesium Stearate	1.0 %	-	1.0 %
Budesonide micr.	2.0 %	2.0 %	-
Lactose carrier	To 100%	To 100%	To 100%

Table 3. Amounts - Diosna batches

Component	Budesonide blends with MgSt (g)	Budesonide naked blends (g)	Coated carrier (g)
Magnesium Stearate	2.5	-	3.0
Budesonide micr.	5.0	5.0	-
Lactose carrier	242.5	245.0	297.0
Total	250.0	250.0	300.0

Table 4. Amounts - Turbula batches

Component	Budesonide blends with MgSt (g)	Budesonide naked blends (g)	Coated carrier (g)
Magnesium Stearate	0.786	-	0.9
Budesonide micr.	1.6	1.6	-
Lactose carrier	77.814	78.4	89.1
Total	80.0	80.0	90.0

The equipment used for manufacturing can be found in table 5 below. Both the Magnesium Stearate and the Budesonide were added to the mixing vessel using the sandwich method, where half the carrier is added before and half after the API/coating agent. During the mixing with the Diosna mixer three stops were made, taking out samples and measuring the temperature after one minute using an IR thermometer, while for the Turbula separate batches were made for the different mixing times and the temperature was measured after 2 minutes. The formula was sieved using the setup in figure 11, where the spoon was used to tap on the sieve for the formulation to move through the mesh. For the high shear mixer two different speeds were used, one low (700 rpm) and one high (1000 rpm), while all the Turbula batches were mixed at the same speed (68 rpm). The Turbula manufactured formula displayed aggregates of what can be presumed to be budesonide during the sieving step, especially for the low mixing times. To keep the drug content uniform, the aggregates were gently pressed through the sieve using a metal spoon.

The bulk density was measured for the different mixing times.

For the manufactured batches and settings, see table 6.

Table 5. Equipment used for manufacturing with the Diosna- respectively Turbula mixer

Equipment	Turbula batches	Diosna batches
Diosna Mixer P1-6		X
Turbula T2C	X	
Scale	X	X
Testo 610 Temp and Humidity meter		X
Sieve 1 mm		X
Sieve 0.71 mm	X	
Testo Thermometer IR	X	X
Bulk density meter	X	X
Timer	X	X

Table 6. Batch names and manufacturing settings

Batch name	Mixer type	Coated or naked	Time for coating (minutes)	Coating speed (rpm)	Speed **H**igh/**L**ow (rpm) API mixing	Time for mixing (minutes)
T-N-10	**T**urbula (low shear)	**N**aked	-	-	68	5*2=**10**
T-N-30	**T**urbula (low shear)	**N**aked	-	-	68	15*2=**30**
T-N-60	**T**urbula (low shear)	**N**aked	-	-	68	30*2=**60**
T-C-10	**T**urbula (low shear)	**C**oated	15*2	68	68	5*2=**10**
T-C-30	**T**urbula (low shear)	**C**oated	15*2	68	68	15*2=**30**
T-C-60	**T**urbula (low shear)	**C**oated	15*2	68	68	30*2=**60**
D-C-L-T-10	**D**iosna (high shear) & **T**urbula (low shear)	**C**oated	4	700	68	5*2=**10**
D-C-L-T-30	**D**iosna (high shear) & Turbula (low shear)	**C**oated	4	700	68	15*2=**30**
D-C-L-T-60	**D**iosna (high shear) & **T**urbula (low shear)	**C**oated	4	700	68	30*2=**60**
D-N-L-3	**D**iosna (high shear)	**N**aked	-	-	**L**ow=700	**3**
D-N-L-6	**D**iosna (high shear)	**N**aked	-	-	**L**ow=700	**6**
D-N-L-9	**D**iosna (high shear)	**N**aked	-	-	**L**ow=700	**9**
D-N-H-3	**D**iosna (high shear)	**N**aked	-	-	**H**igh=1000	**3**
D-N-H-6	**D**iosna (high shear)	**N**aked	-	-	**H**igh=1000	**6**
D-N-H-9	**D**iosna (high shear)	**N**aked	-	-	**H**igh=1000	**9**

D-C-L	**D**iosna (high shear)	**C**oated	4	700	-	-
D-C-L-3	**D**iosna (high shear)	**C**oated	4	700	**L**ow=700	**3**
D-C-L-6	**D**iosna (high shear)	**C**oated	4	700	**L**ow=700	**6**
D-C-L-9	**D**iosna (high shear)	**C**oated	4	700	**L**ow=700	**9**
D-C-H-3	**D**iosna (high shear)	**C**oated	4	700	**H**igh=1000	**3**
D-C-H-6	**D**iosna (high shear)	**C**oated	4	700	**H**igh=1000	**6**
D-C-H-9	**D**iosna (high shear)	**C**oated	4	700	**H**igh=1000	**9**

Figure 10: Picture of the Diosna mixing vessel containing formula.

Figure 11: Picture of sieve and formula

Figure 12: Picture of Turbula mixer.

3.2 Poured bulk density

The bulk density of the formulations was measured (see figure 13). Two different sets were employed. The larger one consists of two cylinders, one with an opening in both ends and one with a closed end. The open cylinder is slightly smaller and intended to be placed into the bigger before the powder is poured using a long and narrow spoon. When filled the inner cylinder is to be carefully removed, making the formulation flow into the bigger. Then using the straight handle of the spoon, scrape of access powder and weighing the content. For the small set, no inner cylinder was used and the access powder scraped of directly. Due to the method being non-destructive, the formulation was not disregarded afterwards.

The big cylinder was used both for the initial measurements of the formulations directly after manufacturing and for measuring the batches after being stored for two months (ambient storage). The small cylinder was used for the samples placed in the desiccator (see 3.7 Storage conditions) as well as for the ambient stored formulations.

The volume of the cylinder was determined by weighing the volume of water (with a surfactant) which could fit inside. The density of water was used for the calculations. For the large cylinder the average volume was 20.2 ml and 5.2 ml for the small one.

Each of the bulk density measurements were performed in duplicates.

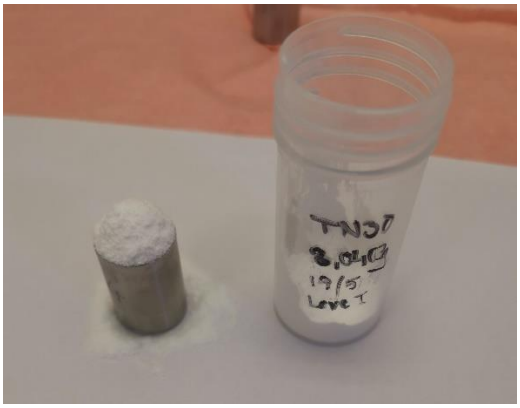

Figure 13. Picture of formulation and the small measuring cylinder.

3.3 Budesonide determination

A calibration curve was established using a precision scale to measure a known amount of budesonide which was then dissolved in EtOH:H2O (50:50) using a volumetric flask, creating a stock solution. The dilution series was then executed by using volumetric flasks to measure equal amounts of stock solution/previous solution and EtOH:H2O (50:50) which was added to a larger flask. This was repeated until acquiring a dilution series ranging between 0,05 mg/ml and 0,003125 mg/ml, as can be seen in figure 14A. The absorbance was measured at 246 nm (peak absorbance for Budesonide, see figure 14B) using Varian Cary 50 Bio UV-Visible Spectrophotometer (UV-vis). Due to the limitations of the UV spectrometer, dilutions resulting in absorption higher than 2 was not used.

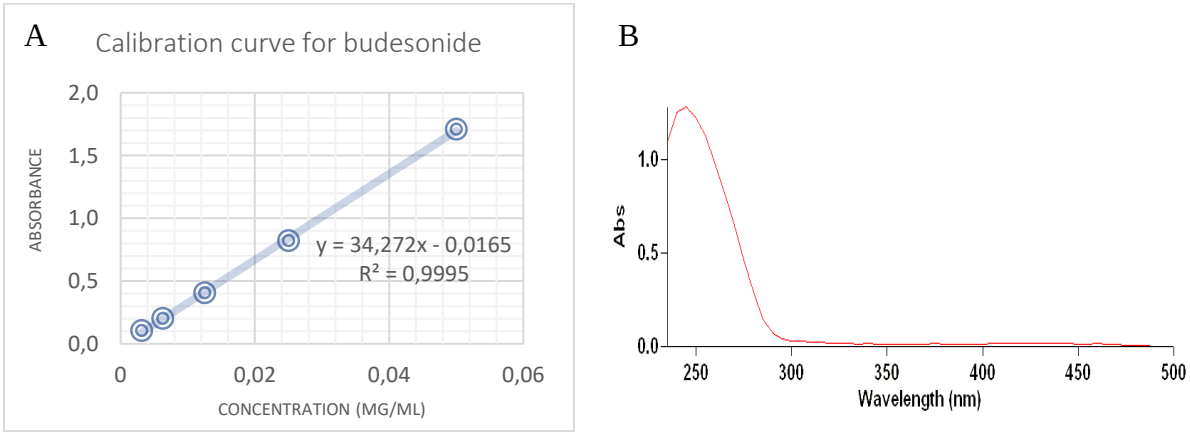

Figure 14: In A, a calibration curve for budesonide measured at 246 nm. In B, absorption curve for budesonide using the 0,025 mg/ml solution.

To determine a suitable wavelength for studying budesonide content an absorption spectrum was obtained using the 0,025 mg/ml solution (one of the solutions created for the calibration curve described above). The result can be seen in figure 14B. The highest absorption occurred around 240-250 nm while after 300 nm there is very low absorption. This information was later used to confirm the wavelengths chosen for the spectrometer.

3.4 Homogeneity

To study the homogeneity of the budesonide content in the fabricated formulation a total of six samples were taken from each batch. The sample size was of order 20-40 mg using a precision scale and diluted in 30 ml of EtOH:H2O using a dispensette. In order for the formula to be dissolved before measuring, the conical flask was placed on a rotating table for 15 minutes and were visually examined before measurements. For the measurements, Varian Cary 50 Bio UV-Visible Spectrophotometer and the computer program advanced reads, were used. The solution was poured into a cuvette (Hellma Analytic) with 10 mm light path, using the program Advanced Reads, two measurements were preformed simultaneously. Based on the information gained from the absorption curve in figure 14B and previous studies, a wavelength of 246 nm was chosen for maximum absorption of budesonide. To subtract any background noise, a measurement at 350 nm was also used. The net absorbance of the two was calculated directly using the program. Using the net absorbance, the API percentage in the solution could be calculated from the equation gained from the calibration curve in figure 14A.

$y = 34.272x - 0.0165$

For the amount of API in the formulations the following calculations were done. The known amount of formulation added to the 30 ml of EtOH:H2O is divided by 30 (ml). By dividing the concentration of budesonide acquired using the above equation, with the concentration of formula in the 30 ml of solution with each other, the result being the percentage of API in the formulation.

The methodology was evaluated after performance due to high RSD on some batches. The first method used weighing boats made out of plastic and relied on the accuracy of the dispensette. During the measurements plastic gloves were used. To reach a lower RSD (<5%) weighing boats made of metal was used instead as well as differential weighing and weighing the liquid. A comparison between the results when using a scale with and without fundament and using or not using gloves was conducted to further investigate the high RSD.

3.5 Aerodynamic particle size distribution

3.5.1 Next generation impactor – NGI

To measure the fine particle fraction, fine particle dose and mass median aerodynamic diameter a Next Generation Impactor (NGI) was used. For the novelizer device, a flow of 80 l/min and 3 seconds inspiration is recommended and thus used. The correlated cut-off diameters for the stages can be found in table 7 below. The impactor consists of seven collection cups which traps particles based on size. Each of the smaller cups was coated with Brij 35 solution on order to prevent bounce. For the small cups, 0.5 ml of Brij 35 solution was used, while the two bigger, 1 ml was applied to achieve the same coverage. An addition of 15 ml of internal standard (IS) solution was added to the pre-separator. The NGI was connected to a trig box that controlled the flow. To capture budesonide particles finer than the collection stages, a filter (Airlife, Bacterial/Viral filter, 303EU) was connected between the trigbox and the NGI. The set up was conducted in accordance to the European Pharmacopoeia.

Table 7. Table presenting the cut-off diameters of the NGI when operating at a flow of 80 lpm.

Stages	Cut-off diameters (µm)
1	11.3
2	6.9
3	3.8
4	2.4
5	1.45
6	0.81
7	0.46
MOC	0.28
Filter	0.10

From each inhaler two replicate NGI measurements were made, each with six doses drawn from the inhaler to create an average. To dissolve the budesonide an IS solution was added to each stage (15 ml), including the throat, pre-separator and filter. The internal standard solution contains equal parts ethanol and water (to dissolve the budesonide), with a known amount of propagin in order to calculate the amount of budesonide in relation to this known amount. To ensure the budesonide on each stage has become dissolved before measurements, the samples were placed on a rotating table for 10 minutes.

The NGI was also used to perform delivered dose measurements. Six separate doses were measured, each into a new filter as can be seen in figure 15.

The samples were analyzed using high performance liquid chromatography (HPLC), the settings used are included in appendix 1.

Each inhaler was weighed before and after measurements to acquire weight per actuated dose.

Figure 15. Picture of the setup used when performing delivered dose measurements.

Figure 16. Picture of the NGI setup used.

3.5.2 Andersen cascade impactor - ACI

Using an Andersen impactor (ACI) the fine particle fraction, fine particle dose and mass median aerodynamic diameter was measured. In order to achieve a flow rate of 80 l/min the seventh stage of the setup had to be removed, instead an additional filter stage was inserted. The cut off diameters of the ACI operating at a flow rate of 80 l/min can be found in table 8. Each stage had a collection plate which was coated using Brij 35 solution (approximately 0.5 ml). On the last filter stage, a filter paper fastened with a rubber band was added, this to collect any particles finer than the last collection stage. The purpose of the Brij solution, as in the NGI, is to prevent bouncing of particles from one collection stage to another, and thus creating a misleading result.

The measurements were performed in duplicates where each measurement consists of six doses drawn from the inhaler. Before and after each measurement the inhalers were weighed to retrieve weight per dose data.

On each collection plate, throat and pre-seperator 15 ml of IS (50:50 H_20/EtOH) solution was added using a dispensette. To ensure dissolution of the API, the parts were placed on a rotating table for 15 minutes. Samples were than drawn using pipettes and poured into a cuvette (Hellma Analytic) with 10 mm light path. Using the program Advanced reads, two measurements were preformed simultaneously, one for the absorption of budesonide at 246 nm and one measurement at 350 nm (to subtract any background noise). From the net absorbance, the API content could be calculated from the equation described previously (in 3.4 Homogeneity).

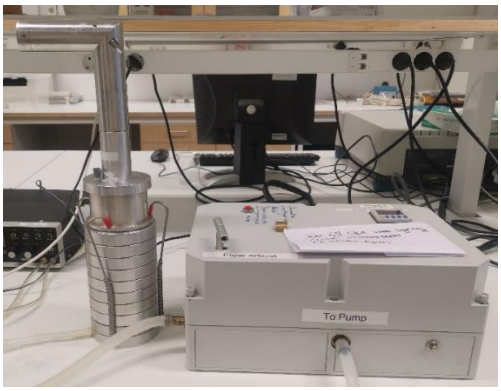

Figure 17. Picture of the Andersen cascade impactor setup used to make the measurements. The seventh stage is removed in the picture and replaced with an extra filter stage.

Table 8. Table presenting the cut-off diameters of the ACI when operating at a flow of 80 lpm.

Stages	Cut-off diameters (µm)
0	7.57
1	4.88
2	3.95
3	2.78
4	1.77
5	0.93
6	0.59

3.6 Laser diffraction particle size analyzing

3.6.1 Malvern Mastersizer

Using the dry Malvern Mastersizer S, the geometric size distribution could be determined for the different formulations using light diffraction. When performing the measurements, a small amount of formula was placed on the feed plate. The machine was set on a jet pressure of seven, this proved optimal to achieve the best measurements, and a feed rate of around three in order to achieve a suitable rate for the measurement. For each run a triplicate measurement was performed and an average and standard deviation calculated (if the RSD was very high additional measurements were made). Due to the occurrence of "ghost peaks", a setting for compressed mode was used, which extinguishes the ghost peaks. These could be due to aggregated formed in the formula, which would highly impact the average and distribution of the measurements and where thus discharged.

3.7 Imaging of surface and morphology

To examine the morphology and surface of the manufactured product a scanning electron microscope (SEM) was used. Using adhesive carbon tape, the powder was distributed thinly onto metal stubs and then sputtered with Au/Pd to avoid charging effects in the material. The carrier gas used during the sputtering was argon gas. For the measurements a voltage of 5 kV was used to accelerate the electrons, making the working distance frequently used 14.9 mm. Three different magnifications were used when studying the samples; 50x, 500x and 300x magnification. Two different detectors were used for imaging, the SEI (upper secondary electron in-lens) and LEI (Lower secondary electron).

Figure 18. Picture of the SEM microscope used to examine the samples.

Figure 19: Picture of the machine used to sputter the samples.

Figure 20. Picture of the metal stubs after the powder has been sputtered.

3.8 Storage conditions

After manufacturing the powders, a study regarding the effects of storage was conducted. The following samples were stored in ambient conditions respectively placed in a Desiccator with silica gel, see table 9. The reason being to lower the moisture content of the powder. The gel is known to keep a humidity level of below 5-10 %.

The manufactured formulations were left in storage for two months. The bulk density of the powders was measured before and after storage.

Table 9. List of the batches placed in the desiccator and which were kept in ambient storage.

Batch name	Ambient storage conditions	Desiccator
T-N-10	X	X
T-N-30	X	X
T-N-60	X	X
T-C-10	X	X
T-C-30	X	X
T-C-60	X	X
T-C	X	X
D-C-L-T-10	X	
D-C-L-T-30	X	
D-C-L-T-60	X	
D-N-L-3	X	
D-N-L-6	X	
D-N-L-9	X	
D-N-H-3	X	X
D-N-H-6	X	X
D-N-H-9	X	X
D-C-L	X	
D-C-L-3	X	
D-C-L-6	X	
D-C-L-9	X	
D-C-H-3	X	X
D-C-H-6	X	X
D-C-H-9	X	X
D-C	X	X

4 Results and discussions

4.1 Mixing

In this section, the mixing of the manufactured formulations will be presented and discussed. This will be discussed in terms of budesonide content, homogeneity and a delivered dose study.

Budesonide content

The budesonide content of the batches manufactured using the Turbula mixer was determined using the calibration curve previously presented in figure 14 (Data can be found in appendix 4). From this it can be seen that the mean budesonide level maintains a more stable level for the coated batches, while the naked formulation exhibits a small decline with increased mixing time, as can be seen in figure 21.

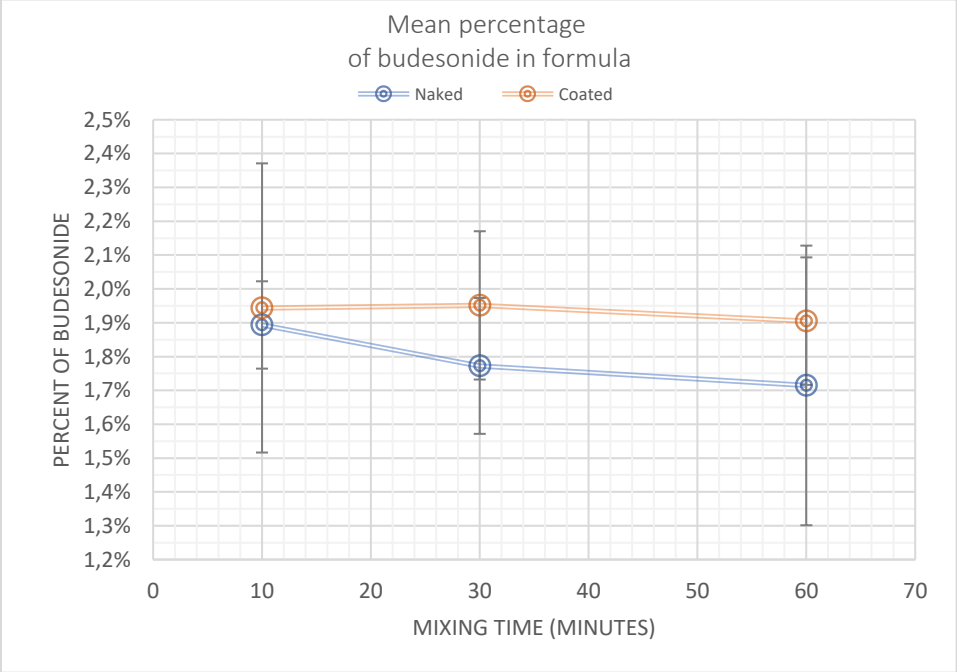

Figure 21. Diagram showing the mean percentage of budesonide in each of the Turbula batches.

As can be noted, the batches T-N-60 and T-C-10 displays a relatively large standard deviation, why it is difficult to make any conclusions regarding this trend.

Homogeneity

By investigating the standard deviation (SD) and the relative standard deviation (RSD) of the budesonide in the powder, it is possible to gain information regarding the homogeneity, i.e., how well the budesonide has been distributed on the carriers. This measurement becomes important since it is desirable to obtain an equal amount of budesonide from each actuated dose when using an inhaler. From figure 21, it is seen that the largest standard deviation, can be found in formula T-N-60 and T-C-10. This indicates that these doses do not display a good uniformity regarding budesonide distribution, which would be problematic if the formulation

were to use for treatment. During the measurements, some fluctuations of the scale was noticed and thus further investigations regarding the formulations and the scale was performed, as can be seen in figure 22.

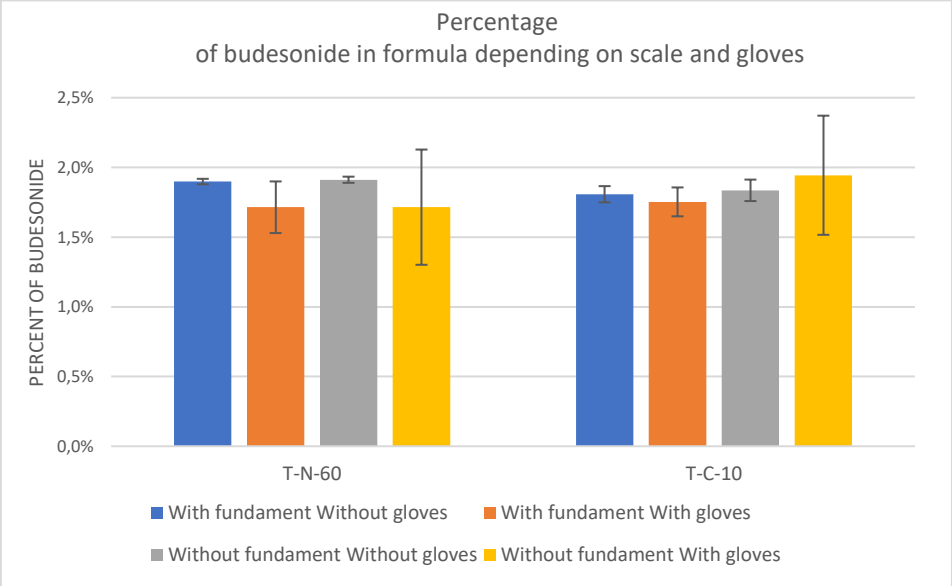

Figure 22. The amount of budesonide and SD at different weighing conditions for T-N-60 and T-C-10.

From figure 22 it can be seen that the amounts when weighing differs to some extent depending on whether the scale is placed on fundaments or not and whether gloves were used when handling the powder and scale. The largest standard deviation and thus inhomogeneity can be found when weighing the powder on a scale not situated on a fundament while using gloves. The second largest is when weighing on a scale on fundament while using gloves. Best results were obtained when not using gloves and having the scale standing on a fundament, closely followed by not wearing gloves and not having the scale on a fundament. A reason for this could be electrostatic effects which are induced due to the usage of plastic gloves. Some electrostatic effects were observed when handling the powder, as can be seen in figure 23.

Figure 23. Formulation observed exhibiting electrostatic effects when handled with a spatula.

The study shows much higher reliability of the measurements when not using gloves, as seen in figure 22. Where, in addition to having a low SD, the mean budesonide content lies very close to each other (”with fundament without gloves” and “with fundament with gloves”) compared to the measurements using gloves.

From this it could be assumed that the batches are uniform in budesonide content and that the high values in SD originated from the measuring technique initially used.

Delivered dose study

To further investigate the uniformity of the powders, the two batches T-N-6o and T-C-10 (with highest SD from the homogeneity assessment) were subjected to a delivered dose study, of which the results can be found in table 10. As can be seen, the batches display a low RSD, below 5 %, which implies high uniformity. Since these batches were the ones which originally displayed the poorest dose uniformity, which could be refuted, it can be assumed that all other batches are of equal or superior grade. This would also be true for the Diosna manufactured batches since it has been shown that the Diosna high shear mixer delivers better dose uniformity compared to the Turbula low shear mixer (Kaialy, 2016). Which is why those batches are not investigated for uniformity in this study.

Table 10. Delivered dose performance of T-C-10 and T-N-30, 6 actuations per batch.

Batch	T-C-10	T-N-60
Mean (µg Bude/ act)	265,67	211,67
SD (µg)	12,91	9,45
RSD%	4,86	4,46

Mixing temperature

The temperature increase occurring due to mixing is presented in figure 24 and 25 below. For the Turbula mixed batches, the first measurement for the naked formulation was forgotten. For the second measurement a decrease in temperature can be seen, this is most likely due to a decrease in room temperature during the mixing procedure rather than a decrease due to the mixing. It can be assumed that the increase was not significant after 10 and 30 minutes of mixing, especially since the sieving step after half the mixing time gives the powder opportunity to cool. For the coated batches manufactured using the Turbula, an almost linear increase can be linked to the mixing time, where after 60 minutes of mixing there was a temperature increase of almost 4° Celsius, as can be seen in figure 24.

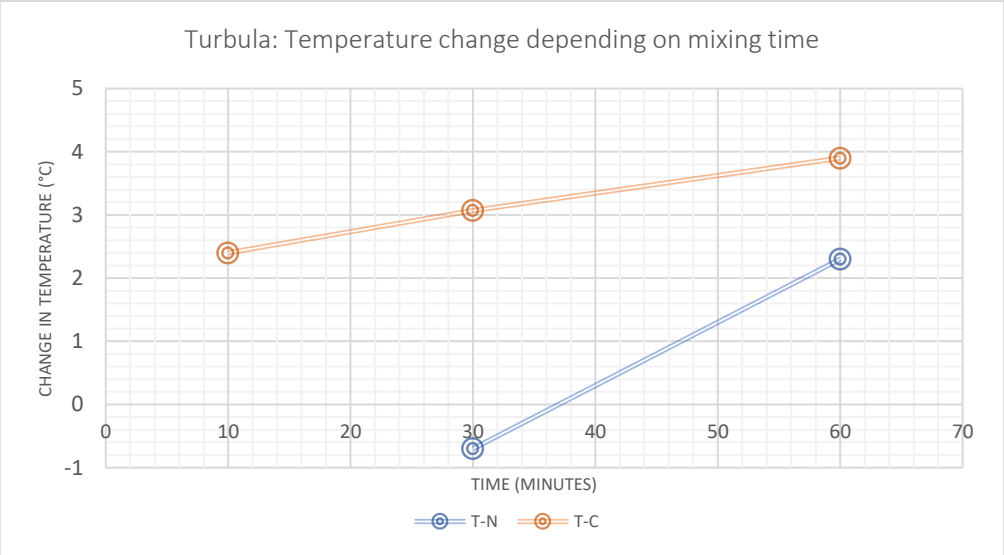

Figure 24. Change in temperature after mixing plotted against the mixing time in minutes. Temperature was measured 2 minutes after mixing ceased.

The Diosna manufactured batches displayed a higher temperature increase on average compared to the Turbula mixed batches. In figure 25 below, it can be seen that the batches mixed on low speed (D-N-L and D-C-L) reaches an increase of around 4 ° Celsius, which was also the highest recorded temperature increase for the Turbula batches. As with the Turbula mixed batches an initial higher temperature of the coated powders can be seen. Though for the low speed formulations, the naked powders exhibit a higher increase for the longer mixing times. For the high mixing speed powders, the coated batches continue to demonstrate a higher heat development compared to their counterparts without coating. A heat development of 7.5 ° Celsius was recorded for the D-C-H-9 batch.

One explanation to why the coated batches yield a larger increase in temperature could be the initial coating step (4 minutes, low speed for Diosna and 2x15 minutes for Turbula). This initial mixing most likely leads to a higher initial starting temperature of the powders which could also explain why D-N-L starts with a lower increase compared to D-C-L, but later displays a steeper increase. For the high speed batches a similar temperature profile is displayed.

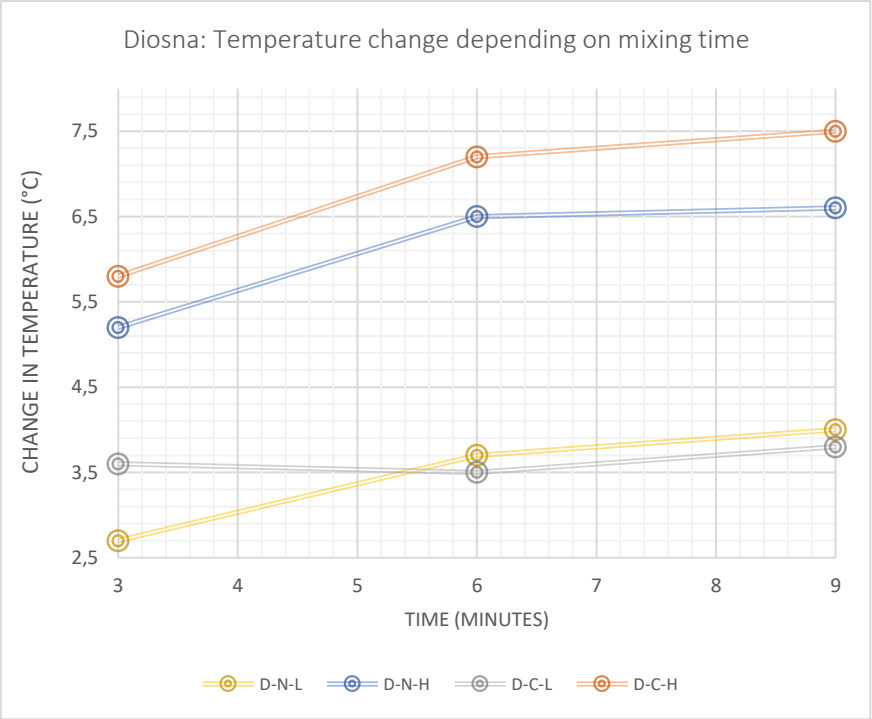

Figure 25. Change in temperature after mixing plotted against the mixing time in minutes. Temperature was measured 1 minute after mixing ceased.

4.2 Aerodynamic particle size distribution

Note that in this chapter "delivered dose" refers to the summation of Budesonide deposited in the NGI (sum NGI) and not the separate delivered dose study described in the methodology.

4.2.1 Turbula batches

Data can be found in appendix 2.

Mass median aerodynamic diameter

Below the mass median aerodynamic diameter is plotted for the Turbula mixed batches (figure 26), calculated from the measurements performed using the NGI. As can be seen the MMAD for coated and the naked batches follow different trends. The MMAD of the naked batches are only to a very small extent affected by the mixing time in the Turbula, see figure 26. From the diagrams it can also be seen that the biggest change occurred during the initial mixing, since there is a small increase in size between 10 and 30 minutes of mixing, while the difference between 30 and 60 minutes of mixing is negligible. Overall, the naked batches display a steady MMAD while the coated batches display a decline.

For the coated particles, the initial size measured after 10 minutes of mixing (T-C-10) can be seen to be marginally larger than the naked batch mixed the same amount of time (T-N-10). However as can be seen in figure 26, the batches with 30 respectively 60 minutes of mixing display significant declining in MMAD values, which are much smaller compared to the naked formulation. This could possibly be due to other deposition mechanisms (of the API) which facilitates a higher release when using MgSt compared to direct deposition on the carrier. This

could indicate that a longer mixing time for the Turbula mixed formulas is necessary to reap the benefits of using a coating agent.

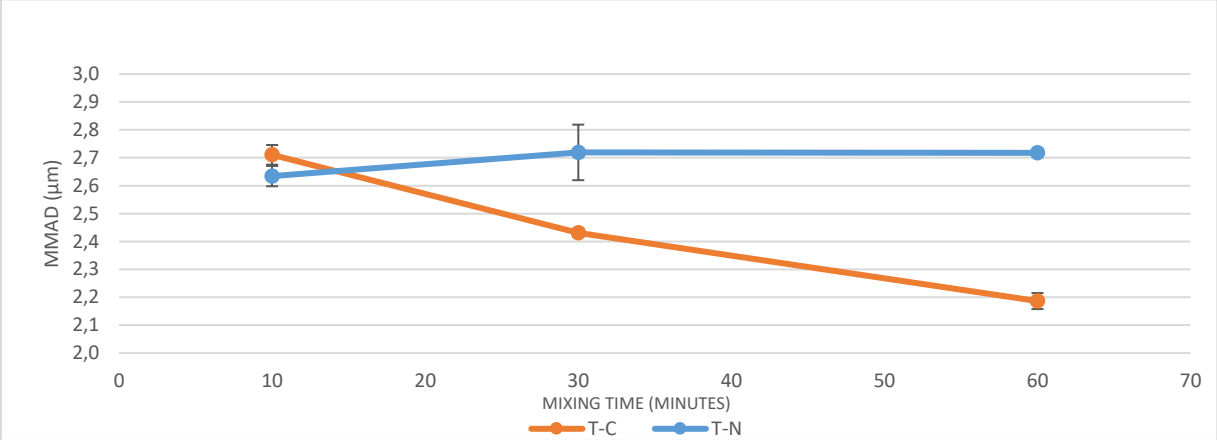

Figure 26. MMAD can be seen for the coated (T-C) and the naked (T-N) batches is plotted beside each other against the mixing time in minutes.

Budesonide amount in each step, fine particle fraction and fine particle dose

Data was calculated from the measurements performed using the NGI setup. The Budesonide amount per actuation for each stage of the NGI is presented below. Each stage has a cut-off diameter which hinders larger particles from passing, resulting in a particle distribution by aerodynamic size. All measurements were performed using the same flowrate and time in the Novolizer inhaler.

As can be seen in figure 27 below, there is an overall higher deposition of budesonide from the coated batches compared to the naked batches. A possible explanation for this could be that the addition of MgSt leads to a better flowability of the powder and thus a higher dose being actuated. This is also evident from the figure 28, where it is shown that the coated batches display a higher total weight per dose and thus also a higher delivered dose of budesonide compared to the naked batches. From the figure 27 showing the amount per stage, it is also evident that there is a higher deposition in the inlet when actuating the coated particles, compared to the naked formulation. This however is only true for the batch T-C-10 and T-C-30, while T-C-60 display a similar amount as the naked formulations. For both the naked and the coated particles there is a decrease of deposition in the inlet connected to a longer mixing time, this is more evident in the coated batches compared to the naked. This could indicate a better release of budesonide linked to longer mixing times, since this would result in less budesonide not being separated from the carrier and thus impacting the inlet/throat. On the stages 1 to 7, there is also an increase of budesonide linked to longer mixing times. Stage 2 has a cut-off of 6,9 µm and stage 3 of 3,8 µm, meaning that particles <5µm will begin to deposit on stage 2 and on the finer stages thereafter, making these important in order to determine the amount which would reach the lungs in vivo.

From the diagram, it is shown that the naked batches display roughly the same deposition regardless of mixing time (only a slight increase can be noted) and this amount is comparable

with that of T-C-10. For the coated batches a direct link between mixing time and deposition amount in these stages can be assumed. The coated batches display a higher total delivered dose and weight per dose compared to that of the naked batches. These measurements seem to be consistent and not depend on mixing time. This would indicate that the higher deposition on the finer stages (and lower results in the inlet) occurring for longer mixing times are due to better separation of the API from the carrier.

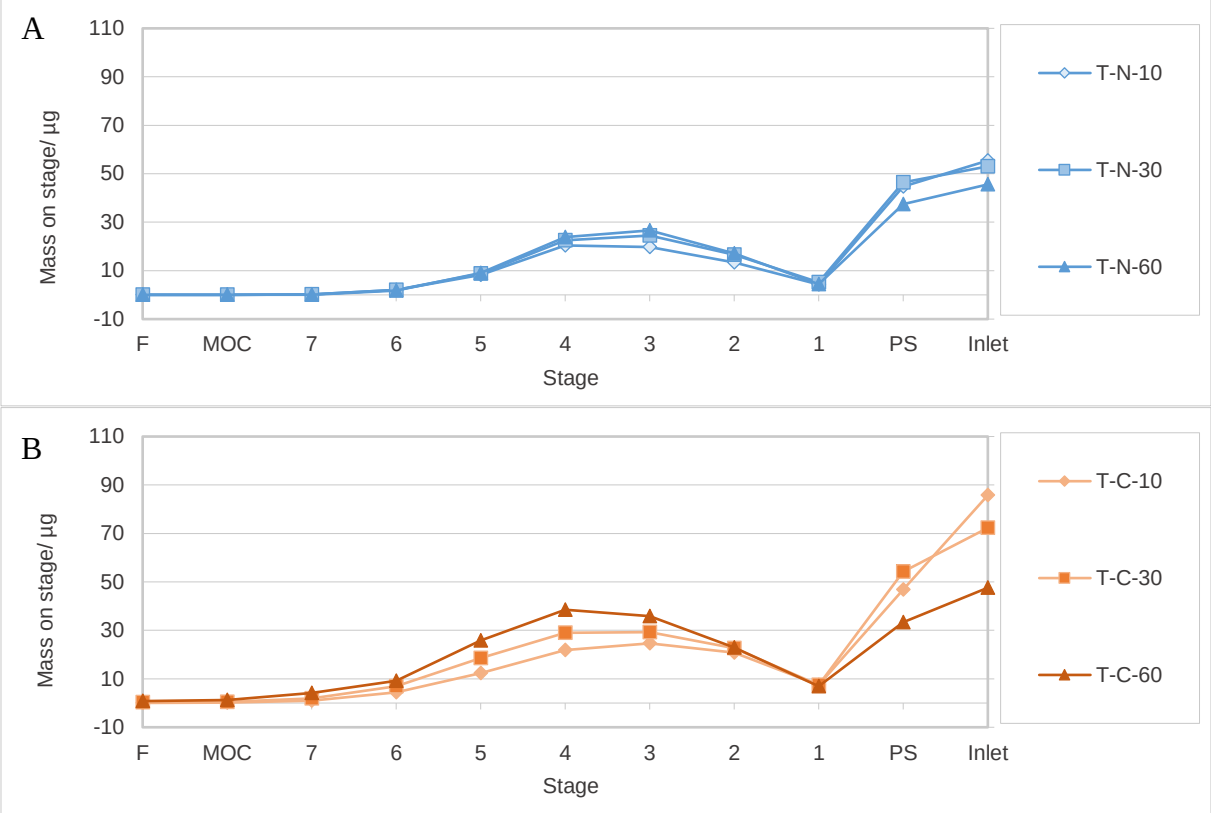

Figure 27. A, showing the deposited amount of Budesonide on each stage in the NGI when testing the naked Turbula batches. B, showing the deposited amount of Budesonide on each stage in the NGI when testing the coated Turbula batches.

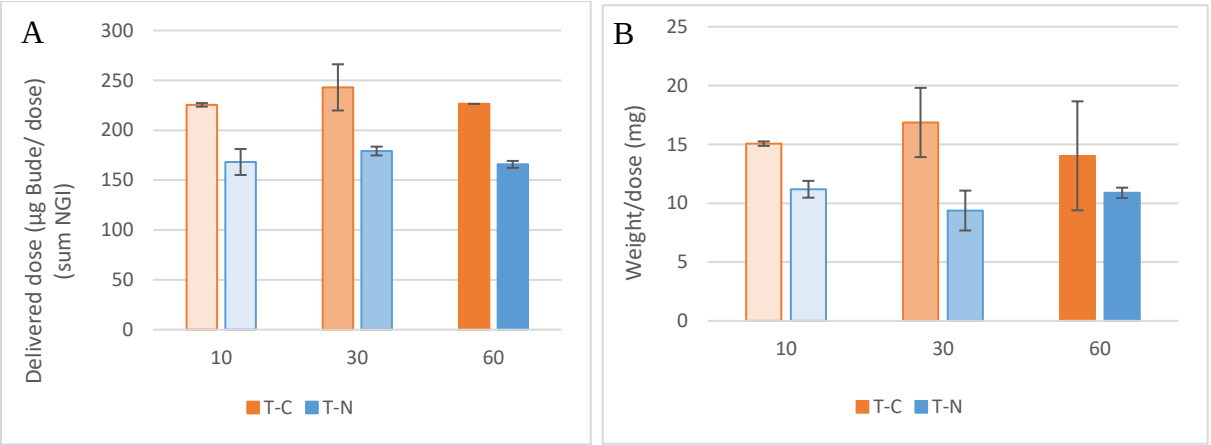

Figure 28. A, showing the delivered dose (=sum NGI) of Budesonide per actuation, for the Turbula mixed batches. B, showing total weight per actuated dose, for the Turbula mixed batches.

As could be seen in figure 27, with budesonide amount per stage, it is further supported that the amount of fine particles (i.e. budesonide available for absorption) is increased with coated carriers compared to naked particles. In figure 29, it is seen that there is an overall higher fine

particle dose in the coated batches, which can be connected to the higher delivered dose and weight per dose of the coated batches. These also display a linear increase with mixing time as can be seen in figure 29. However, there is only a slight increase in FPD with longer mixing time in the naked batches.

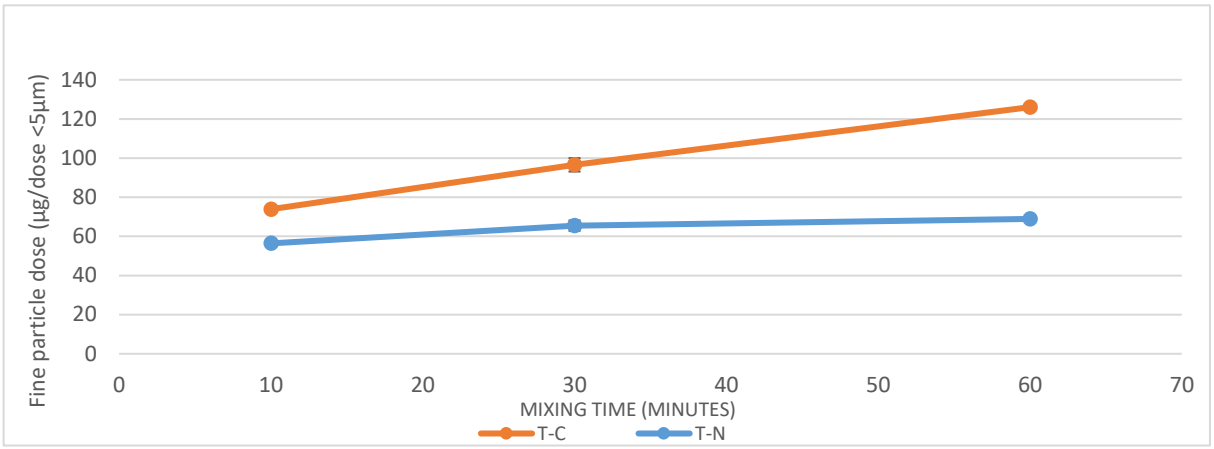

Figure 29. Fine particle dose (amount of particles/budesonide smaller than 5 µm) for the naked and coated batches mixed in the Turbula. FPD for the coated batches (T-C) and the naked (T-N) is plotted beside each other against the mixing time in minutes.

From figure 30, it is clear that the fine particle fraction of T-C-10 and T-N-10 is equal to each other. This means that even though the coated batches have been shown to actuate a higher dose, the fraction of fine particles is the same as for the naked batch when the mixing time is short.

However, there is an increase in FPF both for the naked and the coated batches, though the increase of FPF with longer mixing time is far more rapid in the coated batches. This indicates that the higher FPF is not only due to the larger actuated dose, but linked to the mixing time of the formulations. From the figure it is evident that T-C-60 displayes the highest FPF of somewhere around 55 %, this can be compared to the highest reached value of the naked formulations, only achieving slightly above 40 %. Since the increase does not seem to level out within the mixing times examined, it seems that even longer mixing times would continue to increase the FPF.

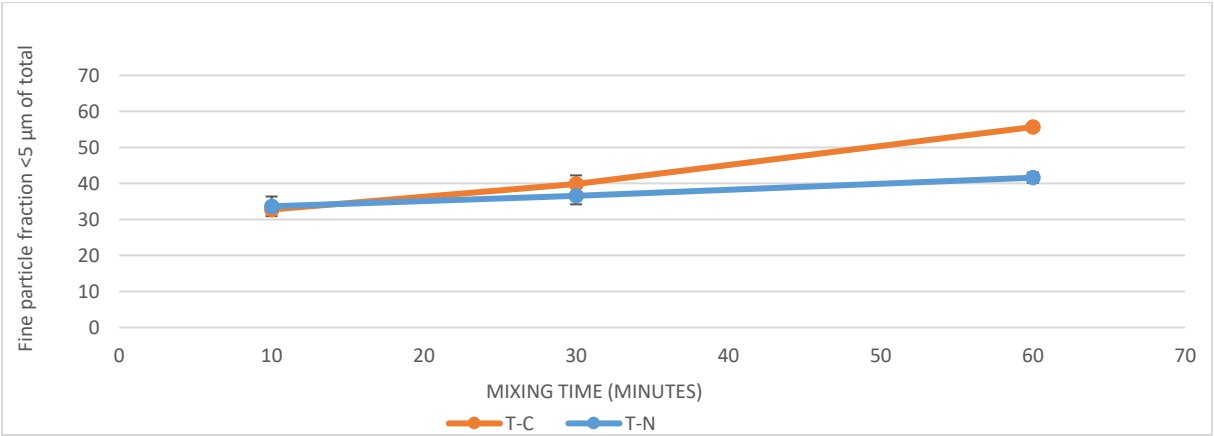

Figure 30. Fine particle fraction (the fraction of particles/budesonide smaller than 5µm) for the naked and coated batches mixed in the Turbula. FPF for the coated batches (T-C) and the naked (T-N) is plotted beside each other against the mixing time in minutes.

4.2.2 Diosna batches

Data can be found in appendix 2.

Mass median aerodynamic diameter

Below, the mass median aerodynamic diameters are plotted for the Diosna mixed batches calculated from the measurements performed using the NGI. As can be seen the MMAD for the coated and the naked batch differs. All the batches display roughly the same MMAD after three minutes of mixing. For the longer mixing times it is shown that the MMAD of the naked batches increase compared to the first batch with short mixing time, however there no difference between 6 and 9 minutes of mixing. For the coated batches, the MMAD stays roughly the same and there is very little difference between the batches mixed at high respectively low speed. D-N-H increases roughly 1 µm in diameter which is a far bigger change compared to the coated batches. This increase of MMAD for 6 and 9 minutes of mixing is quite surprising and was not anticipated.

For the coated batches, there is no such increase with mixing time, instead a very slight decrease can be noted. A possible explanation to this could be that MgSt facilitates the release of the API, thus lowering the mass median aerodynamic diameter.

When manufacturing the batch D-N-H-9, the formulation had to be scraped off the walls of the mixing bowl and suggesting that the formulation is quite adhesive.

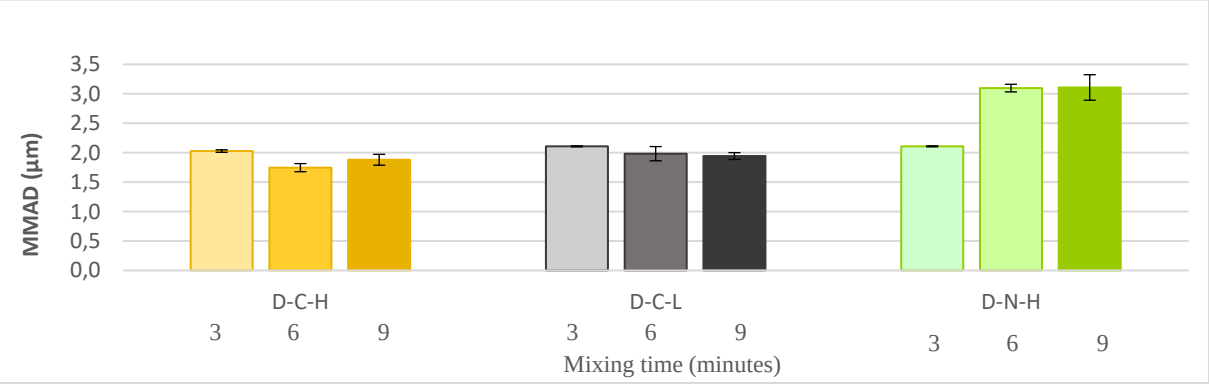

Figure 31.The MMAD based on the NGI measurements for the Diosna mixed batches are here plotted beside each other against the mixing time in minutes.

Mass on stages, fine particle fraction and fine particle dose

For the D-C-H batches in figure 32, one can see that the longer mixing times results in a higher amount deposited in the inlet and pre-separator of the NGI device, and a smaller amount being deposited on the finer stages (2-7). The batch D-C-H-3 shows the lowest amount deposited in the inlet and pre-separator and the highest in the steps finer than 5 µm. From the diagram it is worth noting that there seems to be a tendency towards bounce, since there is an increase in particles being collected in the filter stage. This could indicate that the measurements of the

previous stages also have been subjected to bounce, leading to some degree of uncertainty regarding the amounts.

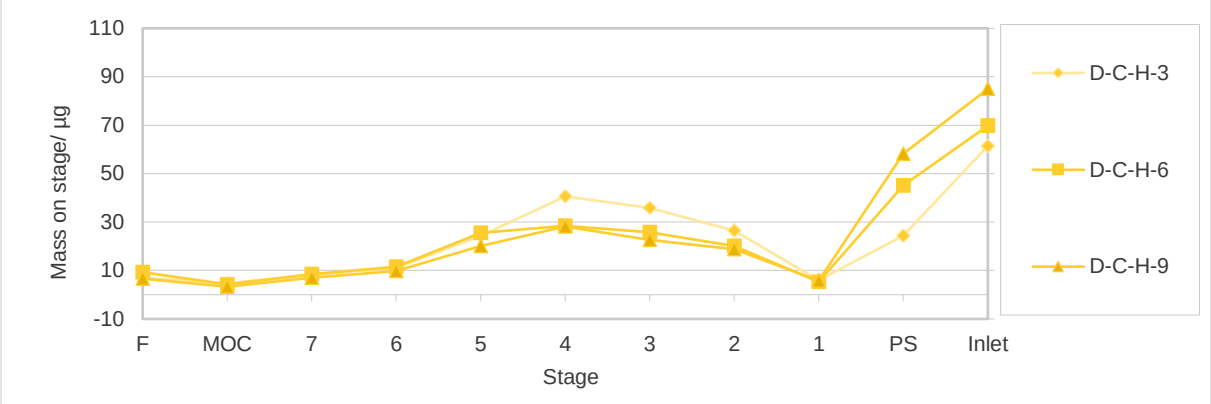

Figure 32. Diagram showing mass on stages for the coated, Diosna high speed mixed batches.

For the D-C-L batches in figure 33, the differences are not as prominent as for the batches mixed at high speed. These batches also display a tendency towards bounce.

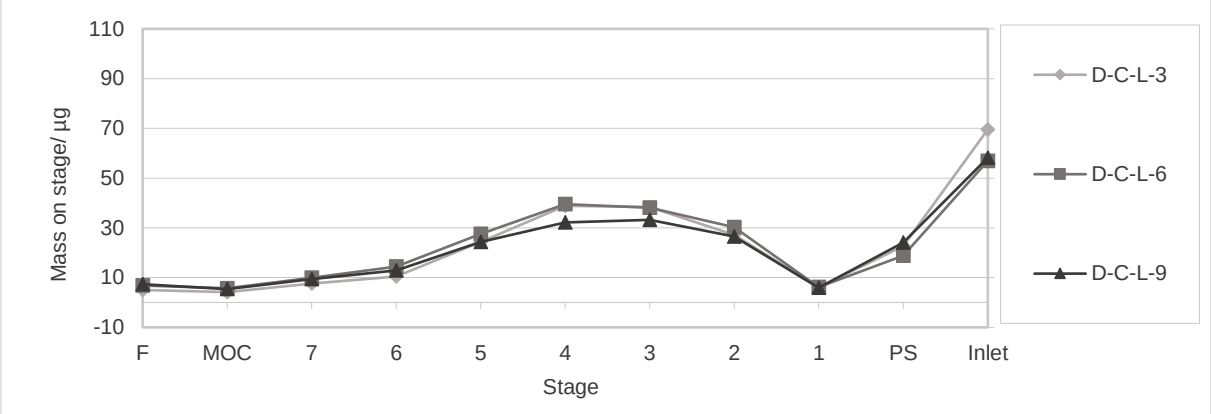

Figure 33. Diagram showing mass on stages for the coated, Diosna low speed mixed batches.

For the D-N-H batches displayed in figure 34, the results look different. D-N-H-9 had the lowest amount of budesonide deposited in the inlet, however this trend does not consist and for the finer stages it displays the lowest deposited amounts of the three batches (as have been seen with the corresponding coated batches). The highest amount deposited on stages (2-6) is the D-N-H-3 batch. Note that compared to the coated batches, there is an overall higher amount being deposited in the inlet and pre-seperator (PS), and a smaller amount on the finer stages of the NGI. For the naked batches, the filter stage shows zero deposition, indicating no bounce.

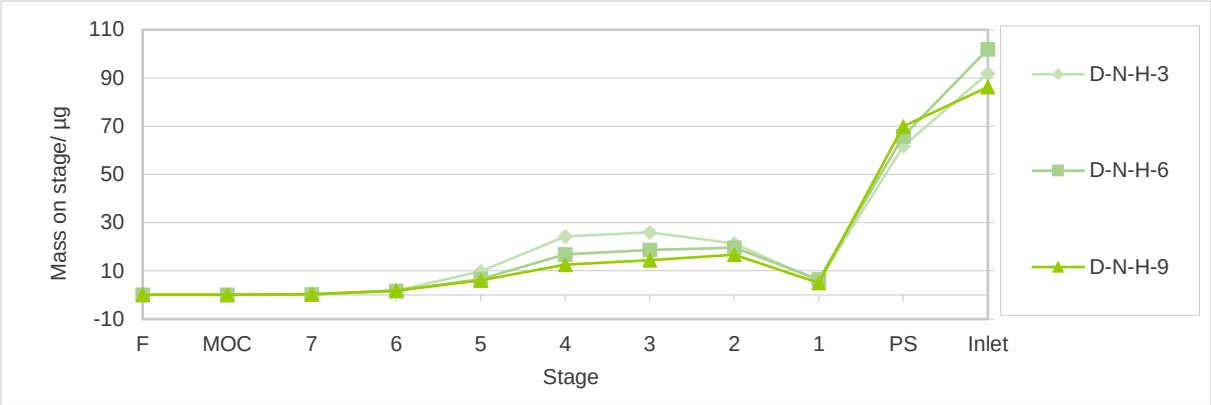

Figure 34. Diagram showing mass on stages for the naked, Diosna high speed mixed batches.

The weight per dose is roughly uniform as can be seen in figure 35, although somewhat lower for the naked formulations. For the delivered dose, the values are roughly the same for the batches, however the naked formulation seem to have a decrease in delivered dose correlating to longer mixing times.

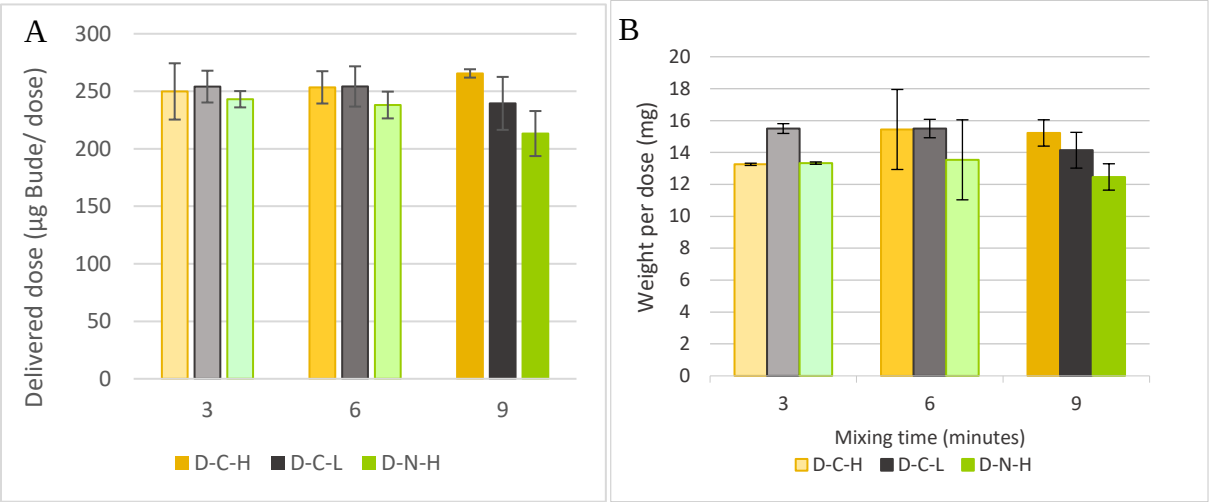

Figure 35. Diagram A displays the delivered dose (=sum NGI) of the Diosna mixed batches measured in the NGI. In B, the weight per dose of the Diosna manufactured batches is displayed.

To summarize the previous section, there is a significantly lower amount of fine budesonide in the naked formulations compared to the coated ones, as can also be seen in figure 36 displaying the FPD. The FPD för the D-N-H batches is notably smaller than for the coated batches. For the high speed mixed (D-C-H) there is a decrease in FPD with the longer mixing times, this is also true for the D-N-H batches. However the D-C-L batches display another tendency, where the values are mostly stable but a slight increase and decrease can be distinguished for 6 respectively 9 minutes of mixing.

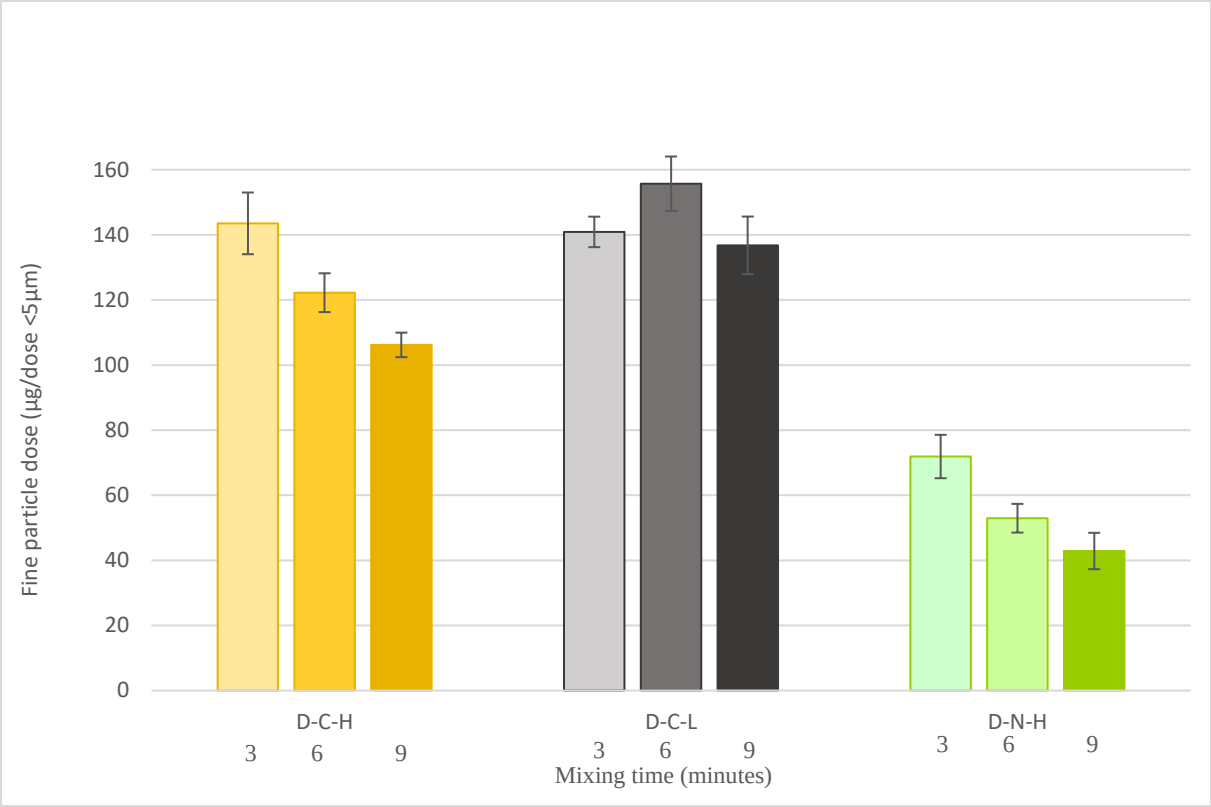

Figure 36. Fine particle dose (amount of particles/budesonide smaller than 5 µm) for the batches mixed in the Diosna.

The same trends can be seen in the FPF shown in figure 37. The FPF for the D-N-H batches is notably smaller than for the coated batches. For the high speed mixed (D-C-H) there is a decrease in FPF with the longer mixing times, this is also true for the D-N-H batches. However the D-C-L batches display another tendency, where the values are mostly stable but a slight increase and decrease can be distinguished for 6 respectively 9 minutes of mixing. The highest value being that of D-C-L-6, displaying a FPF of somewhat over 60 %. Comparing this to the naked batches, the difference is substantial, the highest FPF being only half that of the coated batches.

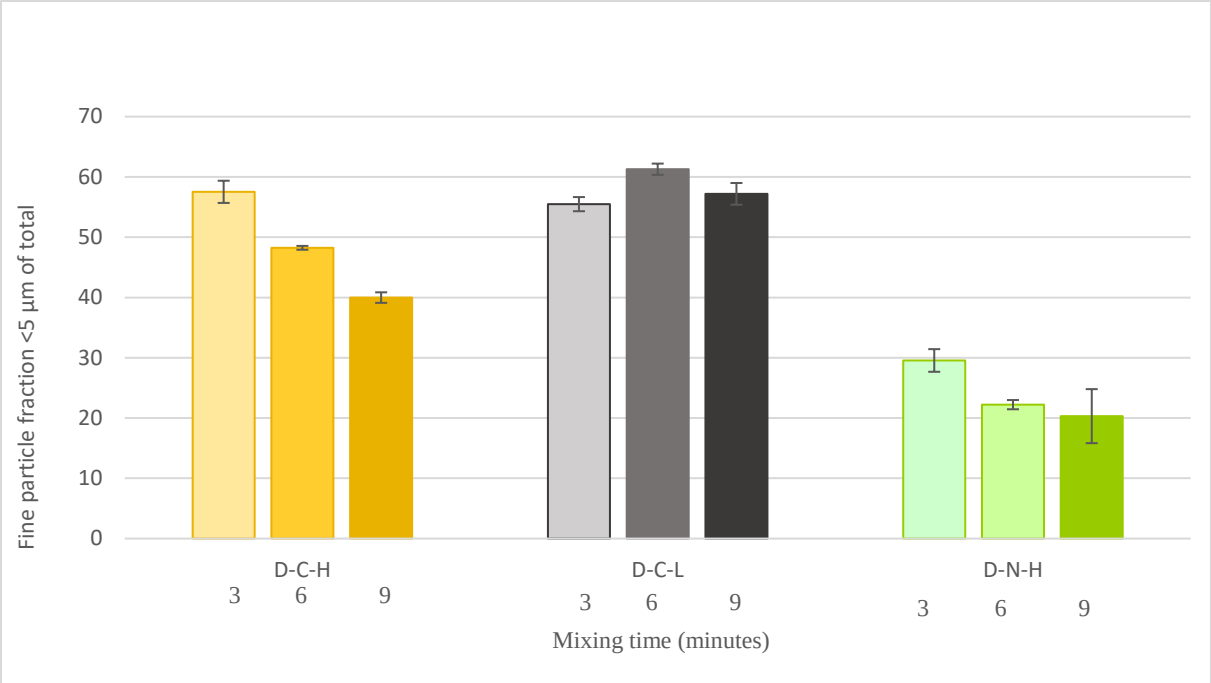

Figure 37. Fine particle fraction (fraction of particles/budesonide smaller than 5 µm) for the batches mixed in the Diosna.

4.2.3 Hybrid batches

Following paragraphs provides information regarding the batches D-C-L-T, which are hybrid batches where the coating is mixed in the Diosna while the API is added in the Turbula mixer. Data can be found in appendix 2.

Mass median aerodynamic diameter, delivered dose and weight per dose

For the hybrid batches, the highest MMAD (2,4 µm) is displayed after 10 minutes of mixing in the Turbula, see figure 38. Following that a decrease can be seen for mixing times of 30 and 60 minutes, roughly about 2,15 µm.

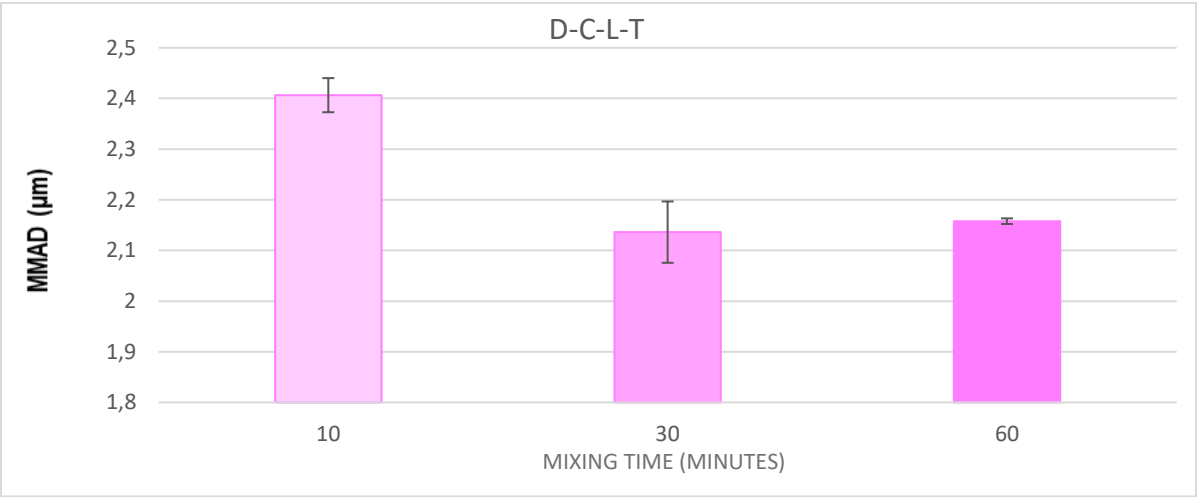

Figure 38. MMAD for D-C-L-T plotted against the mixing time in minutes.

The delivered dose is roughly the same for the different mixing times, about 270 µg. D-C-L-T-10 displays a somewhat lower weight per dose than the longer mixing times.

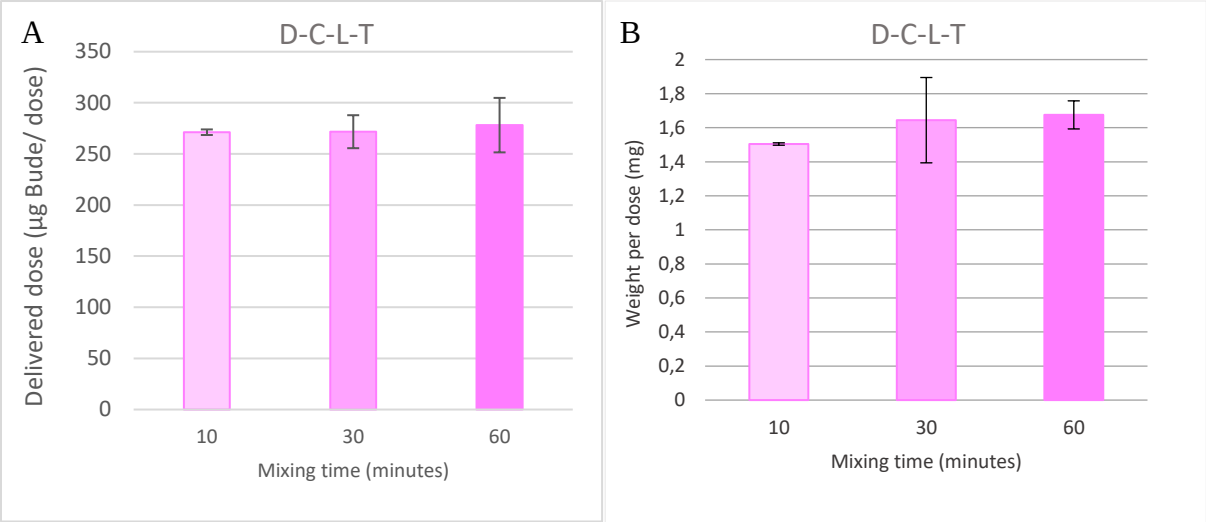

Figure 39. A showing the delivered dose of Budesonide per actuation for D-C-L-T plotted against the mixing time. B showing the weight per dose for D-C-L-T plotted against the mixing time.

Mass on stage, fine particle fraction and fine particle dose

In figure 40, it can be seen that the shorter mixing time of 10 minutes leads to the highest deposition in the inlet, while the deposition on the finer stages follows the same pattern as for D-C-L-T-30. The batch which has the best performance is the D-C-L-T-60, which has the lowest deposition in the inlet and pre-separator and the highest on the finer stages. This indicates that the API in batch D-C-L-T-60 is more successful in detaching from the carrier compared to the batches with shorter mixing time. This is also supported when looking at the FPF and FPD in figure 41, where it is shown that there is an increase in both dose and fraction when the batches are mixed for a longer duration.

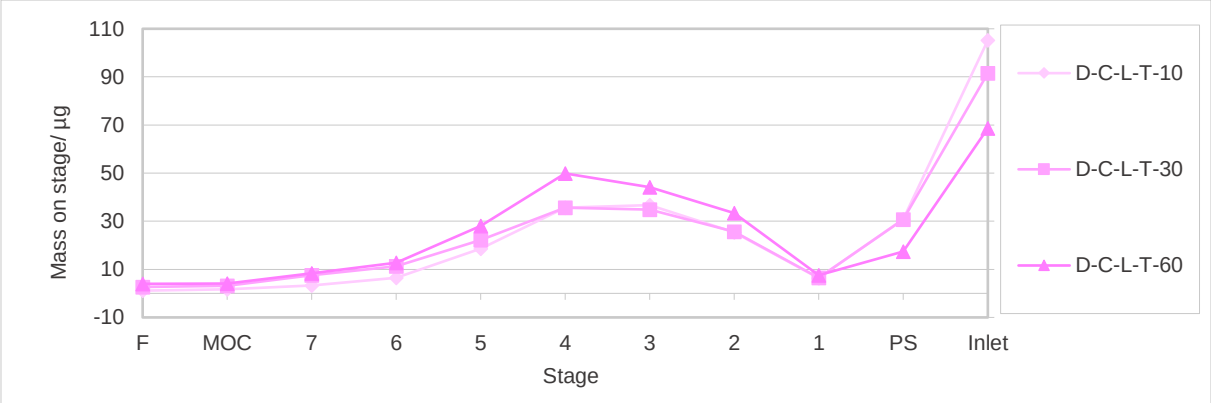

Figure 40. Mass on stage displayed for D-C-L-T batches, one plot per mixing time.

B

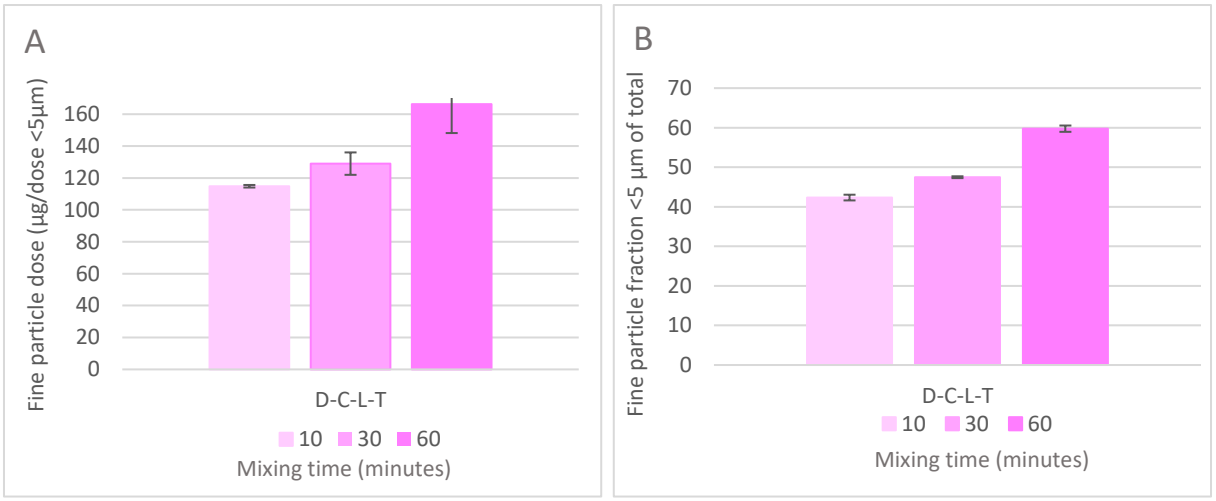

Figure 41. The fine particle dose of D-C-L-T is displayed in A, plotted against the mixing time. In B, the fine particle fraction is plotted against the mixing time for the D-C-L-T batches.

4.2.4 Andersson Cascade Impactor measurements

Due to limited access to the NGI, the naked batches mixed in the Diosna mixer were measured using the ACI. Worth noting is that the cut-off diameters of the stages of the ACI and NGI are not equal, thus the measurements below cannot be used to make a direct comparison with the batches measured using the NGI. To highlight this in the measurement, the result of D-N-H measured using NGI will be included in the figures below. Data can be found in appendix 3.

Mass median aerodynamic diameter

For the naked formulations mixed using the Diosna mixer there was only a slight difference in Mass Median Aerodynamic diameter between the batches. Comparing the powders mixed at low speed and high speed, D-N-L (low speed) displayed a slightly higher MMAD throughout the measurements. Worth noting is the difference due to measurement tool, it can be seen in figure 42 below that there is a difference between the ACI and NGI measurements of D-N-H.

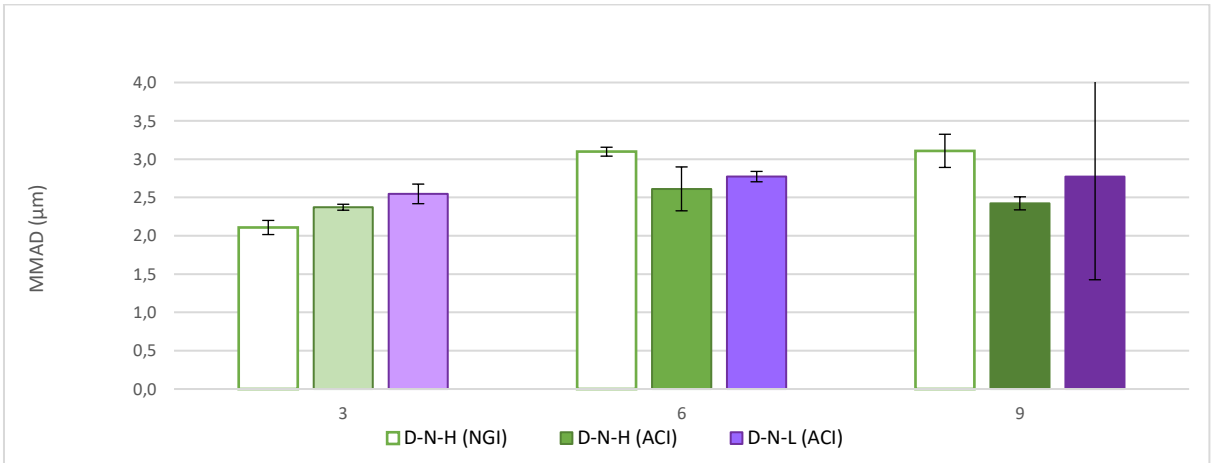

Figure 42. MMAD for D-N-H and D-N-L using the ACI, for reference D-N-H measured by NGI is included, plotted against the mixing time in minutes.

The delivered dose measurements (sum of deposited budesonide on the stages) show a higher D-N-H compared to D-N-L. Here the measurements made with NGI showed a lower dose compared to the ACI, as can be seen in figure 42.

Weight per dose were more or less uniform for the batches. Comparing the results to those when measuring using the NGI there is no significant difference.

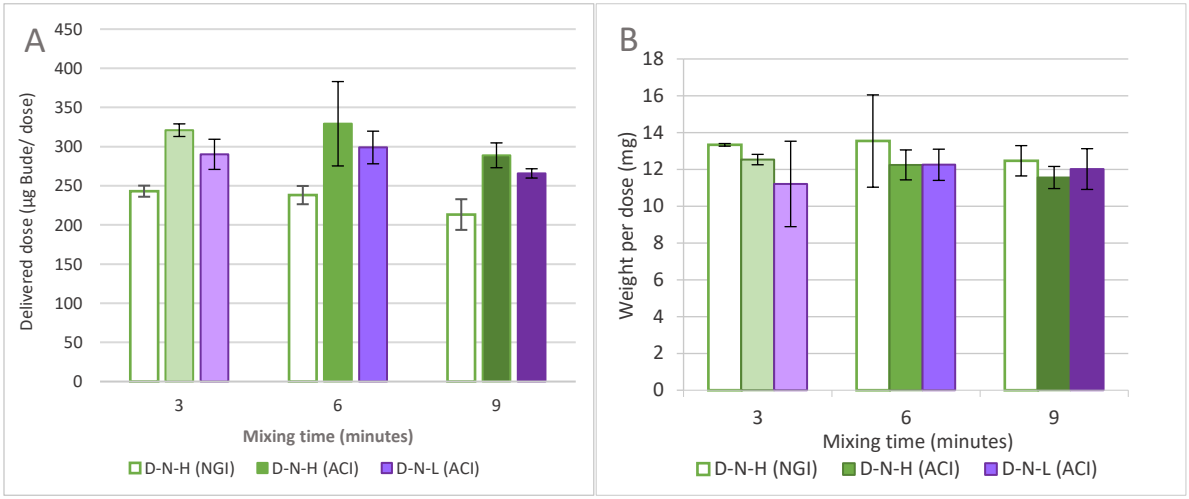

Figure 43. A showing the delivered dose of Budesonide per actuation for D-N-H and D-N-L plotted against the mixing time. B showing the weight per dose for D-N-H and D-N-L plotted against the mixing time. Data is collected from ACI measurements, NGI reference for D-N-H is included.

Mass on stage, fine particle fraction and fine particle dose

Below are the results from the measurements of D-N-H and D-N-L using the ACI. Comparing figure 44 with figure 34 (same batches measured using the NGI) it can be seen thar the ACI delivers higher values compared to the NGI and, probably due to the different cut-off diameters, there is shift to the left (towards the finer stages) compared to when measuring using the NGI. Thus, if comparing the results with those of the NGI it is important to keep this in mind. Comparing D-N-L and D-N-H, figure 44 and 45, it can be seen that D-N-H yield a higher deposition in the inlet. D-N-L displays slightly increased deposition on the finer stages compared to D-N-H.

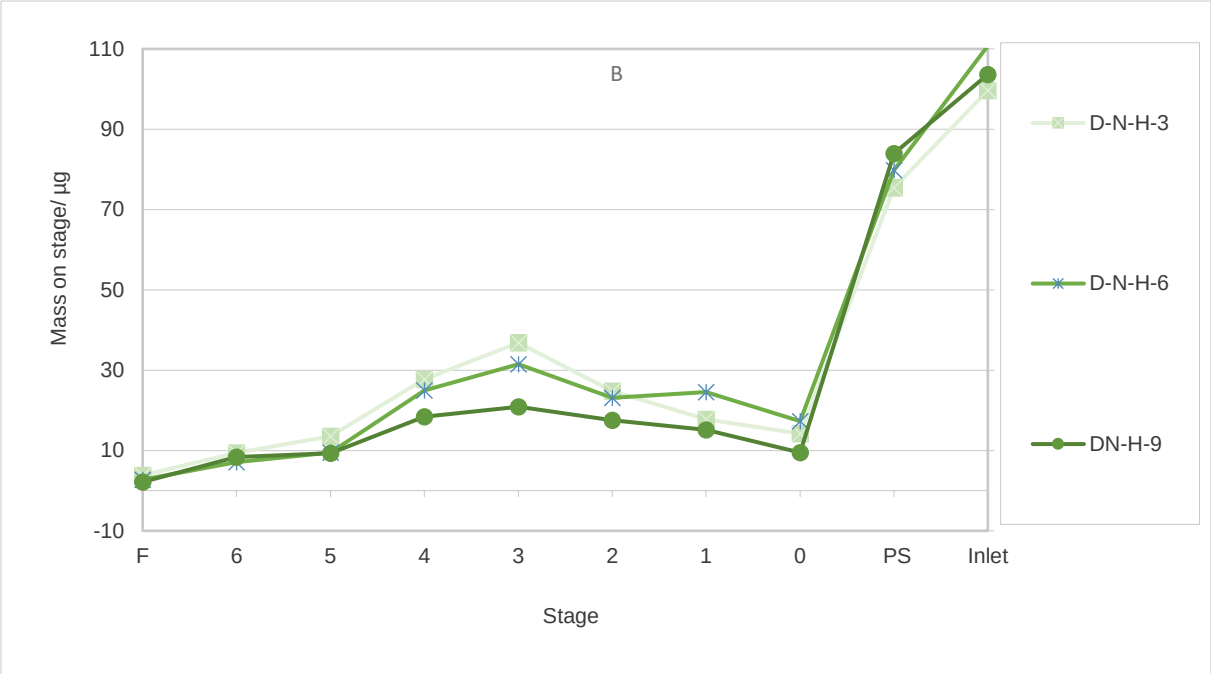

Figure 44. Mass on stage displayed for D-N-H batches measured using the ACI, one plot per mixing time.

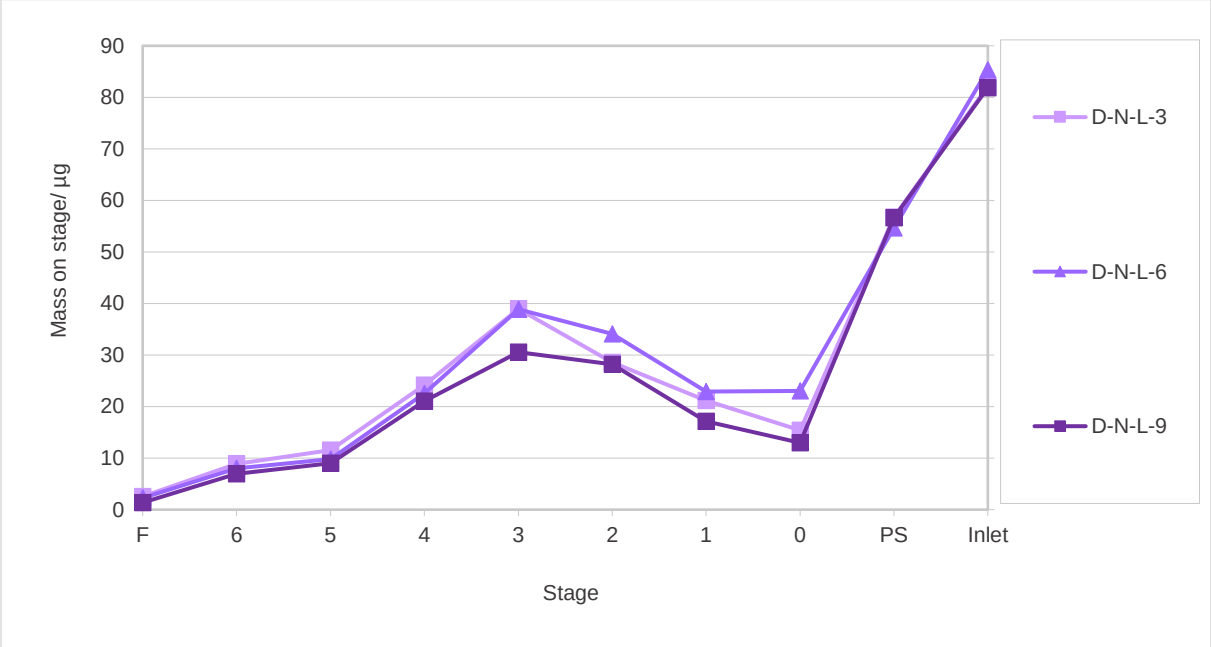

Figure 45. Mass on stage displayed for D-N-L batches measured using the ACI, one plot per mixing time.

The results for the fine particle dose and fine particle fraction can be seen in figure 46 below. Comparing the results of the ACI and NGI, it can be seen that the ACI yields higher values compared to the NGI. The reason is most likely the difference in cut-off diameter. This difference is quite surprising since both types of impactors are in use today.

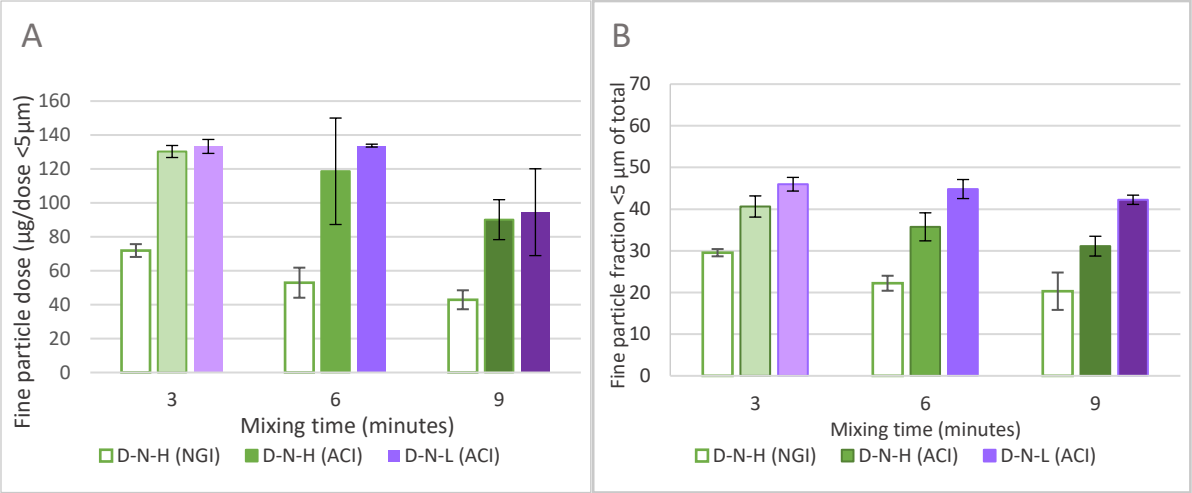

Figure 46. The fine particle dose of D-N-H and D-N-L is displayed in A, plotted against the mixing time. In B, the fine particle fraction is plotted against the mixing time for the D-N-H and D-N-L batches. Both batches are measured using the ACI, for reference the measurements for D-N-H using NGI is included.

4.3 Malvern dry

The results from the geometric particle sizing using the Malvern dry can be seen in the diagrams presented in figure 47 below. In B, the particle size of the Diosna batches can be seen. From the diagram it can be distinguished that coated and the naked batches differ to a small extent in size, where the naked display a somewhat larger size. However, the coated batches independent on the mixing speed seem to display roughly the same size, which seems to also be true for the naked batches.

In A, the particle size of the Turbula manufactured batches can be seen, all batches T-N and D-C-L-T display similar size of the particles, though T-C-30 deviates to some extent, however the standard deviation is quite large for these measurements, why it is hard to draw any conclusions.

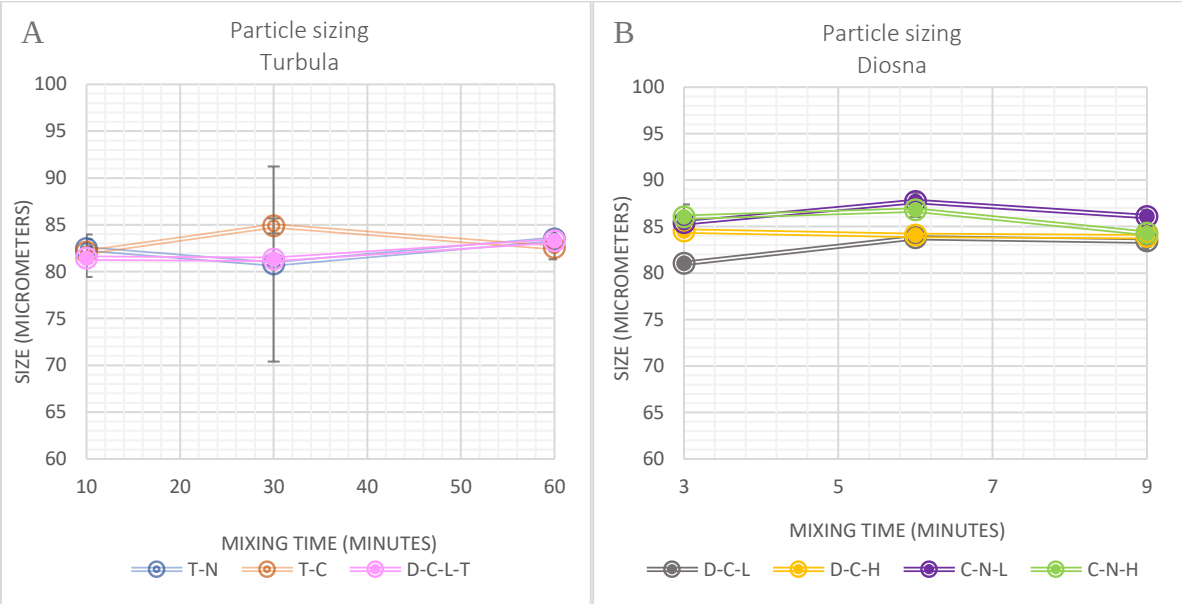

Figure 47. A showing the measured size in µm of the Turbula mixed batches, here plotted against the mixing time in minutes. In B, the particle size in µm of the Diosna manufactored batches can be seen plotted against the mixing time in minutes.

4.4 Bulk density

4.4.1 Initial bulk density (big cylinder)

The initial poured bulk density of the batches was measured directly after mixing using the big cylinders. The results for the Turbula and Diosna mixed batches plotted against the mixing time are shown in figure 48 below. As can be seen the Turbula mixed batches yield a higher bulk density compared to the Diosna mixed batches. The poured bulk density of the carrier (lactohale 206) was measured to 0.64 g/cm^3. Compared to the bulk density of the carrier all the mixed batches except for the naked batches mixed in the Diosna (D-N-H and D-N-L) shows an increase in bulk density i.e. a closer packing of the particles after mixing. For the Turbula mixed batches there is an increase of the bulk density linked to the mixing time. This can also be seen for the naked batches mixed in the Diosna mixer, though very slight for D-N-L. For the coated particles mixed in the Diosna there is instead a decrease in bulk density. Both the particles coated in the Diosna and Turbula yielded a higher bulk density compared to their naked counterparts. The highest bulk density was achieved with D-C-L-T where the particles were coated in the Diosna and the API added in the Turbula.

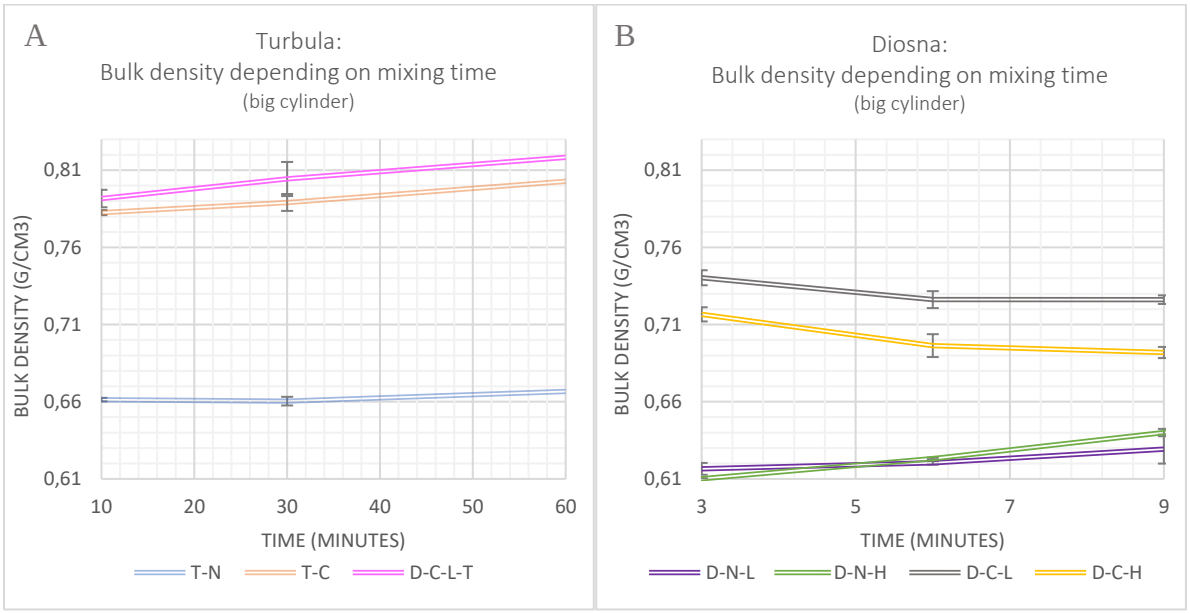

Figure 48. The initial bulk density of the Turbula (A) and Diosna (B) mixed formulation measured directly after fabrication. Error bars showing the standard deviation is included for each batch.

When performing the measurements it was noted that the coated formulations showed better flow properties compared to the naked formulations which were more troublesome to pour. Comparing the Turbula batches with the Diosna, it was more difficult to perform the measurements for the long mixing times in the Diosna. The difficulty being that the powder adhered to the spoon and needed either a tap or steep angle to pour. This was especially evident for the naked batches.

In figure 49 the bulk density of the batches mixed in the Diosna is plotted against the mixing energy (for equation, see theory). From the diagram it may be suggested that the bulk density correlated to the mixing energy as it follows a trend almost overlapping where the mixing

energy is equal for the batches mixed at high and low speed. Here it is almost more evident that with increasing mixing time/energy the bulk density of the naked batch increase while the coated decrease, both coming closer to the initial value of the carrier.

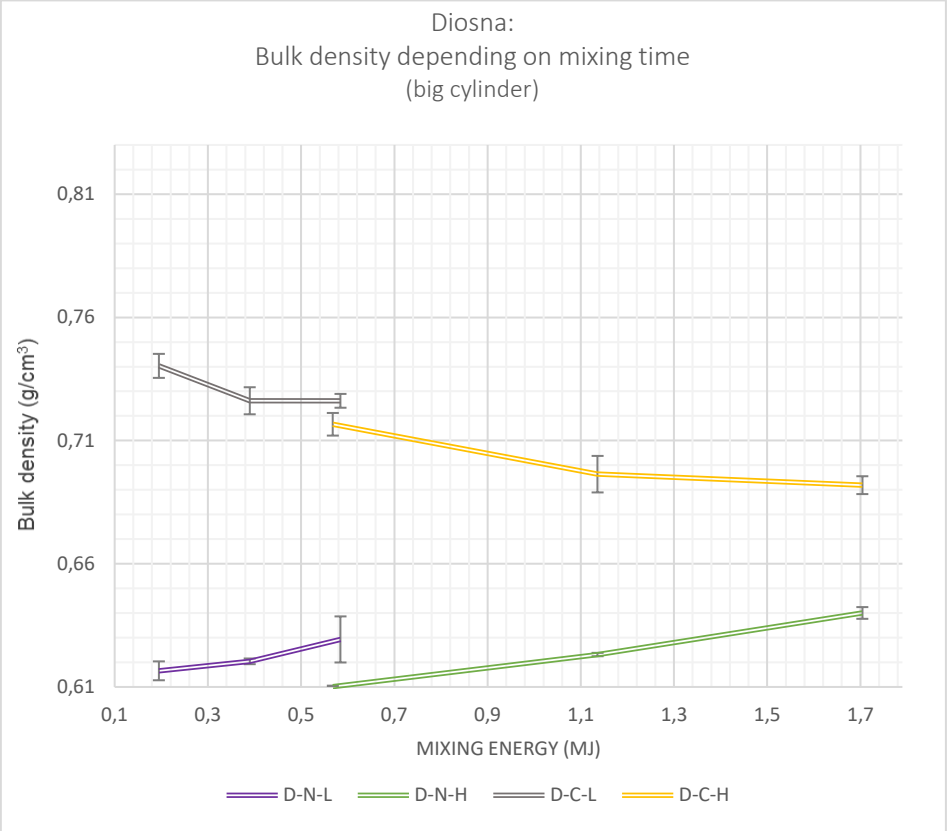

Figure 49. The initial bulk density of the Diosna mixed formulations plotted against the mixing energy.

4.4.2 Storage conditions

All batches were stored for two months in ambient conditions, some of the batches were additionally placed for dry storage in a desiccator (see table 9).

4.4.2.1 Turbula batches

Change after 2 months - ambient (big cylinder)

In figure 50 the results of the bulk density after ambient storage for the Turbula batches is presented. A few trends can be noted for the different batches. D-C-L-T show an increase in bulk density after storage. For the coated batches the results of the initial measurements and after storage are closer to each other, exception being T-C-5. While for the naked batches, there is instead a decrease in bulk density after storage, which deviates from the other batches measured.

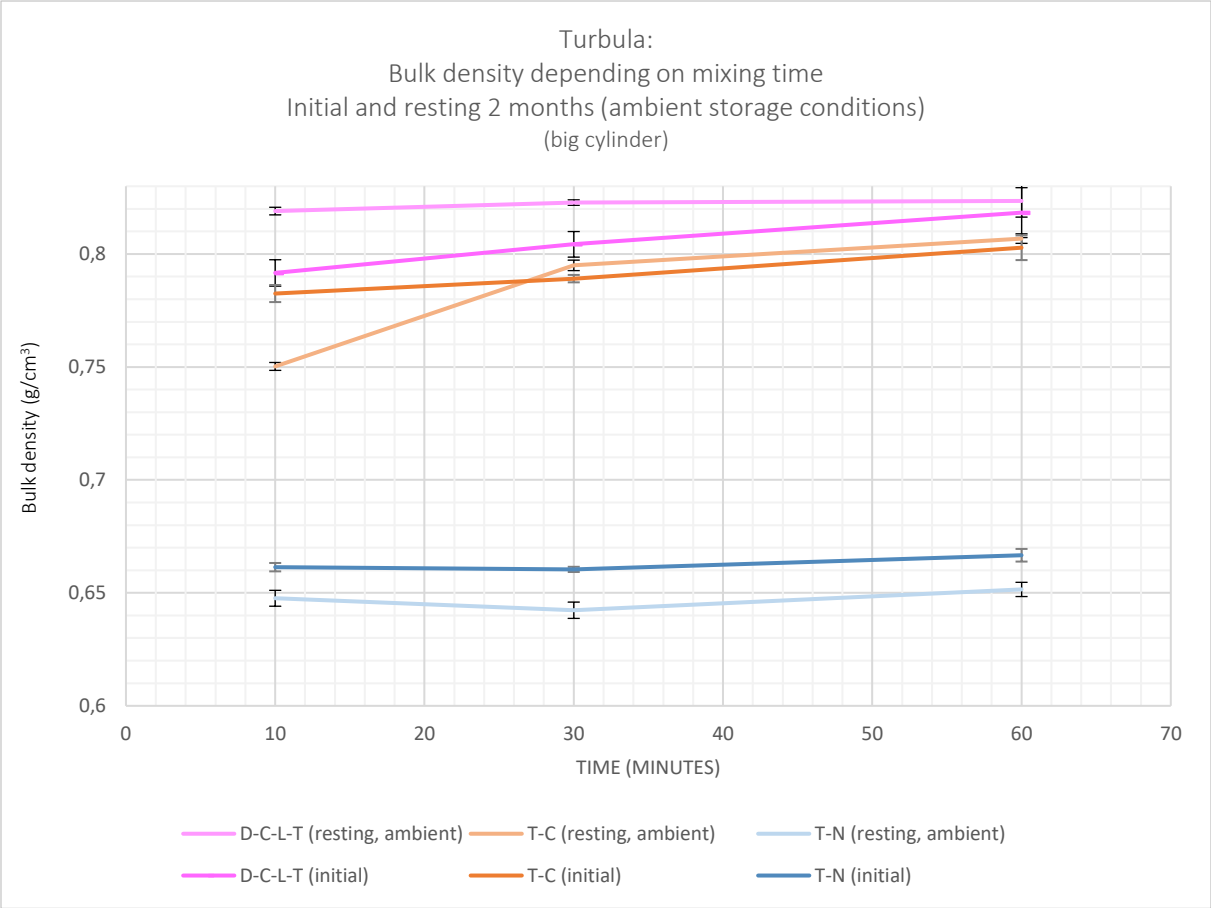

Figure 50. The bulk density of the Turbula mixed formulations stored in ambient condition and the initial measurements using the large cylinder, plotted against the mixing time.

Small and big cylinder

When comparing the measurements of the powder stored in ambient condition using small and large cylinders for measurements a reoccurring difference was noted, were the small cylinder deliver lower results compared to the larger cylinder, as can be seen in figure 51. The difference is seen to be constant and while small, it does significantly affect the result.

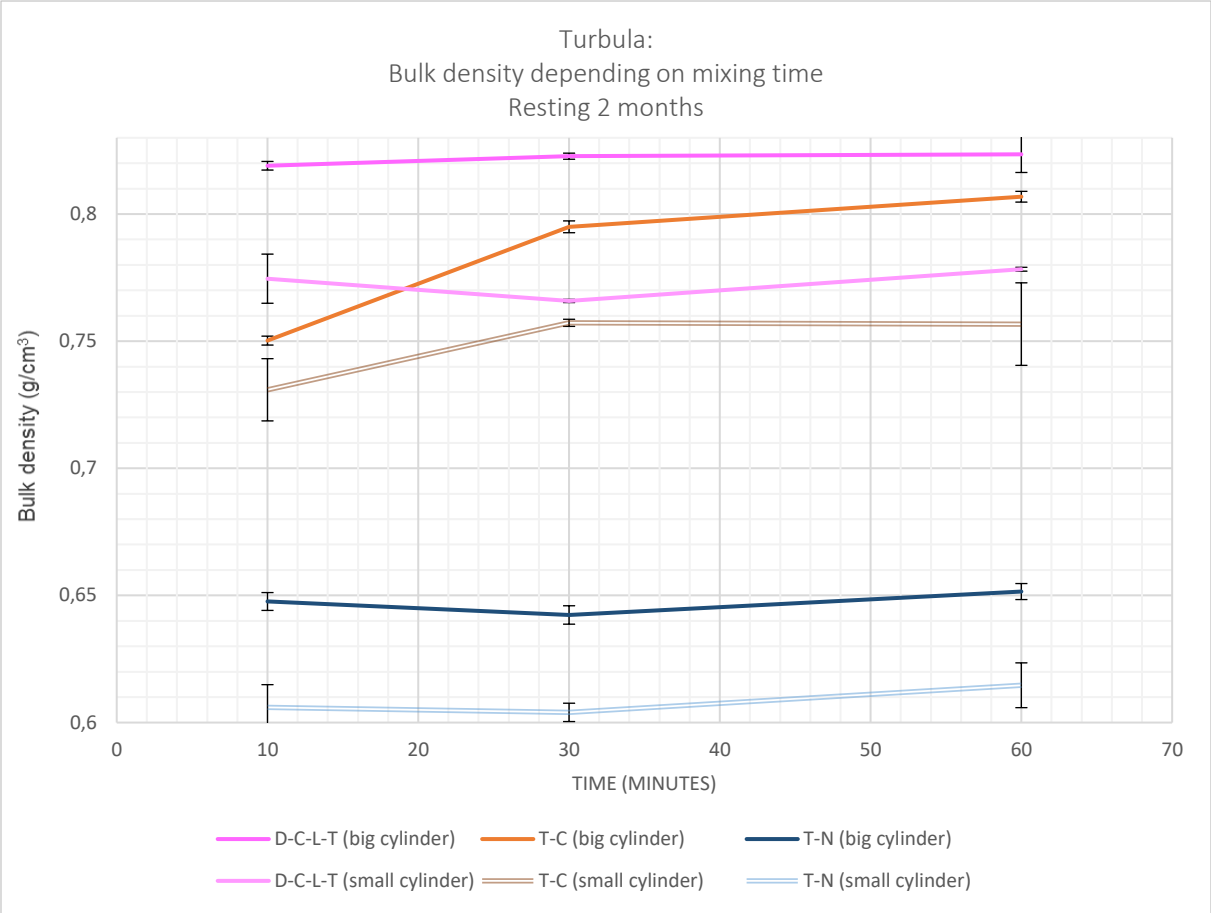

Figure 51. The bulk density of the Turbula mixed formulations stored in ambient condition, here measured using both the small and large cylinder plotted against the mixing time.

Comparison of ambient and dry storage – small cylinder

All the batches stored in ambient conditions were measured and selected batches were placed in a desiccator to study the effects of dry storage, particular interest was placed in the effects of storage on the batches coated with MgSt.

Due to the limited area in the desiccator, the samples had to be small, thus these were measured using the small cylinder for the bulk density measurements.

From the diagram in figure 51 it can be seen that there is almost no difference in bulk density when storing the formulations in dry conditions compared to those stored ambient. This may be due to the relatively long storage time (2 months). It is possible that there would have been a more significant change if the powders were stored for a shorter period since the powders now may have relaxed and thus not exhibiting as much electrostatic effects as expected of dry storage.

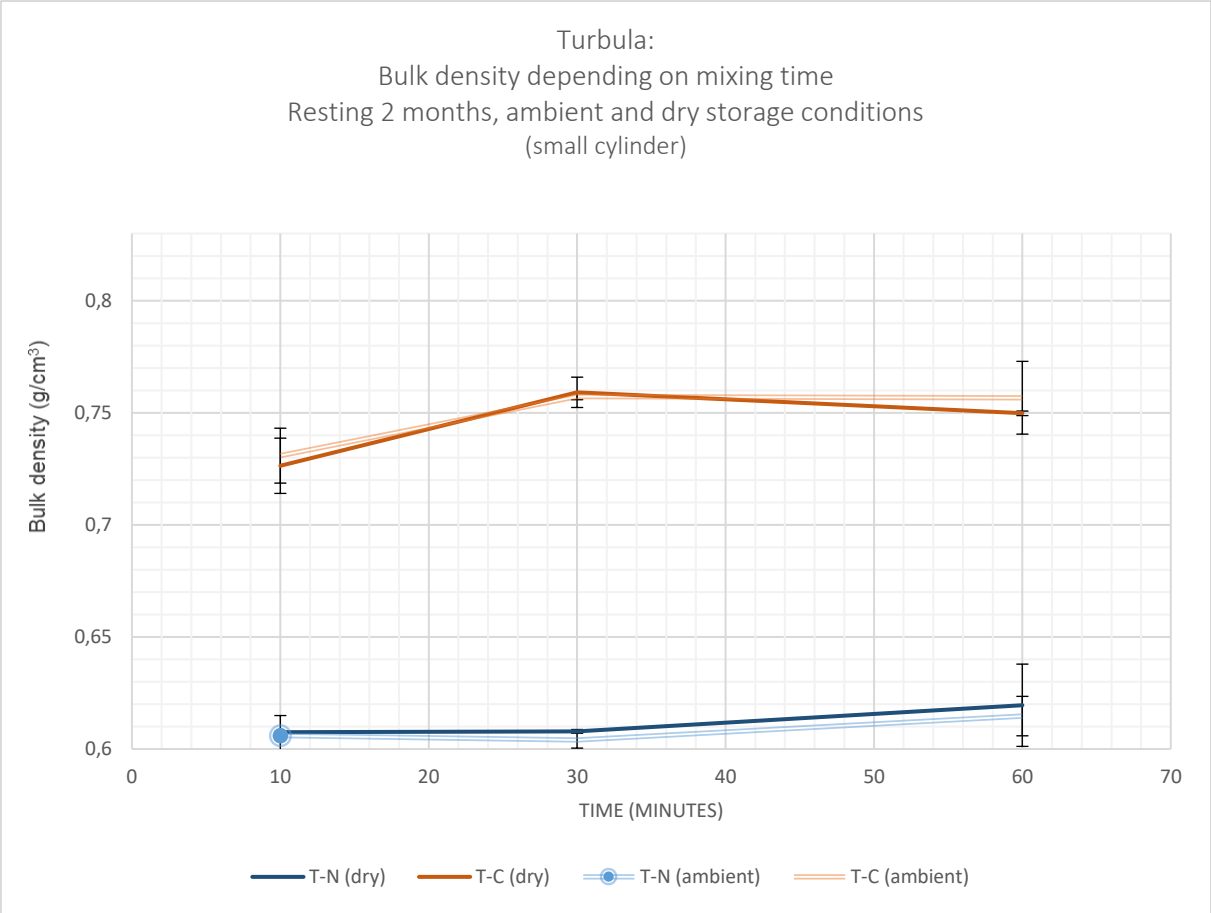

Figure 51. The bulk density of the Turbula mixed formulations stored in ambient and dry condition plotted against the mixing time.

In order to compare the results of the initial measurements to those after storage, figure 52 is presented below. An adjusted initial measurement, based on the mean difference presented in figure 51, has been added in order to make the measurement comparable.

The batches D-C-L-T show an increase in bulk density after storage. For the coated batches the results of the initial measurements and after storage are closer to each other, exception being T-C-5. While for the naked batches, there is instead a decrease in bulk density after storage, which deviates from the other batches measured.

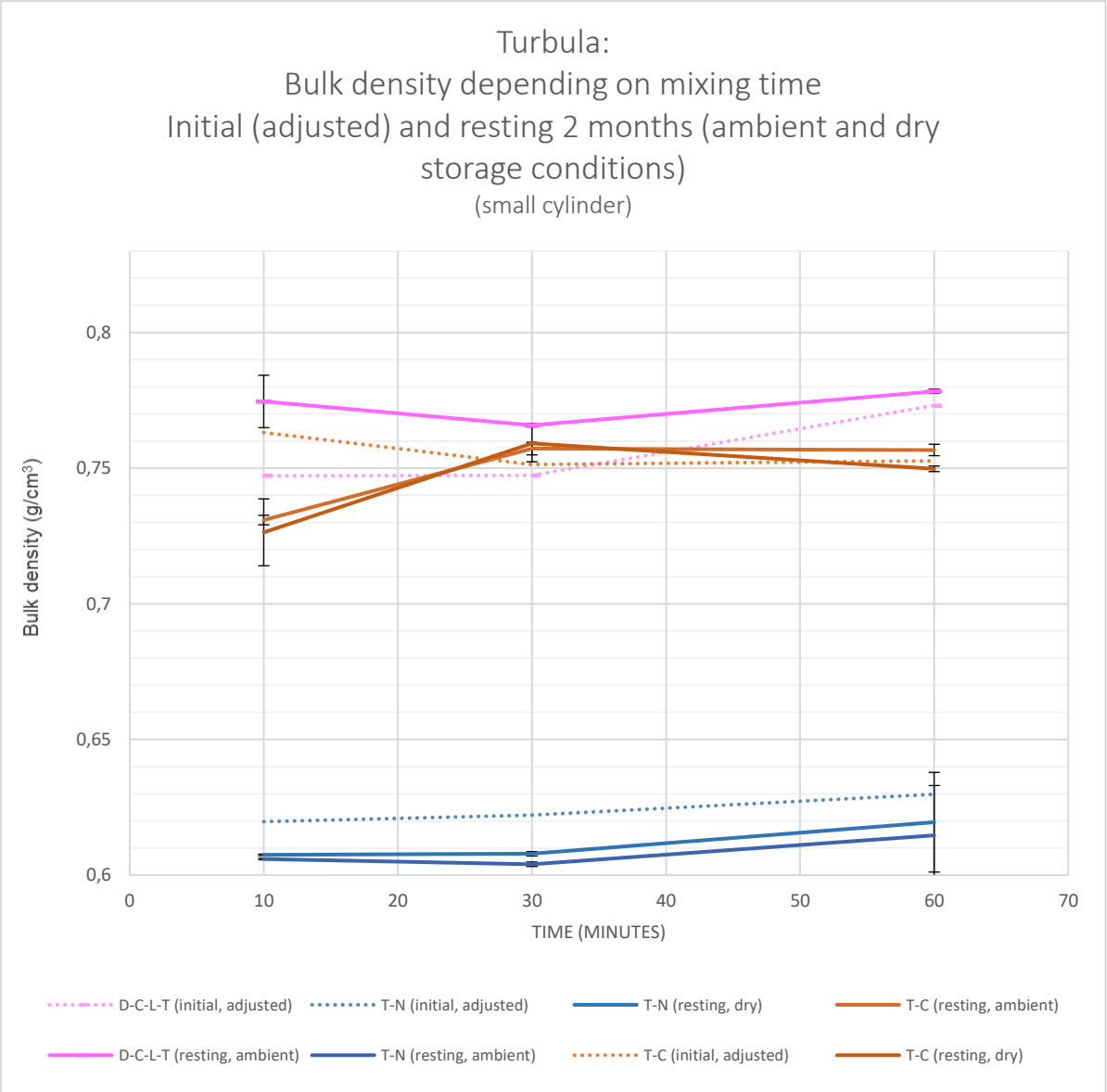

Figure 52. The bulk density of the Turbula mixed formulations stored in ambient and dry condition measured using the small cylinder here plotted together with initial measurements measured using the large cylinder, adjusted with the measured difference, plotted against the mixing time.

4.4.2.2 Diosna batches

Change after 2 months - ambient (big cylinder)

Figure 53 shows a comparison between the initial measurements and the measurements after storage (ambient). Here the bulk density was measured using the big cylinders.

When comparing the initial measurements to those after storage, it is seen that all the formulation are closer packed after storage (exception being D-N-H-9). This could be due to a decrease of electrostatic effects after storage. When performing the initial measurements the formuations showed clear signs of electrostatic effects (e.g. almost not being able to pour the powder for measurements after mixing).

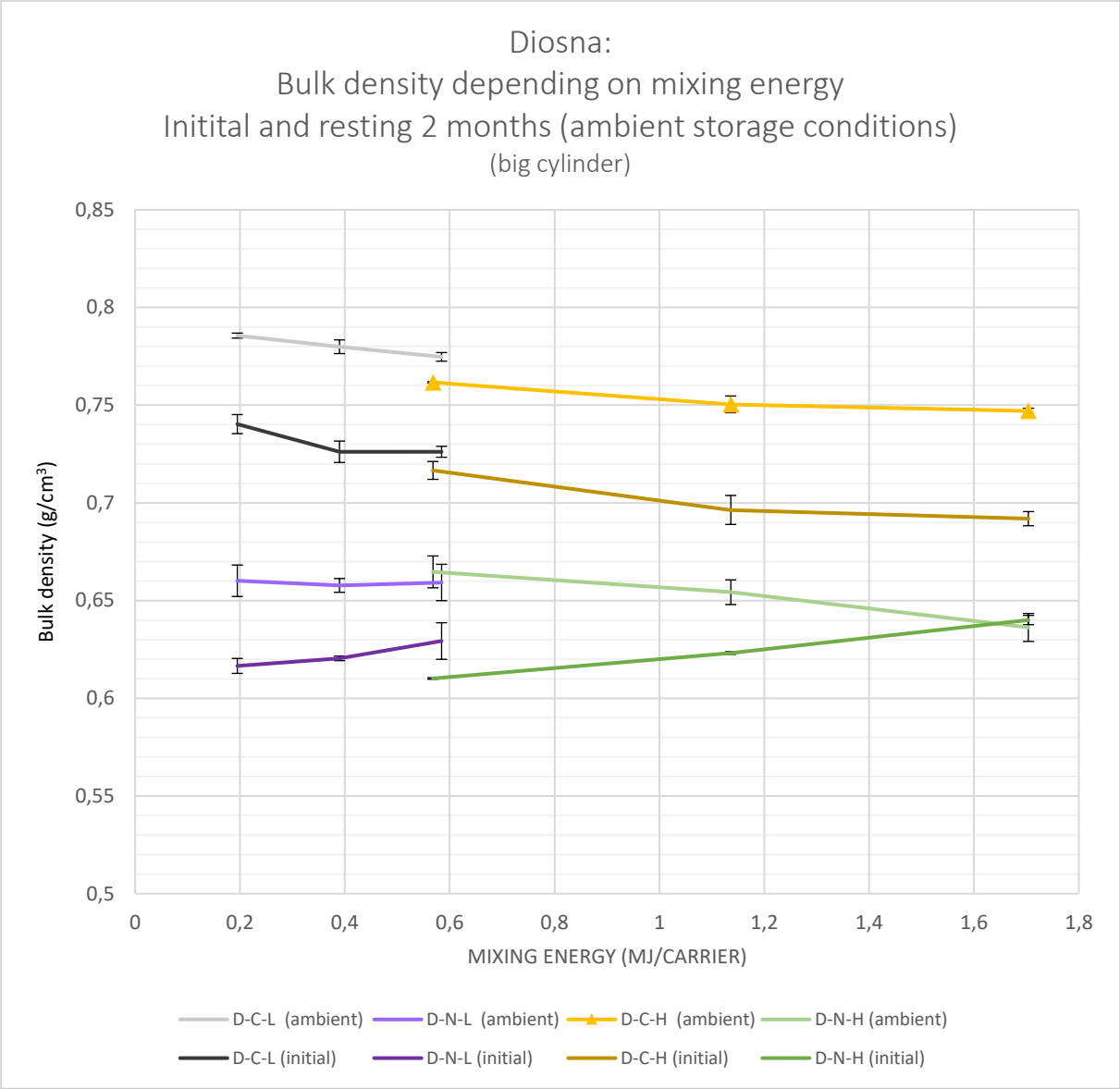

Figure 53. The bulk density of the Diosna mixed formulations stored in ambient condition and the initial measurements using the large cylinder, plotted against the mixing energy.

Small and big cylinder

Comparing the measurements of the formulations stored in ambient condition using both the small and large cylinder for measurements, a difference could once again be spotted. As with the Turbula mixed batches, the big cylinder displays higher values compared to the small, see figure 54.

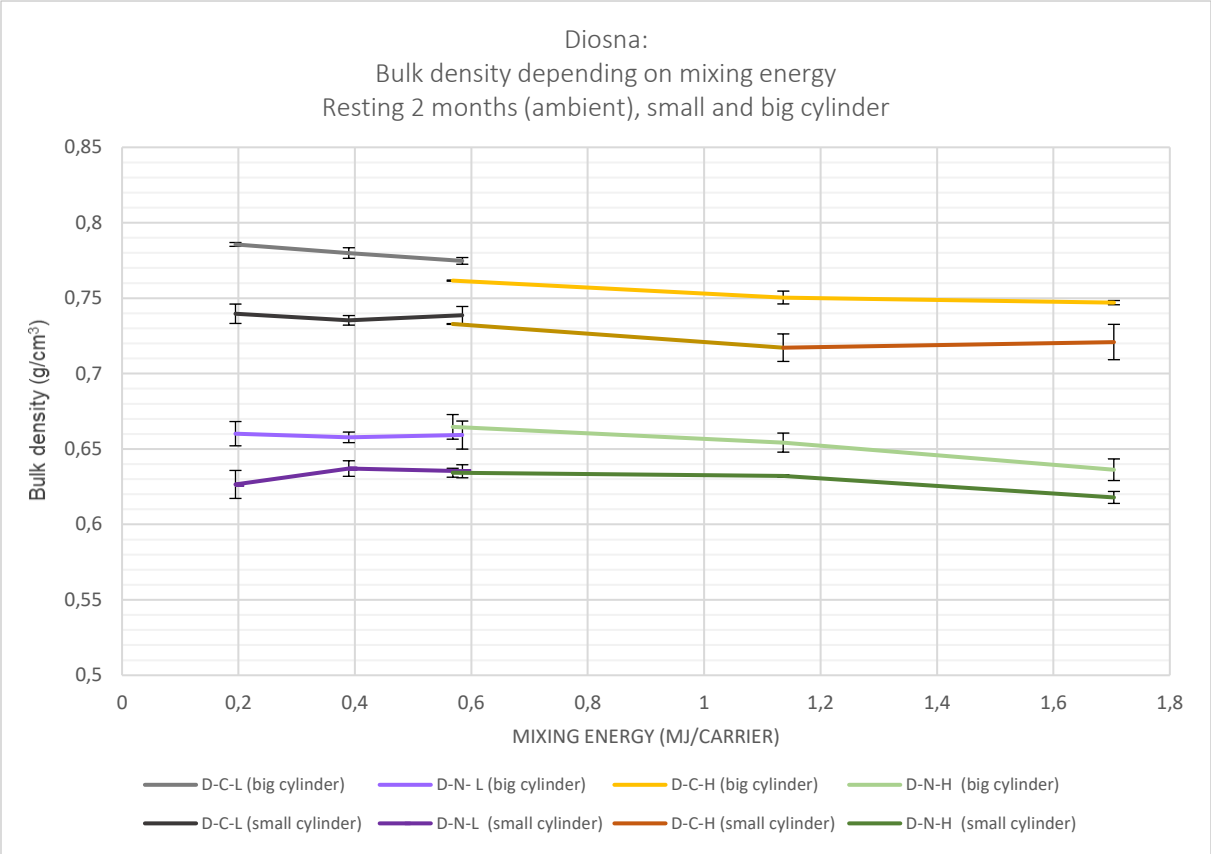

Figure 54. The bulk density of the Diosna mixed formulations stored in ambient condition here measured using both the small and large cylinder plotted against the mixing energy.

Comparison of ambient and dry storage – small cylinder

As for the turbula mixed batches, the bulk density of the formulations stored in ambient compared to dry conditions, could be said to be approximately the same, the figure 55.

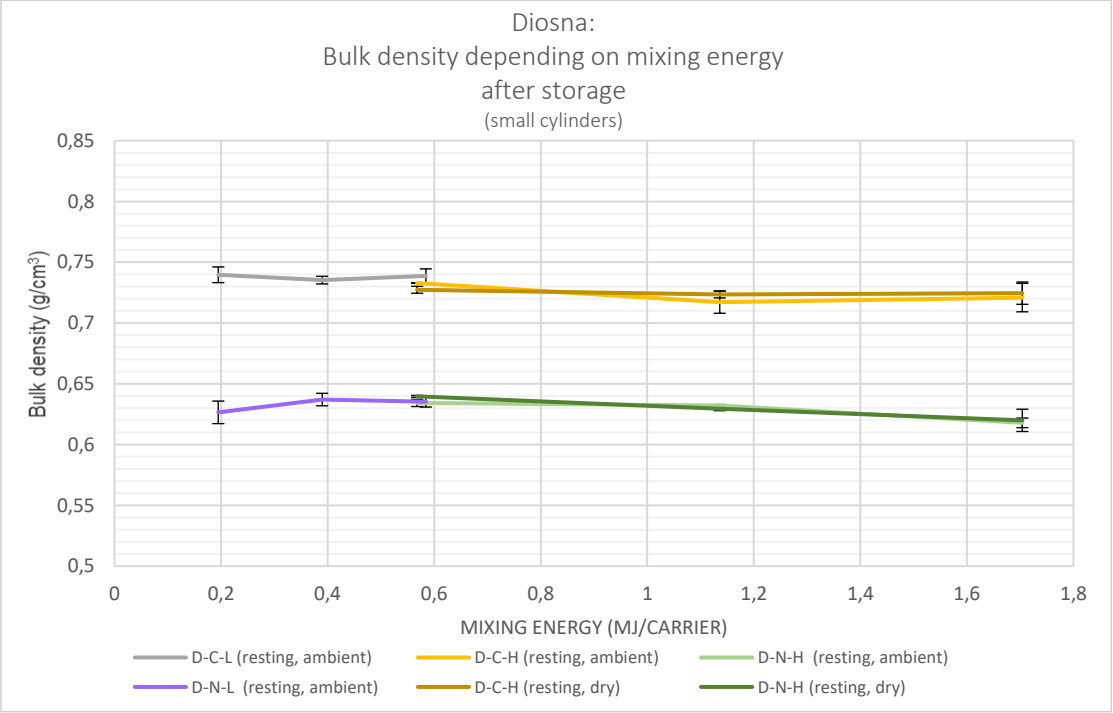

Figure 55. The bulk density of the Diosna mixed formulations stored in ambient and dry condition plotted against the mixing energy.

In order to compare the results of the initial measurements to those after storage, figure 56 is presented below. An adjusted initial measurement has been, created in accordance to those of the Turbula batches in figure 52. The bulk density of the batches stored ambient is almost equal to those stored dry.

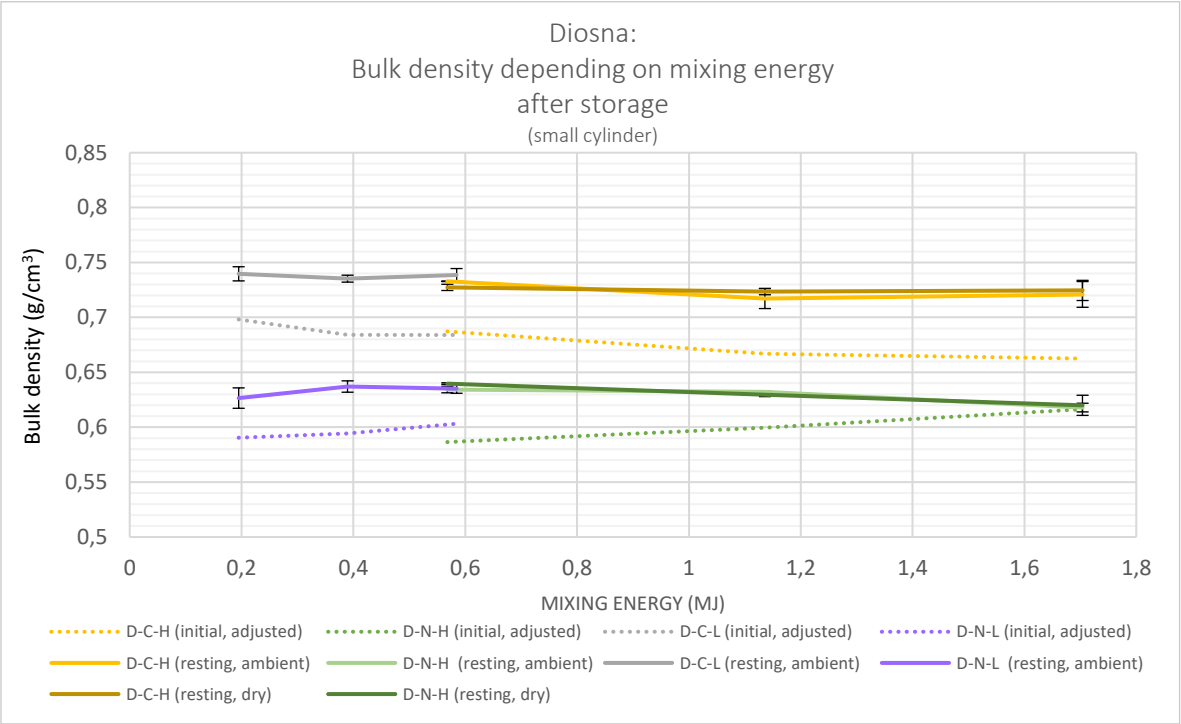

Figure 57. The bulk density of the Diosna mixed formulations stored in ambient and dry condition measured using the small cylinder here plotted together with initial measurements measured using the large cylinder, adjusted with the measured difference, plotted against the mixing energy.

4.4.3 Bulk density after storage – comparison between Turbula and Diosna mixed batches (big cylinder)

Comparing the bulk density measurements of the Diosna mixed and Turbula mixed batches it after storage it can be seen that D-C-L-T yield the highest bulk density, see figure 58. After storage the bulk density of the Diosna manufactured powders increase more compared to those manufactured using the Turbula. The naked batches produced have a bulk density of slightly above 0.65 g/cm^3 after storage, independent of the mixer type used. The bulk density of the mixed formulations are on average higher than that of the carrier, 0,64 g/cm^3.

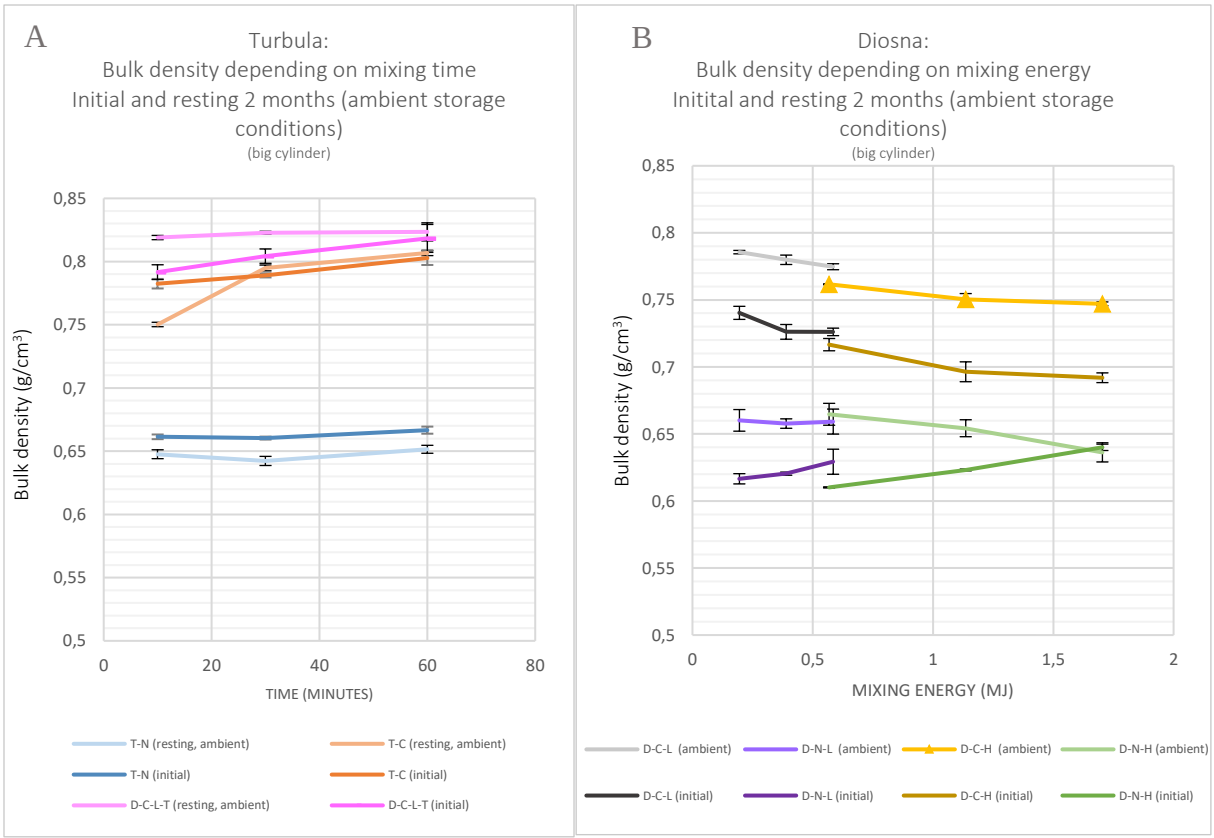

Figure 58. Diagrams showing the initial bulk density and the bulk density after ambient storage conditions of the Turbula (A) and Diosna (B) mixed formulation. Error bars showing the standard deviation is included for each batch.

4.5 Surface and morphology – SEM images

The surface and morphology of a number of selected batches was studied using a Scanning Electron Microscope. The images were taken using two different detectors, the SEI (upper secondary electron in-lens) and LEI (Lower secondary electron). In figure 59, the bare lactose particles are imaged. As can be seen in the pictures with higher magnification, the surface of the carriers has some lactose fines innately. Looking at the particles with added MgSt in figure 60, a slight increase in particles on the surface can be spotted.

Lactose carrier particles - LH206

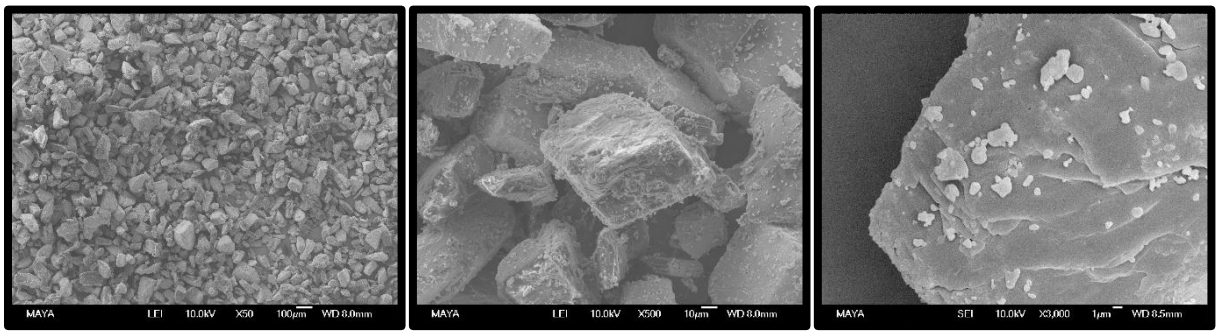

Figure 59. SEM images of lactose carrier (LH206) with an accelerating voltage of 5.0 kV, working distance 8,0 and 8,5 mm and magnification of 50X, 500X and 3000X respectively (note that the last image is taken using a SEI detector).

MgSt coated lactose carriers

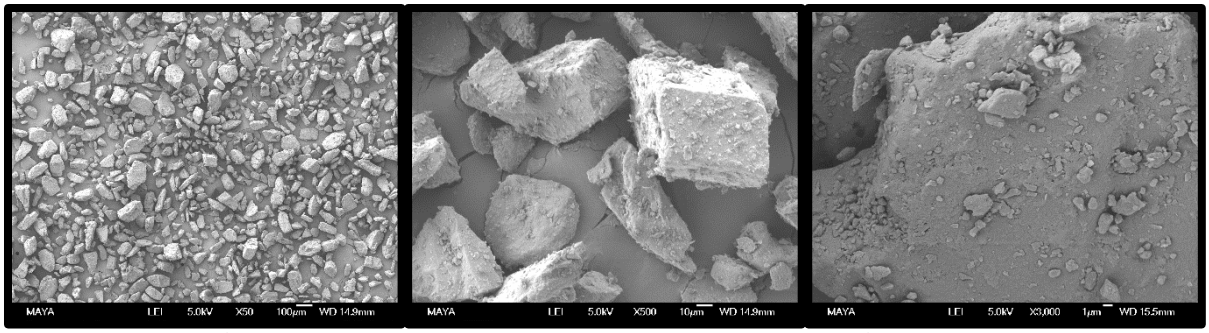

Figure 60. SEM images of lactose particles coated in the Diosna mixer with an accelerating voltage of 5.0 kV, working distance 14,9 and 15,5 mm and magnification of 50X, 500X and 3000X respectively.

Batches D-N-L-6 (figure 61) and D-C-L-6 (figure 62) can be compared to each other, to note the visual effects of adding a coating agent. Looking at the images with 500X magnification, an increase in fine particles may be spotted, this however is not as obvious when looking at 3000X magnification, thus it may be only on this site. However when comparing the Diosna coated batches with the Turbula mixed, it seems that the Diosna batches present smaller "knob" like particles on the carriers compared to the Turbula batches, this can be observed on the 3000x magnification images.

D-N-L-6

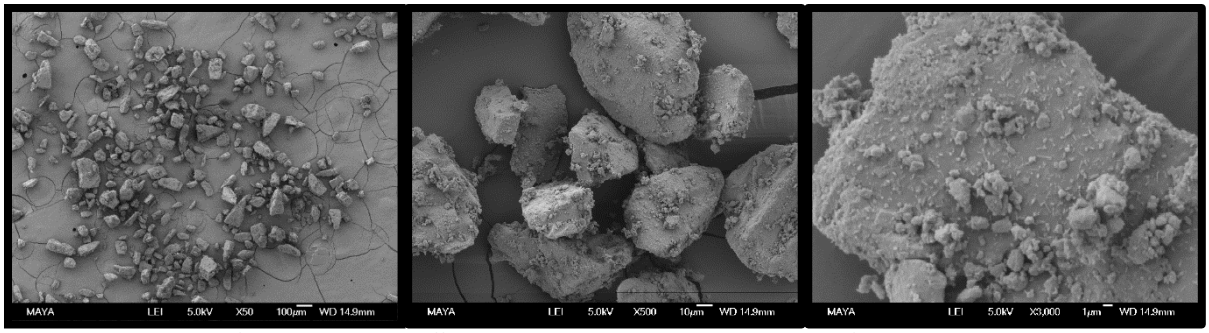

Figure 61. SEM images of D-N-L-6 on three different locations with an accelerating voltage of 5.0 kV, working distance 14,9 mm and magnification of 50X, 500X and 3000X respectively.

D-C-L-6

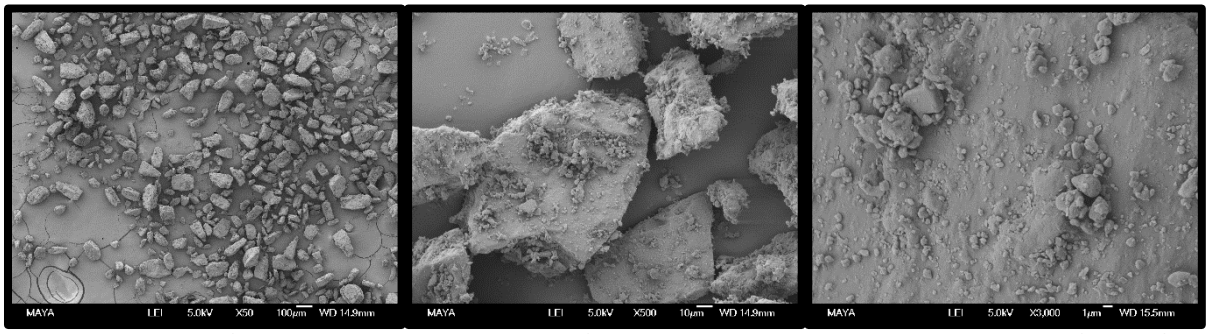

Figure 62. SEM images of D-C-L-6 with an accelerating voltage of 5.0 kV, working distance 14,9 and 15,5 mm and magnification of 50X, 500X and 3000X respectively.

Comparing T-C-30 and T-C-60 it would seem that T-C-60 has a higher amount of fines on the carrier when looking at figure 63 and 64 at 500X and 3000X magnification. Comparing T-C-60 and T-C-L-60, there is not a significant visual difference between the batches.

T-C-30

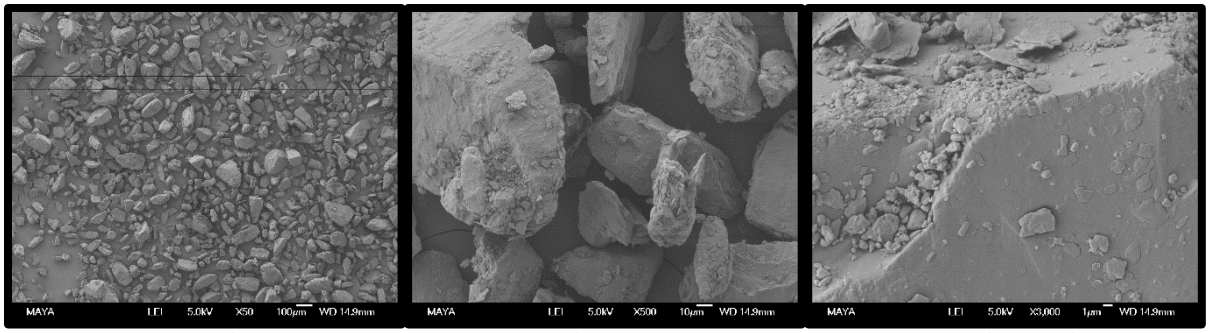

Figure 63. SEM images of T-C-30 with an accelerating voltage of 5.0 kV, working distance 14,9 mm and magnification of 50X, 500X and 3000X respectively.

T-C-60

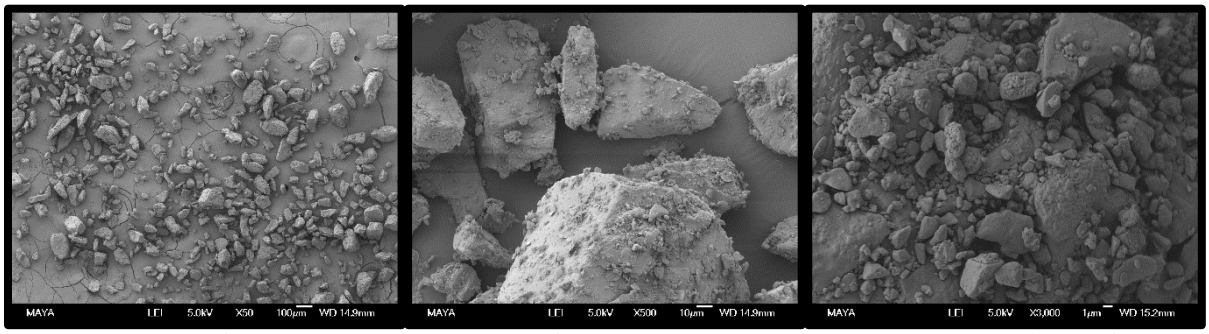

Figure 64. SEM images of T-C-60 with an accelerating voltage of 5.0 kV, working distance 14,9 and 15,2 mm and magnification of 50X, 500X and 3000X respectively.

D-C-L-T-60

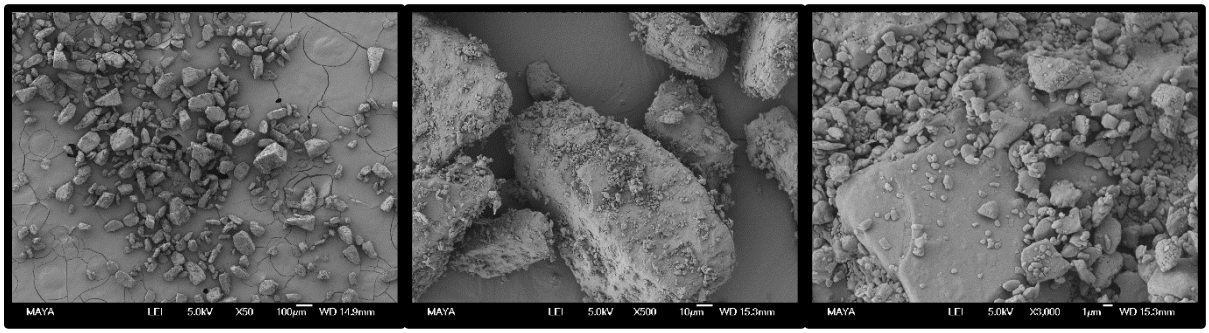

Figure 65. SEM images of D-C-L-T-60 on two different locations with an accelerating voltage of 5.0 kV, working distance 14,9 and 15,3 mm and magnification of 50X, 500X and 3000X respectively.

Comparing the naked lactose carrier particles and the MgSt coated carrier particles (figure 59 and 60) with the batches mixed for longer duration, it seems that the naked and coated carrier display sharper edges compared to the mixed formulations, when studying the particles at 500X magnification. This may be due to an abrasive effect of the mixing process.

4.6 Final comparison – FPD, FPF, MMAD and weight per dose

Compilation of the results gained from the FPF and FPD measurements using the NGI can be viewed below in figure 66. Fine particle dose and fine particle fraction are two important measurements since the first tells how much API is able to reach the lungs and the second how big fraction of the API was able to separate from the carrier. The results of D-N-L have not been included since these batches were measured using the ACI. It can be seen that D-C-L-T-

60 yields the highest fine particle dose (slightly above 160 µg/dose) and second highest fine particle fractioned, highest being that of D-C-L-6 (slightly above 60 %). The lowest values measured was that of D-N-H performing approximately half or less that of the previously mentioned batches.

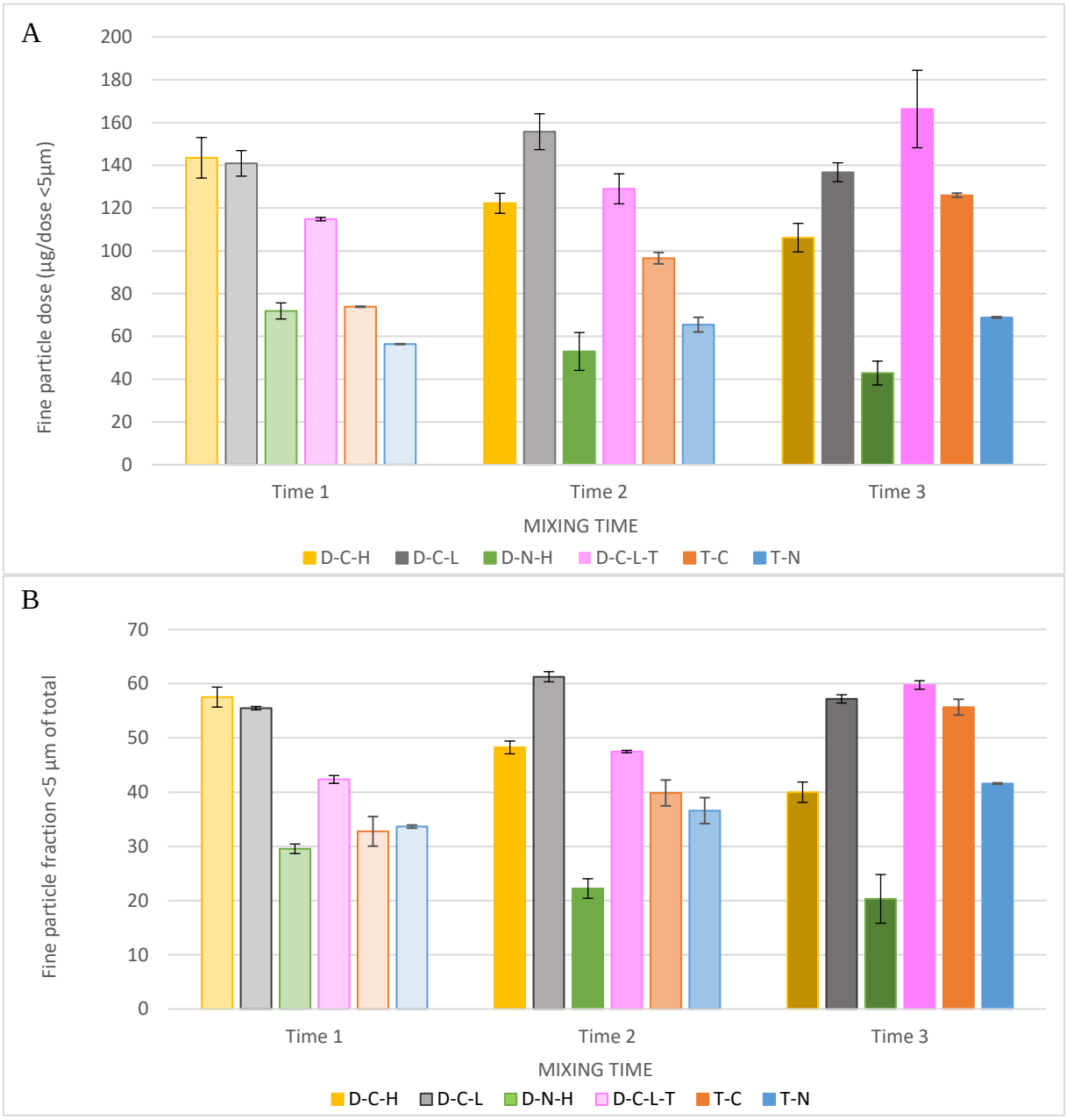

Figure 66. The fine particle dose of all batches measured using the NGI is displayed in A, plotted for each mixing time/batch. In B, the fine particle fraction is plotted against the mixing time/batch for the all batches measured using the NGI.

The weight per dose of the batches measured using the NGI is compiled in figure 67 below. It can be seen that the inhaler actuates smaller doses with the naked formulations, compared to the coated.

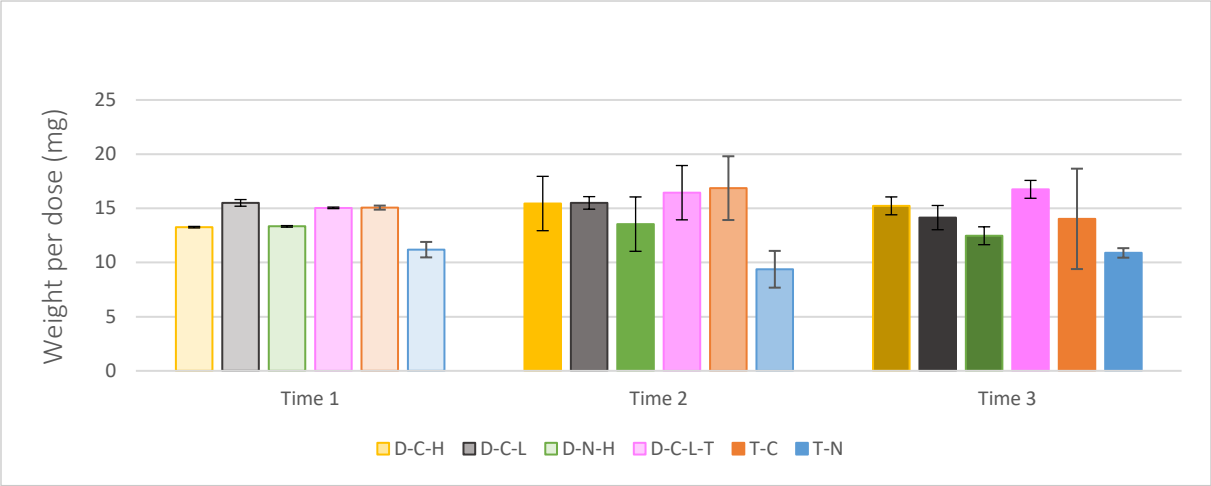

Figure 67. The weight per dose for all batches measured using the NGI is displayed and plotted for each mixing time/batch.

4.6.1 Comparison of Diosna batches based on mixing energy

To further analyze the results from the Diosna mixed batches, the results were plotted against the mixing energy instead of the mixing time. Mixing energy has gained interest as a key parameter in performance of dry powders for inhalation and is thought to offer explanation to how the particles are affected by mixing (Thalberg, 2022).

The mixing energy was calculated according to the equations described in the theory. Using the experimental data gained from the ACI and NGI measurements, lines were fitted to predicted values. The modeling equation used for describing the fine particle fraction is the following (Thalberg, 2022):

$$FPF = [A + \frac{B}{1 + e^{-k_1 x}}](e^{-k_2 x})$$

The equation takes into consideration the increase and decrease of the FPF, k_1 respectively k_2 (rate constants) in the equation. X is the mixing energy exerted on the particles. For the batches displaying only a decrease the following formula, Ce^{-kx}, is used instead.

Comparing the results of figure 68 and 69, differences in the FPF curve can be spotted (note that D-Cs experimental values were gained using the NGI while D-N was measured with ACI, which is why a direct comparison is not possible). An explanation offered by Thalberg (2022) to the initial increase of the coated powder is the interactions between the API and coating, which is described by the parameter k_1. Further, it is believed that the smearing of the coating agent on the carrier will facilitate a higher drug load.

From table 11, it would also seem like the rate of the decrease in FPF is somewhat higher for the naked formulations compared to the coated.

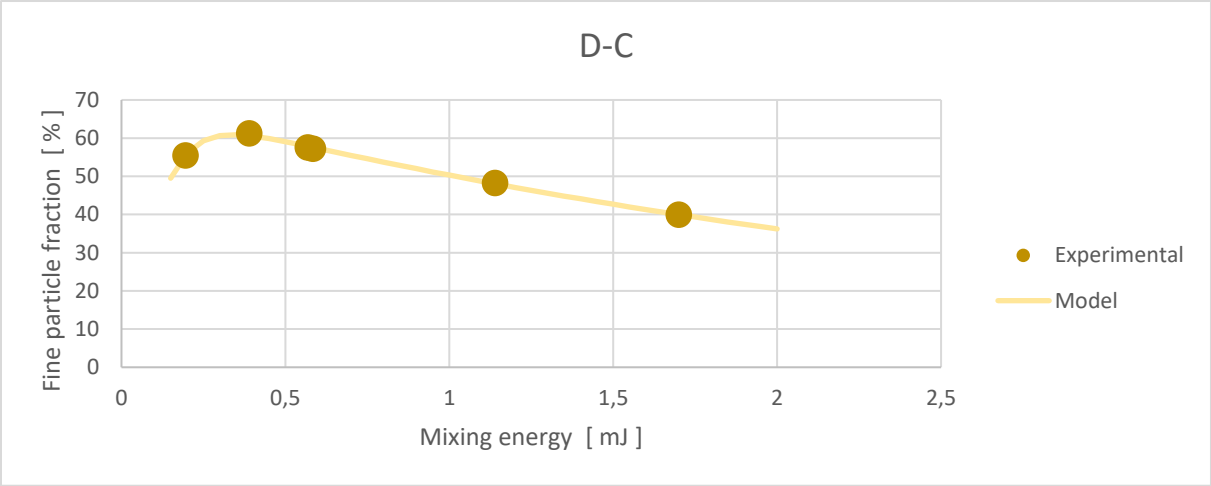

Figure 68. Curves fitted to the experimental values of the FPF measured using the NGI of the coated Diosna batches, plotted against the mixing energy. Model being used to approximate the curves, limited to A+B/2 >0 (see equation for FPF). The value before a mixing energy of 0,15 mJ have been extinguished since there cannot be any FPF before mixing.

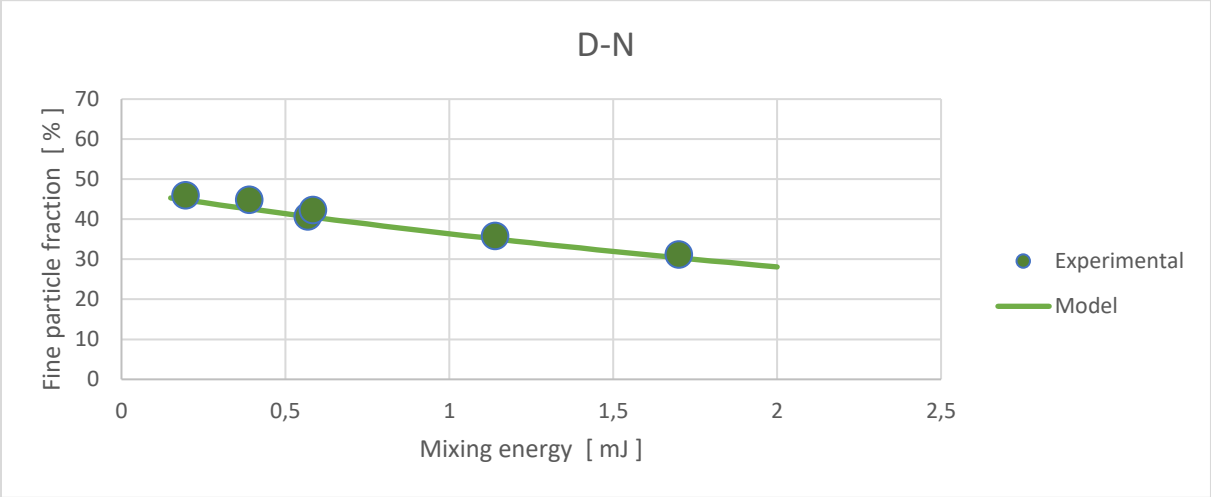

Figure 69. Curves fitted to the experimental values of the FPF measured using the ACI of the naked Diosna batches, plotted against the mixing energy. Model used to approximate the curve (equation Ce^{-kx}). The value before a mixing energy of 0,15 mJ have been extinguished since there cannot be any FPF before mixing.

The MMAD of the batches were plotted similarly, see figure 70 and 71. The coated and naked batches display a similar decrease in MMAD with increasing mixing time.

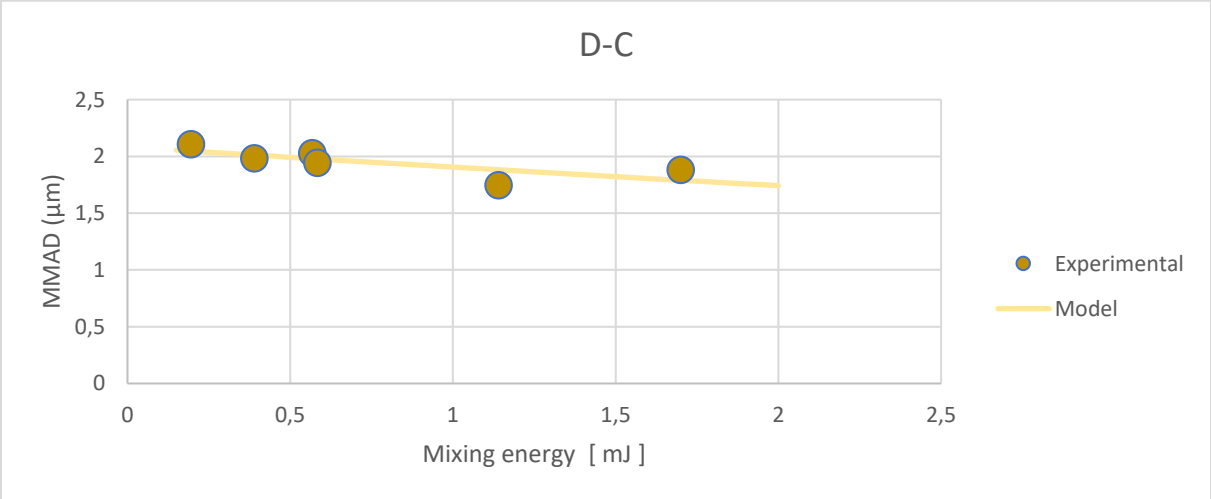

Figure 70. Curves fitted to the experimental values of the MMAD measured using the NGI of the coated Diosna batches, plotted against the mixing energy. Model used to approximate the curve. The value before a mixing energy of 0.15 mJ have been extinguished.

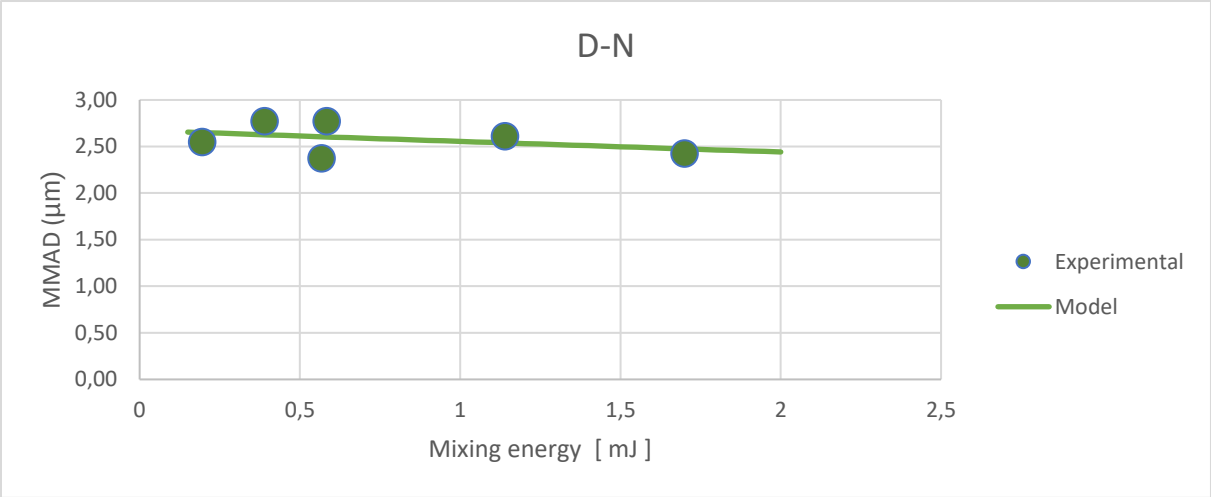

Figure 71. Curves fitted to the experimental values of the MMAD measured using the ACI of the naked Diosna batches, plotted against the mixing energy. Model used to approximate the curve. The value before a mixing energy of 0.15 mJ have been extinguished.

The rate constants k1 and k2 can be found in table 11 below.

Table 11. The rate constants are presented for the Fine Particle fraction and Mass Median Aerodynamic Diameter of D-N and D-C.

Fine Particle Fraction	**K1**	**K2**
D-N	12.83	0.33
D-C	-	0,26
Mass Median Aerodynamic Diameter	**K1**	**K2**
D-N	-	0.09
D-C	-	0.05

5 Conclusion

5.1 Impact of the study

The aim of the study was to investigate the impact of mixing time and mixer type and how it may affect the formulation and contribute to further understanding of the performance of the finished product. The use of magnesium stearate (a coating) has the potential to assist the separation of the API and carrier particle, thus it was also studied how magnesium stearate is affected by the mixing and the forces involved. The hope being to help gain knowledge for formulation of inhalation medicine.

5.2 Main findings

From the results gained, it is clear that the task of formulating is complex with many aspects to consider. From this study, it is evident that adding a coating agent to the lactose carrier improves the delivery of the API.

Throughout, it has been noted that the coated formulations have performed better regarding FPF, FPD and actuating higher doses (weight per dose/flowability). Comparing the coated and naked formulations in regard to bulk density, it could easily be seen that the coated formulations were able to be closer packed (higher bulk density) compared to their naked counterparts. The batches furthermore had an increase in bulk density after storage. This could possibly be linked to electrostatic effects associated with the manufacturing process, which are reduced during storage of the formulations. When manufacturing the powders, it was noted that the Diosna formulations adhered more to the measuring spoon compared to the Turbula formulations. This may be linked to why the Diosna batches display a larger difference in bulk density when comparing before and after storage. The actuated dose (weight per dose) was also somewhat higher for the coated formulations compared to the naked, indicating a somewhat better flowability which may also be linked to the bulk density.

In terms of fine particle fraction and fine particle dose, the best-performing batches where D-C-L-6 and D-C-L-T-60. Interesting here is that D-C-L-T showed no sign of stagnating whereas D-C-L-6 would be very close to a peak value based on the mixing energy curve.

From the results gained when plotting the mixing energy curves, it may also be assumed that the energy exerted on the carriers is an important aspect to consider when designing formulations. Depending on whether a coating agent has been added or not, the FPF behaves differently. The results of this study indicate that naked formulations benefit from low mixing energy, only to reach uniformity, while coated formulations require more mixing due to interactions between API and coating.

Elaborating on the low mixing energy requirement when mixing API, it would seem the opposite is true regarding the coating agent. Results indicate that better results are acquired using the high-shear mixer (or requiring very long mixing times using a low-shear). However,

when adding the API, as with D-C-L-T, it may be advantageous to use the Turbula blender. This could be due to a gentler mixing compared to the Diosna high-shear mixer, which may cause damage to the particles. A challenge with using the Turbula mixer compared to the Diosna is achieving good uniformity of the blends, this however was tested and obtained satisficing results in this study.

Moving over to high mixing energy. From the mixing energy curves, it became evident that a high mixing energy, either from long mixing times or high mixing speeds, affects the formulations in a negative manner. This overmixing resulted in lower FPF as well as lower FPD, which continue to decrease linked to higher mixing energy. This pushes the importance of finding the right amount of mixing energy, which is governed by both the mixing time and mixing speed, in order to achieve a successful dry powder formulation.

5.3 Way forward

Engineering a successful formulation is a complex task, where the interplay between formulation, device and patient is crucial. From this thesis work, some insight has been gained regarding the impact of coatings, mixer type and mixing time, but there is plenty more to be studied. The results gained showed an interesting prospect for the batch D-C-L-T, and further studies of this would be exciting due to the many promising results. One such thing would be to investigate even longer mixing times since there was no sign of stagnating for either the FPF or FPD. It would also be interesting to see the impact of adding lactose fines to the formulation since this is known to increase the FPF. Furthermore, establishing a way of calculating the mixing energy exerted on a formulation when using the Turbula mixer would have the potential to gain further insight into predicting and maximising the quality outcome. This may also help to create a bridge between the outcome of high and low-shear mixers.

To further investigate the flowability and effects of storage, one way of moving forward would be to measure the compressed bulk density and calculate the Hausner ratio which is an indication of this. (European Pharmacopoeia. Chapter 2.9.18. Aerodynamic assessment of fine particles)

There is also still a lot of ground to be explored regarding the mechanisms of API release connected to the surface of the carrier (and coating), thus another way forward would be to investigate this using Atomic Force Microscopy or even synchrotron light (MAX IV).

6 References

Aulton, M. E. (2017). *Aulton's Pharmaceutics: The Design and Manufacture of Medicines.* Elsevier.

Biddiscombe, M. F., & Usmani, O. S. (2014). Is there room for further innovation in inhaled therapy for airways disease? *Breathe, 14*(3), 216-224. doi:10.1183/20734735.020318

European Pharmacopoeia. Chapter 2.9.18. Aerodynamic assessment of fine particles. (n.d.).

Fenton, C., Keating, G., & Plosker, G. (2003). Novolizer®. *Drugs*. doi:10.2165/00003495-200363220-00010

Gumani, D., Newmarch, W., Puopolo, A., & Casserly, B. (2016). Inhaler Technology. *International Journal Respiratory and Pulmonary Medicine, 3*. doi:10.23937/2378-3516/1410064

Kaialy, W. (2016). On the effects of blending, physicochemical properties, and their interactions on the performance of carrier-based dry powders for inhalation — A review. *Advances in Colloid and Interface Science, 235*, 70-89. doi:10.1016/j.cis.2016.05.014

Kohler, D. (2004). The Novolizer: overcoming inherent problems of dry powder inhalers. *Respiratory medicine*. doi:10.1016/j.rmed.2004.02.005

Kulkarni, V. S. (2009). Kulkarni, V. S. (2009). Handbook of Non-Invasive Drug Delivery Systems: Science and Technology. *Elsevier Science*. doi:10.1016/B978-0-8155-2025-2.10009-5

Kushner, J. (2012). Incorporating Turbula mixers into a blending scale-up model for evaluating the effect of magnesium stearate on tablet tensile strength and bulk specific volume. *International Journal of Pharmaceutics, 429*, 1-11. doi:10.1016/j.ijpharm.2012.02.040

Peng, T., Lin, S., Niu, B., Wang, X., Huang, Y., Zhang, X. &., Wu, C. (2016). Influence of physical properties of carrier on the performance of dry powder inhalers. *Acta Pharmaceutica Sinica B.* doi:10.1016/j.apsb.2016.03.011.

Saharan, V. A., Kukkar, V., Kataria, M., Kharb, V., & Choudhury, P. (2008). Ordered Mixing: Mechanism, Process and Applications in Pharmaceutical Formulations. *Asian Journal of Pharmaceutical Sciences* , 240-259.

Sanders, M. (2007). Inhalation therapy: an historical review. *Primary care respiratory journal : journal of the General Practice Airways Group, 16*, 71-81. doi:10.3132/pcrj.2007.00017

Shur, J., Price, R., Lewis, D., Young, P. M., Woollam, G., Singh, D., & Edge, S. (2016). From single excipients to dual excipient platforms in dry powder inhaler products. *International Journal of Pharmaceutics, 514*(2), 374-383.

Spahn, J. E., Zhang, F., & Smyth, H. D. (2022). Mixing of dry powders for inhalation: A review. *International Journal of Pharmaceutics, 619*.

Telko, M. J., & Hickey, A. J. (2005). Dry powder inhaler formulation. *Respiratory care, 50*(9), 1209-1227.

Thalberg, K. (2022, August). Formulation developmentof adhesive mixtures for inhalation - A multi-factorial optimization challange: Part 2. *Inhalation*, 22-29.

Thalberg, K., Berg, E., & Fransson, M. (2012). Modeling dispersion of dry powders for inhalation. The concepts of total fines, cohesive energy and interaction parameters. *International journal of pharmaceutics, 427*(2), 224–233.

Thalberg, K., Papathanasiou, F., Fransson, M., & Nicholas, M. (2020). Controlling the performance of adhesive mixtures for inhalation using mixing energy. *International journal of pharmaceutics*. doi:10.1016/j.ijpharm.2020.120055

Weiler, C., Egen, M., Trunk, M., & Langguth, P. (2017). Force Control and Powder Dispersibility of Spray Dried Particles for Inhalation. *Journal of pharmaceutical sciences, 99*(1), 303-316. Retrieved from https://doi.org/10.1016/j.ijpharm.2017.03.055

Appendix 1 – Settings for HPLC

Column	SUPELCOSIL LC-18, HPLC Column, 5cmx4.6mm,5µm
Column temperature	Ambient
Mobile phase	Ethanol (96%)/water 44/56 (vol/vol)
Flow rate	1.2 mL/min
Injection volume	50 µL
Detection wavelength, UV	240 nm
Run time	About 4 minutes

Table 12. Settings for the HPLC used when analyzing the samples from the NGI measurements.

Appendix 2- Data for the formulations analyzed using NGI

Fine Particle Fraction

FPF < 5 µm % of sum	3 min	6 min	9 min
D-C-H	57.53	48.24	39.98
D-C-L	55.48	61.28	57.19
D-N-H	29.55	22.22	20.31
	10 min	30 min	60 min
T-C	32.76	39.85	55.67
T-N	33.65	36.58	41.59
D-C-L-T	42.34	47.48	59.75

Fine Particle Dose

FPD < 5 µm ug/dose	3 min	6 min	9 min
D-C-H	143.52	122.22	106.18
D-C-L	140.89	155.70	136.76
D-N-H	71.90	52.94	42.87
	10 min	30 min	60 min
T-C	73.87	96.55	126.02
T-N	56.40	65.48	68.90
D-C-L-T	114.82	129.01	166.31

Mass Median Aerodynamic Diameter

MMAD (µm)	3 min	6 min	9 min
D-C-H	2.03	1.75	1.88
D-C-L	2.11	1.98	1.94
D-N-H	2.11	3.10	3.11
	10 min	30 min	60 min
T-C	2.71	2.43	2.19
T-N	2.63	2.72	2.72
D-C-L-T	2.41	2.14	2.16

Weight per dose

Weight/dose (mg/dose)	3 min	6 min	9 min
D-C-H	13.26	15.44	15.23
D-C-L	15.50	15.50	14.14
D-N-H	13.33	13.54	12.47
	10 min	30 min	60 min
T-C	15.06	16.86	14.03
T-N	11.18	9.37	10.88
D-C-L-T	15.04	16.44	16.75

Delivered dose (sum NGI)

Delivered dose (µg)	3 min	6 min	9 min
D-C-H	249.88	263.15	265.53
D-C-L	254.09	254.09	239.48
D-N-H	243.10	238.08	213.25
	10 min	30 min	60 min
T-C	225.45	242.97	226.38
T-N	168.15	179.15	165.75
D-C-L-T	271.24	271.75	278.16
Standard deviation (µg)	3 min	6 min	9 min
D-C-H	24,47	14,04	3,63
D-C-L	13.83	17.51	23.04
D-N-H	7.09	11.65	19.59
	10 min	30 min	60 min
T-C	1.79	23.16	0.06
T-N	13.02	4.44	3.50
D-C-L-T	2.72	16.13	26.64
Relative standard deviation (%)	3 min	6 min	9 min
D-C-H	9.79%	5.54%	1.37%
D-C-L	5.44%	6.89%	9.62%
D-N-H	2.92%	4.89%	9.18%
	10 min	30 min	60 min
T-C	0.79%	9.53%	0.03%
T-N	7.74%	2.48%	2.11%
D-C-L-T	1.00%	5.94%	9.58%

Appendix 3 - Data for the formulations analyzed using ACI

Fine Particle Fraction

FPF < 5 µm % of sum	3 min	6 min	9 min
D-N-H	40.63	35.75	31.13
D-N-L	45.98	44.82	42.25

Fine Particle Dose

FPD < 5 µm ug/dose	3 min	6 min	9 min
D-N-H	130.28	118.64	90.10
D-N-L	133.27	133.78	94.50

Mass Median Aerodynamic Diameter

MMAD (µm)	3 min	6 min	9 min
D-N-H	2.37	2.61	2.42
D-N-L	2.55	2.77	2.77

Weight per dose

Weight/dose (mg/dose)	3 min	6 min	9 min
D-N-H	12.53	12.24	11.56
D-N-L	11.21	12.25	12.02

Delivered dose (sum ACI)

Delivered dose (µg)	3 min	6 min	9 min
D-N-H	320.97	329.17	288.87
D-N-L	290.16	298.90	265.80
Standard deviation (µg)	3 min	6 min	9 min
D-N-H	8.04	53.89	15.84
D-N-L	19.27	20.84	5.90
Relative standard deviation (%)	3 min	6 min	9 min
D-N-H	2.50%	16.37%	5.48%
D-N-L	6.64%	6.97%	2.22%

Appendix 4 – Homogeneity and budesonide content

Scale without fundament – with gloves

T-N-10 (test nr)	Weight (mg)	Absorbance	Concentration (mg/ml)	Concentration of budesonide (mg/ml)	Fraction of budesonide in formula	Amount of budesonide in formula
1	31.90	64.615%	106.333%	1.934%	1.818%	0.580
2	32.60	67.185%	108.667%	2.008%	1.848%	0.603
3	31.80	69.825%	106.000%	2.086%	1.967%	0.626
4	36.10	70.145%	120.333%	2.095%	1.741%	0.628
5	27.20	55.680%	90.667%	1.673%	1.845%	0.502
6	34.20	81.995%	114.000%	2.441%	2.141%	0.732
				Mean:	1.893%	
				STD:	0.129%	
				RSD:	6.819%	

T-N-30 (test nr)	Weight (mg)	Absorbance	Concentration (mg/ml)	Concentration of budesonide (mg/ml)	Fraction of budesonide in formula	Amount of budesonide in formula
1	26.40	51.045%	88.000%	1.538%	1.747%	0.461
2	25.00	55.595%	83.333%	1.670%	2.004%	0.501
3	29.40	60.510%	98.000%	1.814%	1.851%	0.544
4	34.20	52.145%	114.000%	1.570%	1.377%	0.471
5	34.70	66.955%	115.667%	2.002%	1.731%	0.601
6	32.00	68.695%	106.667%	2.053%	1.924%	0.616
				Mean:	1,772%	
				STD:	0,201%	
				RSD:	11,327%	

T-N-60 (test nr)	Weight (mg)	Absorbance	Concentration (mg/ml)	Concentration of budesonide (mg/ml)	Fraction of budesonide in formula	Amount of budesonide in formula
1	33.90	79.040%	113.000%	2.354%	2,084%	0.706
2	36.10	80.000%	120.333%	2.382%	1,980%	0.715
3	25.90	60.640%	86.333%	1.818%	2,105%	0.545
4	36.80	75.290%	122,667%	2.245%	1,830%	0.673
5	36.20	47.220%	120.667%	1.426%	1,182%	0.428
6	34.30	41.755%	114.333%	1.266%	1,108%	0.380
				Mean:	1,715%	
				STD:	0,413%	
				RSD:	24,101%	
T-C-10 (test nr)	Weight (mg)	Absorbance	Concentration (mg/ml)	Concentration of budesonide (mg/ml)	Fraction of budesonide in formula	Amount of budesonide in formula

1	32.30	86.695%	1.07666667	0.02578	2.394%	0.7733281
2	29.20	66.465%	97.333%	1.987%	2.042%	0.5962447
3	29.50	84.920%	98.333%	2.526%	2.569%	0.7577906
4	35.40	56.695%	118.000%	1.702%	1.443%	0.510723
5	36.10	61.030%	120.333%	1.829%	1.520%	0.5486695
6	32.70	61.670%	109.000%	1.848%	1.695%	0.5542717
				Mean:	1.944%	
				STD:	0.00427	
				RSD:	21.9861%	

Scale on fundament – with gloves

T-N-60 (test nr)	Weight (mg)	Absorbance	Concentration (mg/g)	Concentration of budesonide (mg/g)	Fraction of budesonide in formula	Amount of budesonide in formula
1	35,90	57,690%	126,580%	1,731%	1,368%	0,519
2	25,20	50,495%	88,954%	1,522%	1,710%	0,456
3	35,90	78,670%	126,621%	2,344%	1,851%	0,703
4	29,90	66,475%	105,614%	1,988%	1,882%	0,596
5	40,00	89,140%	141,293%	2,649%	1,875%	0,795
6	23,60	44,070%	83,430%	1,334%	1,599%	0,400
				Mean:	1,714%	
				STD:	0,00185	
				RSD:	10,8077%	

T-C-10 (test nr)	Weight (mg)	Absorbance	Concentration (mg/g)	Concentration of budesonide (mg/g)	Fraction of budesonide in formula	Amount of budesonide in formula
1	31,90	73,130%	112,989%	2,182%	1,931%	0,655
2	30,50	59,370%	107,601%	1,780%	1,655%	0,534
3	29,50	62,205%	104,285%	1,863%	1,787%	0,559
4	21,00	39,835%	74,166%	1,210%	1,632%	0,363
5	30,00	60,055%	106,142%	1,800%	1,696%	0,540
6	24,70	52,705%	87,350%	1,586%	1,816%	0,476
				Mean:	1,753%	
				STD:	0,104%	
				RSD:	5,906%	

Scale on fundament – without gloves

T-N-60 (test nr)	Weight (mg)	Absorbance	Concentration (mg/g)	Concentration of budesonide (mg/g)	Fraction of budesonide in formula	Amount of budesonide in formula
1	23.70	51.960%	83.564%	1.564%	1.872%	0.469
2	34.70	78.140%	122.488%	2.328%	1.901%	0.698
3	24.60	54.960%	86.765%	1.652%	1.904%	0.496
4	23.90	52.950%	84.420%	1.593%	1.887%	0.478
5	21.90	49.680%	77.358%	1.498%	1.936%	0.449
6	20.70	45.790%	73.178%	1.384%	1.892%	0.415
				Mean:	1.899%	
				STD:	0.020%	
				RSD:	1.038%	

T-C-10 (test nr)	Weight (mg)	Absorbance	Concentration (mg/g)	Concentration of budesonide (mg/g)	Fraction of budesonide in formula	Amount of budesonide in formula
1	21.20	44.435%	75.090%	1.345%	1.791%	0.403
2	25.10	53.470%	88.550%	1.608%	1.816%	0.482
3	33.30	70.230%	117.718%	2.097%	1.782%	0.629
4	20.30	43.015%	71.694%	1.303%	1.818%	0.391
5	21.30	42.845%	75.361%	1.298%	1.723%	0.389
6	29.20	66.180%	103.263%	1.979%	1.917%	0.594
				Mean:	1.808%	
				STD:	0.058%	
				RSD:	3.211%	

Scale without fundament – without gloves

T-N-60 (test nr)	**Weight (mg)**	**Absorbance**	**Concentration (mg/g)**	**Concentration of budesonide (mg/g)**	**Fraction of budesonide in formula**	**Amount of budesonide in formula**
1	23.00	50.610%	80.689%	1.525%	1.890%	0.457
2	29.60	65.775%	104.068%	1.967%	1.890%	0.590
3	24.20	53.505%	85.18%	1.609%	1.891%	0.483
4	20.50	46.085%	72.027%	1.393%	1.934%	0.418
5	25.90	59.280%	91.523%	1.778%	1.942%	0.533
6	21.80	48.955%	76.816%	1.477%	1.922%	0.443
				Mean:	1.912%	
				STD:	0.022%	
				RSD:	1.154%	

T-C-10 (test nr)	Weight (mg)	Absorbance	Concentration (mg/g)	Concentration of budesonide (mg/g)	Fraction of budesonide in formula	Amount of budesonide in formula
1	20.30	43.385%	71.902%	1.314%	1.828%	0.394
2	39.80	86.640%	140.410%	2.576%	1.835%	0.773
3	20.10	42.800%	71.055%	1.297%	1.825%	0.389
4	26.80	62.925%	94.650%	1.884%	1.991%	0.565
5	26.20	53.470%	92.698%	1.608%	1.735%	0.482
6	22.40	47.230%	79.216%	1.426%	1.800%	0.428
				Mean:	1.836%	
				STD:	0.077%	
				RSD:	4.195%	